Identification and validation of novel aptamers against fungal cells.

by

Beth Milnes

A thesis submitted in partial fulfilment for the requirements for the degree of MSc (by Research), at the University of Central Lancashire

March 2019

STUDENT DECLARATION FORM

Type of Award **Msc (by Research)**

School **School of Pharmacy and Biomedical Sciences**

1. Concurrent registration for two or more academic awards

*I declare that while registered as a candidate for the research degree, I have not been a registered candidate or enrolled student for another award of the University or other academic or professional institution

2. Material submitted for another award

*I declare that no material contained in the thesis has been used in any other submission for an academic award and is solely my own work

3. Collaboration

Where a candidate's research programme is part of a collaborative project, the thesis must indicate in addition clearly the candidate's individual contribution and the extent of the collaboration. Please state below:

4. Use of a Proof-reader

*No proof-reading service was used in the compilation of this thesis.

Signature of Candidate _____

Print name: _____

Abstract

We encounter thousands of species of fungi each day, only a few of these are pathogenic to humans and even fewer are life threatening. However, current fungal infection treatments come with a wide variety of issues. With some exhibiting high nephrotoxicity due to targeting issues, and others a lack of efficiency.

Aptamers are short oligonucleotides, which exhibit affinity and specificity for a target molecule. These aptamers are determined through the process of SELEX. This is where target molecules, or in this case whole cells, are incubated with a pool of random aptamers. Non-binding aptamers are removed and binding aptamers are eluted and amplified by PCR. This enriches the pool with binding aptamers. This process continues as a cycle with each round of selection removing non-binding aptamers, and further amplifying the numbers of binding aptamers. Once rounds of selection are completed then the aptamers can be tested individually for their binding properties. Aptamers have already been found to be useful in industrial settings, with some aptamers even beginning to show in clinical settings.

This study took whole cell A. fumigatus and C. albicans, in order to select aptamers that were specific to these cells without limiting the targets by incubating with individual target molecules. This study found isolated 11 aptamers with binding potential; these were then tested further to determine the binding capabilities, and their specificity. These aptamers were then isolated, sequenced and characterised to compare against each other and to attempt to determine key binding regions of the aptamers.

Table of Contents

Acknowledgments

I would like to thank my supervisors, Dr. Clare Lawrence and Dr. Vicky Jones for their continuing support throughout my research. Without them I wouldn't have been able to get this far.

1.0 Introduction

1.1 Fungi

There are estimated to be around 611,000 species of fungi on Earth, approximately 7% of all eukaryotic species (Mora *et al*., 2011). Of these around 600 species are human pathogens (Brown, Denning and Levitz, 2012), although a relatively small number, this group encompasses both those that cause mild infections and those that have the potential to cause life threatening infections. Around 3 million people each year acquire an invasive fungal infection, with around 50% of these dying from the infection (Brown et al., 2012). The overall number of invasive fungal infections is on the rise with the increase in invasive medical interventions like haemopoietic stem cells transplants (Vazquez, Miceli and Alangaden, 2013) bringing with them an increased risk of infection. Also, the rise of immunosuppressive conditions like HIV/AIDS, where patients are especially vulnerable to fungal infections (Armstrong-James, Meintjes and Brown, 2014).

1.2 Systemic Fungal Infections

As with bacteria, most life threatening complications arise when microorganisms enter the tissue and bloodstream of a patient. Most healthy individuals have the immune capacity to prevent this from happening, however, patients with pre-existing conditions or patients who have undergone invasive surgical procedures are most at risk (Brown *et al,.* 2012).

Mucosal Candidiasis is one of the early and most predominant infections in HIV infected patients (Greenspan and Greenspan, 1996). Up to 90% of patients with HIV suffer from at least one case of oral candidiasis in their progression to AIDS. (Cassone and Cauda, 2012). This correlation is thought to be caused by the depletion of CD4 cells specific to *Candida albicans,* meaning that the immune systems no longer has the full capacity to control the spread of *Candida* (Nanteza et al., 2014). Other kinds of immunosuppression include conditions where the immune system neutrophil count is lowered, like with haemopoietic stem cell transplant or

certain kinds of chemotherapy, that can lead to cases of invasive Aspergillosis, as neutrophils play an important role in the control of *Aspergillus* species infection (Mircescu *et al*., 2009).

A common risk of infection is patients that have undergone invasive treatments, for instance urinary catheterisation is a common cause of nosocomial infection especially in patients catheterised for a prolonged length of time. Urinary tract infections (UTI) caused by *Candida* species account for 10-15% of UTIs (Bukhary, 2008).

1.3 *Candida* species

Candida are a species of polymorphic fungi responsible for a wide range of cases of systemic fungal infections, referred to as Candidiasis. The most prevalent of these species is *Candida albicans*, which is responsible for the highest number of both invasive and superficial fungal infections. This opportunistic fungus lives commensally on the skin, the gastrointestinal tract and mucosal membranes of up to 75% of the population (White, 2004). Public Health England (2018) reported 42% of cases of candidiasis as being caused by *C. albicans*, 24% being caused by *Candida glabrata* and 10% caused by *Candida parapsilosis* (Table 1.1).

	2013		2014		2015		2016		2017	
	No.	%	No.	%	No.	%	No.	%	No.	%
Candida spp.	**1829**	100	**1796**	100	**2065**	100	**2150**	100	**2211**	100
C. albicans	853	47	793	44	919	45	905	42	919	42
C. auris	0	0	0	0	3	<1	16	<1	5	<1
C. dubliniensis	13	<1	23	1	36	2	32	1	48	2
C. famata	7	<1	2	<1	2	<1	4	<1	3	<1
C. glabrata	465	25	460	26	473	23	539	25	525	24
C. guilliermondii	16	<1	7	<1	8	<1	17	<1	12	<1
C. kefyr	2	<1	8	<1	9	<1	5	<1	2	<1
C. krusei	21	1	38	2	26	1	21	<1	37	2
C. lusitaniae	21	1	28	2	32	2	31	1	28	1
C. parapsilosis	192	10	193	11	205	10	200	9	229	10
C. tropicalis	67	4	48	3	77	4	67	3	71	3
Candida spp., other named	40	2	40	2	33	2	45	2	40	2
Candida spp., sp. not recorded	132	7	156	9	242	12	268	12	292	13

† data presented are for routine laboratory reports only and may not match those presented in other sources

* including *C. blankii, C. catenulate, C. ciferrii, C. fabianii, C. fermentati, C. haemulonii, C. inconspicua, C. lipolytica, C. magnolia, C. metapsilosis, C. navariensis, C. orthopsilosis, C. pararugosa, C. pelliculosa, C. peltata, C. utilis, C. zeylandoides*

Table 1.1 (Public Health England, 2018) A summary of *Candida spp.* and the % of *Candida* infections they cause, in the UK from 2013 to 2017.

The overall increase in infections since 2013 suggest that *Candida* species infections are a continuing threat. There are also a number of concerns regarding the development of drug resistant strains of these fungi. One of the fastest emerging species is *Candida auris* (Chowdhary, Sharma and Meis, 2017), with instances of this strain worldwide having increased over the past few years. This strain is commonly misdiagnosed as *Candida haemulonii*, their close phylogenetic relationship only being differentiated by sequence analysis of the D1/D2 domain of the large ribosomal subunit of 26S rRNA gene and the internal transcribed spacer regions of the nuclear rRNA gene operon (Satoh *et al*., 2009).

Along with the problem of frequent misdiagnosis, this strain has developed resistance to many commonly used anti-fungal drugs. The strain is likely almost always resistant to fluconazole but relatively susceptible to the group echinocandins (Arendrup *et al*., 2017).

1.4 *Candida albicans* morphology

C. albicans is a polymorphic fungus that grows in several different forms depending on a range of environmental cues. Under conditions that provide opportunity for infection, like low cell densities of competing organisms, (Hornby et al., 2001) *Candida albicans* will appear more in their hyphal form (known as psuedohyphae shown in figure 1.1). However, when living commensally, they exist in their more yeast like form (Lu, Su and Liu, 2014).

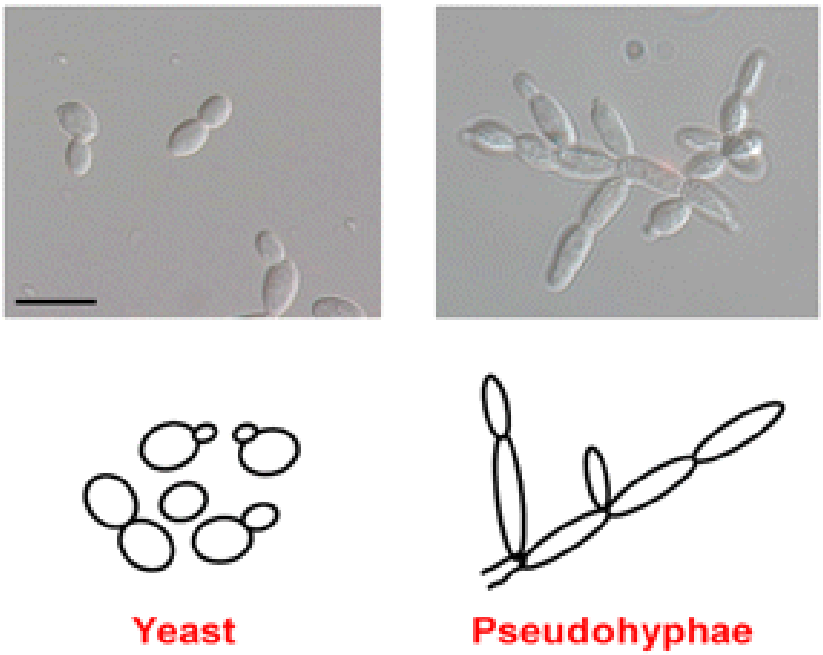

Figure 1.1 Major morphologies of *C. albicans.* (Thompson, Carlisle and Kadosh, 2011). Visualised by differential image contrast (DIC) scale bar 10µm. Left, *C. albicans* in their yeast like form and schematic representation underneath. Right *C. albicans* in their pseudohyphal form and below a schematic representation of this.

Although *C. albicans* predominantly exists in its yeast like form, when environmental aspects such as microbiota, temperature or host immunity change this gives *C. albicans* the opportunity to infect the host through its hyphal form. Initiation of the transformation can be triggered in a number of ways depending on the environmental cue, CO_2 for example directly activates Cyr1 (Hall *et al*., 2010) whereas glucose as a signalling molecule activates expression of the Ras1 protein (Leberer *et al*., 2001) which then results in a signalling cascade of adenyl

cyclase Cyr1. This activates production of cAMP then activation of protein kinase A leading to the production of hyphae, critical for *C. albicans* virulence. Studies have shown that strains of *C. albicans* unable to produce hypha are avirulent (Lo *et al*., 1997).

The presence of other microbes has also been shown to inhibit early stage morphogenesis of *Candida albicans* from their yeast like form to their hyphal form (Matsubara *et al*., 2016), (Cruz *et al*., 2013). For instance, within the gut biome *Clostiridum difficile* are a common organism and produce a substance called p-Cresol, which is toxic in high concentrations to most microbes but has been shown to directly inhibit the hyphal and biofilm formation of *C. albicans* (van Leeuwen *et al*., 2016). Studies like this have shown that there is more to the morphogenesis of *C. albicans* than environmental cues, and in complex environments like the gut biome, *C. albicans* may rely more on other microbes for signalling the start of infection.

Biofilm formation is an important factor in the pathogenesis of *C. albicans*. A biofilm is a community of adherent cells with properties different to that of free floating cells. The formation of *C. albicans* biofilm is closely linked to its hyphal state and the formation of these biofilms is an important step in systemic infections. Cells adhere to a surface, regulated by Bcr-1 and including Hwp1 and Als3 (Nobile *et al*., 2006) and begin to form hyphae which act as structural support for biofilm formation and with the regulation of Bcr-1 allows for the hyphae to adhere to one another (Nobile and Mitchell, 2005). These biofilms then produce an extracellular matrix, and release cells continuously. These released cells, although similar to *C. albicans* in their commensal state, exhibit increased adherence properties, the ability to form biofilms more readily and in mouse models, have shown increased virulence (Uppuluri *et al*., 2010).

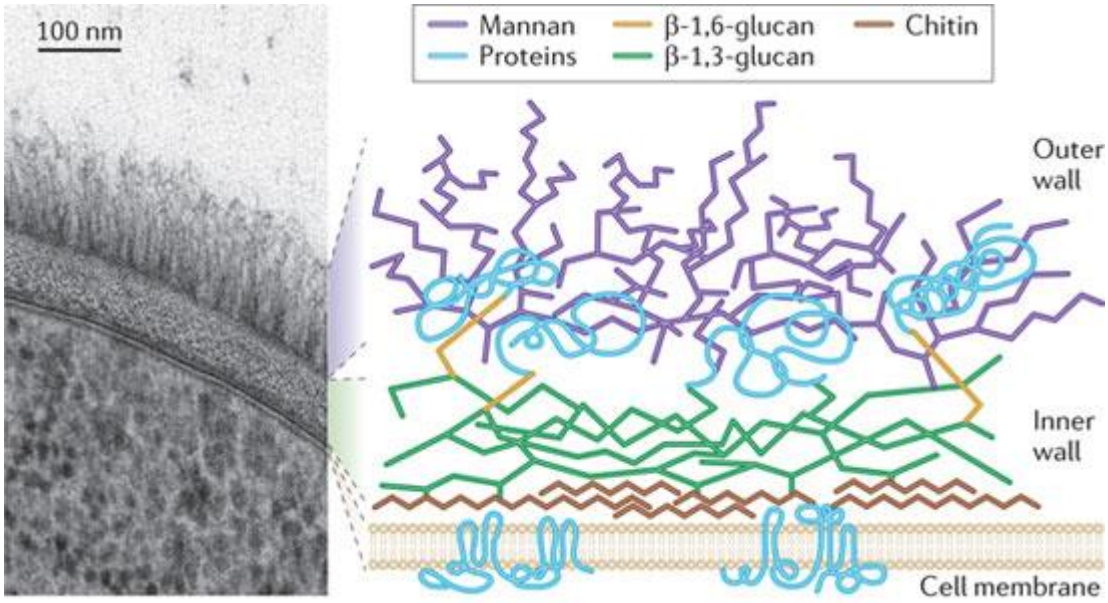

Figure 1.2 Structure of *Candida albicans* cell wall and membrane. The cell membrane is the inner most layer surrounding the contents of the cell, made up of a phospholipid bilayer. This is then surrounded by a layer of chitin, β 1,3 and β 1,6 - glucan comprising the inner wall. The outer wall is then a layer of mannoprotein (taken from Gow et al., 2011).

The cell wall plays a crucial role in the virulence of *C. albicans*, containing many key proteins for the stages of infection. Figure 1.2 shows a schematic diagram, along with an image of *C. albicans* cell wall and membrane. The cell wall has a layered structure with the inner wall comprised of chitin, a linear polysaccharide linked to β-1,3-glucans which provides the cell with structural integrity. β-1,6-glucan links the inner wall to the outer wall which is mainly comprised of mannan and β-1,6-glucan along with cell wall proteins. Beneath the cell wall is the cell membrane, structured the same as all mammalian cells, with a lipid bilayer. This lipid bilayer is interspersed with ergosterol (cholesterol in mammalian cells) an important sterol for the maintenance of the integrity, fluidity and rigidity of the plasma membrane (Abe, Usui and Hiraki, 2009).

1.4.2 *Candida albicans* pathogenicity

Approximately 75% of women worldwide suffer from at least one case of vulvovaginal candidiasis in their life, with 40-50% of these suffering a reoccurrence (Sobel, 2007). Treatments for vulvovaginal candidiasis are readily available and infection causes a relatively small amount of damage to the host. However more serious infections occur in immunocompromised patients, as the host immune system, which monitors commensal growth and responds to pathogenic growth (mainly the formation of hyphae) is not fully functional thus allowing *Candida albicans* to readily form hyphae (Rast *et al*., 2016).

There are three main stages of infection, adhesion, invasion and damage. The formation of hyphae is triggered by the adhesion of the cell to a mucosal membrane leading to the expression of two key hyphal proteins Hwp1 (Staab *et al*., 1999) and agglutinin-like sequence 3 (Als3) (Zhao, 2004). Hyphal growth penetrates the epithelial tissue and secretes a cytolytic toxin called Candidalysin, a peptide encoded by the hypha-associated *ECE1* gene, which causes significant damage. Candidalysin, when secreted in sufficient quantities, intercalates and permeabilises host epithelial membranes and induces cell lysis (Moyes *et al*., 2016). This leads to the formation of multiple necrotic nodules, which cause extensive organ damage and can eventually lead to organ failure.

However, penetration of *Candida albicans* in the epithelial tissue is not the only concern. In 2017 the rate of candidaemia was 3.6 per 100,000 population found in blood isolate. 42% of these were *Candida albicans* (Public Health England, 2018).

1.5 *Aspergillus fumigatus*

The thousands of species of fungi existing in many environmental niches make human contact with fungi a common occurrence. *Aspergillus fumigatus* are a ubiquitous human fungal

pathogen, living in soil and decaying plant matter. The abundance of this organism is due to their ability to survive many environmental conditions. Like most human pathogens *A. fumigatus* has an optimal growth temperature of 37°C, however, unlike most other pathogens it has a high tolerance for temperature changes up to 60°C (Beffa, *et al.* 1998). The causes of this have been investigated and a link between thermotolerance and virulence was found. *A fumigatus* grows in hyphal form and spreads through its dispersion of spores. In order for *A. fumigatus* spores to form hyphae they must germinate, in this process the number of ribosomes increases 10 fold to support hyphal growth (Brogden *et al*., 1984)

Aspergillus fumigatus is the most commonly recovered species from patients with aspergillosis followed by *Aspergillus niger, flavus* and *terreus* (Morgan *et al.* 2005).

1.5.2 *Aspergillus fumigatus* morphology

A. fumigatus are saprotrophic fungi thriving in soil with decaying plant and animal matter. *A.* fumigatus grows in multicellular branched structures in their hyphal form. However, when conditions are unfavourable *A. fumigatus* produces spores called conidia on specialised hyphal structures called conidiophores by a series of signalling cascades. These spores are then very efficiently (Taha *et al*., 2005) released into the air, where humans are estimated to inhale 100-1000 conidia each day. Due to their small size(2-3µm) they can reach the alveoli of the lungs (Latgé, 1999) where they adhere to the surface. The cell wall of *A. fumigatus* conidia is similar to that of most fungal cell walls, with the presence of β 1,3 and β 1,6 - glucans and chitin, however they also contain a protective coating of melanin. The melanin is one of the reasons why the spores are so resilient. Melanin provides resistance to environmental stresses UV radiation and oxidising agents (Rosa *et al*., 2010). The spores are able to reproduce asexually. Once the spores are established in an ideal growing environment the spores can then

germinate into full hyphae. The adherence of the spores to a suitable surface (like lung alveioli) is what triggers hyphal growth.

1.5.3 *Aspergillus fumigatus* pathogenicity

Rates of *Aspergillus fumigatus* infection in the UK are thought to be more substantial than previously reported. Groups of at risk patients include those living with AIDS, Patients who have undergone Haemopoietic stem cell transplants and those with chronic asthma (Baddley, 2011).

Invasive Infection	Risk Group	Number of Expected Cases	Rates per 100,000 population
Invasive aspergillosis	All risk groups* except critical care patients	2901-2912	4.59 - 4.61
	Critical care patients	387-1345	0.61 - 2.13
Chronic pulmonary aspergillosis - all	All risk groups**	204-3600	0.32 - 5.70
Allergic bronchopulmonary aspergillosis (ABPA)	All risk groups***	110,667-235,070	175 - 372
Severe asthma with fungal sensitisation (SAFS)	All risk groups****	121,734-413,724	192- 654

Table 1.2. (Pegorie, Denning and Welfare, 2017) Total Estimates of the burden of various types of aspergilliosis on the at risk UK population. * Risk groups include: Allogeneic hematopoietic stem cell transplantation (HSCT) and autologous HSCT patients; solid organ transplants; people living with AIDS; Acute myeloid leukaemia (AML), Acute lymphoblastic leukaemia (ALL), Chronic myeloid leukaemia (CML), Chronic lymphocytic leukaemia (CLL), Non Hodgkin lymphoma (NHL), Hodgkin lymphoma (HL) and Myeloma patients; Chronic granulomatous disease (CGD) patients; Chronic obstructive pulmonary disease (COPD): emergency hospital admissions,; critical care patients; patients with lung cancer. ** Risk groups include: pulmonary tuberculosis (PTB), non-tuberculous mycobacterial lung infection, COPD, sarcoidosis, and allergic aspergillosis complicating asthma. *** Risk Groups include: Asthma and Cystic Fibrosis. **** Risk Groups include: Severe Asthma, usually those with poor

control of the condition (treatment- resistant severe asthma, undiagnosed severe asthma and difficult to treat severe asthma).

Table 1.2 shows the estimated rates of various *A. fumigatus* infections on at risk patient groups. Severe asthma with fungal sensitivity is predicted to be the most prevalent estimated to occur in 192-654 patients per 100,000.

Little work has been done on determining the incubation time of *A. fumigatus*, however, Bénet *et al*., (2013) found that incubation times in patients with acute myeloid leukaemia can be around 15 days. This has a knock on effect in many aspects of fungal infection firstly in determining the location of infection source, meaning that other cases of infection cannot easily be prevented. Also that treating infections early are very difficult as by the time the patient becomes symptomatic the infection is already deep within the tissue.

Once adhered *A. fumigatus* establishes hyphal growth and, as previously described in *C. albicans*, biofilms are also formed by *A. fumigatus.* These are often highly resistant to antifungal therapies, as pathogenic aspergilli can expel antifungal compounds using multidrug efflux pumps, this means that a high concentration of antifungal drug is necessary to successfully treat infection. (Kaur and Singh, 2014).

The previously discussed melanin coating on the spores contribute greatly to the infectious capabilities *A. fumigatus*.

1.6 Fungal infection diagnosis

Currently fungal infections are diagnosed with a series of laboratory test including the use of microscopy, sample culture and histopathology. Sample culture is the starting point for most suspected cases of fungal infection. A sample is taken and grown on a variety of growth mediums to determine the type of infection. However, in the case of invasive Candidiasis, this process can take between 24 - 72 hours and can miss infection in around 50% of patients when

sampled from blood culture (Ostrosky-Zeichner, 2012) and may only yield a positive result in late stages of infection (Ellepola and Morrison, 2005).

Symptoms of *Aspergillus fumigatus* infection include a fever, chest and joint pain, shortness of breath and coughing up blood. Once symptoms present, diagnosis can be a difficult and lengthy process. Current diagnoses are based on the results following treatment with broad spectrum antibiotics. As the symptoms are non-specific they are often treated as a bacterial infection, after no response to antibacterial drugs thoracic imaging is used. Primarily a CT scan of the lungs is the first port of call (Lim *et al*., 2012).

1.7 Fungal infection treatments

There are four main classes of antifungals. Firstly azoles, including the commonly prescribed fluconazole. These act by inhibiting synthesis of the cell membrane component ergosterol, by inhibiting the cytochrome p450 enzyme 14-α lanosterol demethylase which catalyses the conversion of lanosterol to ergosterol (Kathiravan *et al*., 2012).

The next class are polyenes, most commonly prescribed being Amphotericin B which again targets ergosterol in the cell membrane. Amphotericin B binds to ergosterol in the membrane causing the formation of pores which leads to depolarisation of the membrane, leakage of intercellular components and eventually cell death (Brajtburg *et al*., 1990).

Echinocandins are lipoproteins that act as non-competitive inhibitors of β 1, 3 – glucan synthase required for the synthesis of cell wall component β 1, 3 -glucans (Perlin, 2011). Defects in the synthesis of cell wall components affect the integrity of the cell and result osmotic sensitivity, reduced sterol contents and thickened cell wall.

Finally, pyrimidine analogs like 5- flucytosine, impair fungal cells ability to synthesise proteins and DNA during nuclear division. (Waldorf and Polak, 1983. Diasio *et al.* 1978). This comes as a

result from the rapid conversion of 5-FC to 5-fluorouracil in susceptible fungal cells by the enzyme cytosine deaminase.

1.8 Fungal infection treatment complications including the similarity of fungal cells to human cells

Antifungal treatments have been proven to be relatively effective over the years, with variations in drug types and their targets meaning there are a wide range of options available for treatments. However, as with bacterial infections, treatment options are becoming much narrower with the emergence of antifungal resistant strains of fungi.

The class of antifungals echinocandins for example have seen reported cases of resistance after just one week of treatment (Lewis *et al.* 2013). Mechanisms of resistance vary by treatment and species of target. The most common factors contributing to antifungal resistance are the selective pressures these treatments place on the population of fungi. The most common being mutations that result in conformational changes to the target site. In *C. albicans* multiple strains resistant to azoles have been found to have a single mutation Tyr^{132} to Phe substitution in Cyp51 (Cools, 2008).

Another factor of resistance is in the formation of biofilms during infection. There is an extracellular matrix present around the cells that comprise the biofilm, this extracellular matrix in *A. fumigatus* contains galactomannan, galactosaminogalactan, α-1,3 glucans, monosaccharides, polyols, melanin, and proteins (Beauvais and Latgé, 2015). In addition to this in a biofilm *A. fumigatus* releases extracellular DNA, which aids antifungal resistance (Rajendran *et al*., 2013 and Jöchl *et al*., 2009)

A major issue of anti-fungal treatments is the target cells similarity to human cells. The main sterol component of fungal cell membranes is ergosterol, this is very similar to the cell

membrane sterol cholesterol in mammalian cells. Cholesterol is also synthesised in a pathway utilising members of the cytochrome p450 enzyme class. However, amphotericin B exhibits high nephrotoxicity (Torrado et al., 2008). These adverse effects are not limited to one class of antifungals, Itraconazole for example was found to have a 23% chance of treatment being discontinued due to adverse effects (Wang *et al.* 2010).

Echinocandins have low bioavailability due to their large molecular weight; this means that they must be administered intravenously. However, they have relatively low toxicity toward mammalian cells as they target the cell wall of fungi and therefore don't affect mammalian cells (Shapiro, Robbins and Cowen, 2011).

1.9 Aptamers

The term aptamer refers to a section of DNA/RNA or protein that has specific binding to a target. These highly specific molecules have a high affinity for their targets as a result of the way in which they are produced. SELEX (Systemic Evolution of Ligands by Exponential enrichment), the means for *in vitro* selection of aptamers, was developed in the 1990s and demonstrates the ability of aptamers to bind to a wide variety of targets, from small molecules to large protein complexes (Tuerk and Gold, 1990).

1.9.2 Systematic Evolution of Ligands by Exponential Enrichment (SELEX)

SELEX is carried out by taking a target cell or molecule and incubating with a pool of random aptamers. Non-binding aptamers are removed and binding aptamers, eluted and amplified by Polymerase chain reaction (PCR). These aptamers are then incubated with targets again. This process is repeated and with each round of SELEX the pool of aptamers reduces to aptamers that bind specifically to the target. Some studies performed include the introduction of a counter selection step where the aptamer is incubated with a protein or cell type similar to the

target. Aptamers that do not bind during the counter selection step are taken forward to incubation with the target, whilst aptamers that did bind during counter selection are discarded. This helps to ensure the aptamers specificity by eliminating binding to unwanted targets.

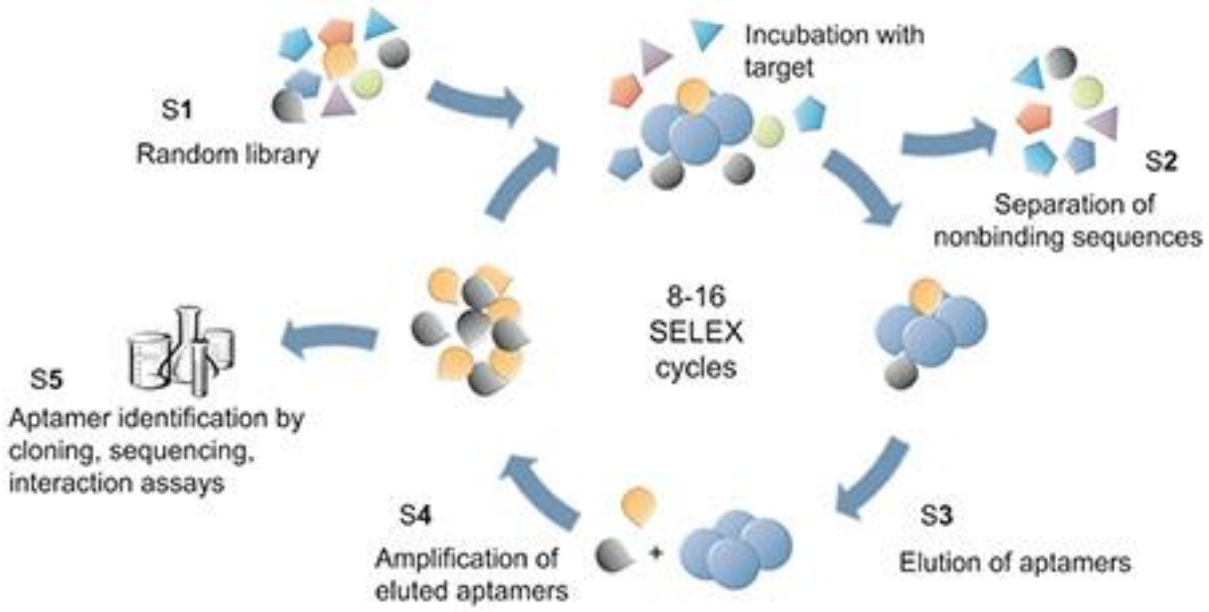

Figure 1.3, SELEX. A schematic diagram of the SELEX process. A random library of aptamers is incubated with the target molecule to determine which will bind. Non-binding sequences are separated off, and binding aptamers are eluted and amplified. The binding aptamers can then be identified and sequenced. The process is then repeated with the addition of new random aptamers to increase numbers of binding aptamers. (Blind and Blank, 2015).

Figure 2 shows the SELEX process and how aptamers are identified for specific targets through the amplification of binding sequences and elimination of non-binding sequences. Once identified, aptamers have a number of uses including the identification of target cells or aiding treatments.

1.9.3 Structure and Function

Aptamers are single-stranded DNA or RNA of 20-100 bases in length. Their unique properties are based on their ability to fold into unique secondary and tertiary structures because of the wide variations in size and sequence of each strand.

1.9.4 Aptamers versus Antibodies

Antibodies also have the ability to bind to specific targets, however, aptamers have a number of key advantages. Firstly in order to carry out the SELEX process the target of the aptamer does not have to be predetermined. This means that an aptamer will be selected on the affinity of its binding not the suitability of the target. Whereas antibodies are produced based on their specific antigen. Aptamers also offer many other advantages over antibodies, due to their oligonucleotide properties. (Sun *et al.* 2014). Aptamers have a lower molecular weight of around 8-24 kDa compared to antibodies at around 150 kDa, because of this, aptamers can penetrate tissue faster and more efficiently enabling smaller doses of drugs to be used as more would get to the target tissue and not be distributed and lost to the other parts of the body. Also directly compared to antibodies, aptamers have been shown to penetrate tissue faster and more efficiently in cases of cancer where tumours are denser than the surrounding tissue (Xiang *et al*., 2015) which, with antibodies, would mean reaching the centre of the tumour would be difficult.

They have also been shown to not illicit an immune response *in vivo* (Eyetech study group, 2002), which brings fewer complications for patients. Another issue with antibodies is their stability. A common cause of physical instability is aggregation of antibodies (Shire, Shahrokh and Liu, 2004). The higher the concentration of antibodies the more likely they are to form aggregates. Aggregates of immunoglobulin have also been shown to cause renal failure (Demeule, Gurny and Arvinte, 2006). Aptamers are more stable, due to the conditions which affect the folding of aptamers like pH, Magnesium (Mg) concentration and temperature. In a

clinical setting, within patients or patient samples these values do not vary enough to affect the binding and folding of DNA. If a selection is carried out under the right conditions the aptamer will continually fold in the same way meaning that problems of aggregation don't occur. Aptamers can be made more stable with the addition of post SELEX modifications (Boomer *et al*., 2005, De Smidt *et al*., 1991).

1.9.5 Previously Identified aptamers

In regards to microorganisms, previous studies mainly focus on the application of aptamers in bacterial treatments/detection. Chang *et al.* (2013) found two aptamers that selectively bind to *Staphylococcus aureus* with high affinity. Hamula *et al.* (2008) performed selections against live whole bacterial cells. Tang *et al.* (2016) found aptamers that specifically bound to β 1,3 - glucan in the membrane of *C. albicans*.

1.9.6 Aptamers as therapeutic agents

Aptamers have been used to fluorescently tag and bind to tumour initiating cells, a common precursor in brain cancer, thus indicating their diagnostic potential as a means of detecting tumour initiating cells (Kim *et al.,* 2013). Many groups have demonstrated that aptamers with specificity to cell surface receptors can greatly aid the internalisation of drugs such as doxorubicin in cancer cells (Tan *et al.* 2011, Meng *et al*., 2012, Chu, 2006).

2.0 Materials and Methods

2.1 Fungal cell growth and maintenance

Candida albicans (C.*albicans*), strain SC5314, and *Saccharomyces cerevisiae* (S. *cerevisiae*), strain BY4741a a derivative of S288C (*MATa his31 leu20 met150 ura30) (Baker Brachmann et al., 1998)* were grown in YPD broth (1% yeast extract, 1% peptone and 2% dextrose) at 30^{o}C with shaking at 180 rpm and stored on YPD agar (YPD broth, 1% agar). *Aspergillus fumigatus* (A. *fumigatus*), strain ATCC 4660, was grown on Sabouraud (SAB) agar (4% glucose, 1% peptone, 2% agar, pH5.6) at 30^{o}C.

2.1.2 HeLa cells

The HeLa cell line (obtained from ATCC, Manassas, USA) were maintained in Eagle's Minimum Essential Media (EMEM, Earle's Balanced Salt Solution, non-essential amino acids, 2 mM L-glutamine, 1 mM sodium pyruvate, and 1500 mg/L sodium bicarbonate.) supplemented with 10% Foetal Bovine Serum (FBS), 1% non-essential amino acids (NEAA), 2mM L-glutamine, 1mM sodium pyruvate and 10U/ml Pen-Strep. Cells were grown in a 75ml flask, in a 37^{o}C, 5% CO_2 static incubator to around 80% confluency before being passaged. Cells were washed twice with phosphate buffered saline (PBS) (10mM phosphate, 137mM sodium chloride, 27mM potassium chloride, pH 7.41) then adding 3ml of 1x trypsin and incubating for 5 minutes at 37^{o}C, in order to detach cells from the surface of the flask. Once detached the trypsin was neutralised by adding an equal quantity of EMEM (all solutions pre warmed to 37^{o}C), before being centrifuged at 570g for 5 minutes and pelleted cells re-suspended in fresh EMEM. Cells were only passaged to around passage 15, at this point cell lines were disposed of and a new line taken from cryogenic storage, defrosted and grown.

2.2 Systematic evolution of ligands by exponential enrichment using cell lines (cell-SELEX).

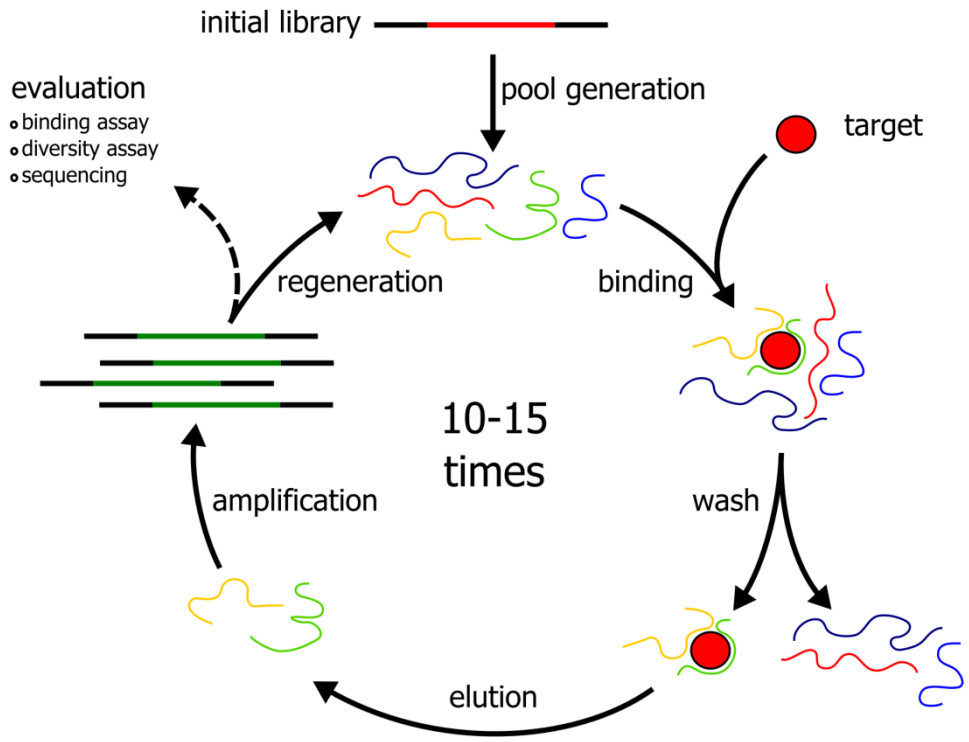

Figure 2.1 A summary of the SELEX protocol (Schütze et al., 2011). The diagram shows the amplification of the initial library to generate the starting pool of aptamers, these are then incubated with the target. Non-binding aptamers are washed from the target, and the remaining bound aptamers are eluted and then amplified. These either form the pool for the next round of selection or are used for binding and diversity assays or sequencing.

2.2.1 Amplification and purification of DNA Aptamer Library

Figure 2.1 shows an overview of the SELEX process. Starting with a random library of aptamers, which were used to provide the stock aptamer library. This library consists of a random 10^{15} DNA aptamers, synthesised by Integrated DNA Technologies (IDT, UK) through machine mixed randomisation. Each sequence (green) was flanked by aptForward (red) and aptReverse (blue) primer specific to the aptamer library.

5'- ATCCTAATACGACTCACTATGGGGAGAGGATTCTGGGCACAAGCGAATTTATATAAAGC CCGGCTCAACTGGCAAAGCAATCGGTCGAGTTTACCGCAGAATT – 3'

For amplification of each aptamer by PCR both primers are needed.

An initial amplification of the aptamer library was undertaken by Polymerase Chain Reaction (PCR), the conditions of which are detailed in tables 2.1 and 2.2.

Table 2.1 Reagents used in the PCR reaction for amplification of aptamers.

Reagent	Final Concentration
10x Taq Buffer	1x
Deoxynucleotide Solution (10mM)	200µM
AptForward (100µM)	2µM
AptReverse (100µM)	2µM
Sample/ Aptamer Library (100µg/µl)	10µg/µl
$MgCl_2$ (25mM)	4mM
DMSO	5%
DNA Taq Polymerase (4U/µl)	0.02 U/µl

Table 2.2 PCR conditions for amplification of aptamer library.

Action	Time (sec)	Temperature (^oC)
Initial Denaturation	300	95
	Phase One (10 Cycles)	
Denaturation	30	95
Annealing	30	60 (decreased 1^oC/cycle)
Extension	30	72
	Phase Two (10 Cycles)	
Denaturation	30	95
Annealing	30	64
Extension	30	72
Final Extension	420	72

Confirmation of aptamer amplification was by visualisation of the PCR product on a 2% agarose gel, containing 0.005% Gel Red (see section 2.2.5) PCR products were pooled and concentrated by ethanol precipitation (see section 2.2.6).

2.2.2 Aptamer preparation

Concentrated PCR products (see section 1.2.4) were added to binding buffer (25mM glucose, 0.1% bovine serum albumin, 0.25mM $MgCl_2$ and 1x PBS), and heated to 95^oC for 5 minutes. The DNA aptamers were then snap cooled on ice for at least 10 minutes and kept on ice or at 4^oC until required.

2.2.3 Negative Selections

The DNA aptamer library and aptamers from each subsequent round were first incubated with HeLa cells, to ensure only aptamers that did not bind to HeLa cells were selected. HeLa cells were prepared for either room temperature or 4°C by first, washing in wash buffer (1x PBS, 25mM glucose, 0.25mM $MgCl_2$), before being re-suspended in 175µl binding buffer at the required concentration, approx. 60,000 cells/ml (total 10,000 cells). HeLa cells were then incubated for 1 hour at 4°C or room temperature on a rotor at 20rpm. Samples were then centrifuged at 570g the supernatant was removed and kept for positive selection, while the pellet containing the cells and any bound aptamers was discarded.

2.2.4 Positive Selections and controls

C. albicans and *S. cerevisiae* cultures were diluted to a concentration of $3x10^6$CFU/ml during exponential growth phase. Cells were then centrifuged at 2660g for 2 minutes, washed with washing buffer to remove any remaining YPD media, and then re-suspended in 175µl of binding buffer. *A. fumigatus* spores were prepared by using an inoculating loop to gently scrape the spores from the surface of the plate and re-suspend in binding buffer. Aptamers were incubated at 4°C to restrict active uptake processes in the cell, in order to select an aptamer which bound the cell wall. Room temperature selections were performed to allow these processes to happen, in order to find an aptamer that is internalised by the cell.

The supernatant from the negative selection was incubated with either C. *albicans* or A. *fumigatus* for 1 hour at 4°C or at room temperature on a rotor spinning at 20rpm. After incubation cells were washed 5 times with washing buffer, to remove any unbound aptamers, before being resuspended in 200µl of dH_2O and heated at 95°C for 10 minutes to elute bound aptamers. The samples were centrifuged at 15,000g for 1 minute and the supernatant retained. A test PCR was initially conducted to ensure elution of aptamers, before further amplification by PCR, purification and concentration, by ethanol precipitation. The resulting

PCR product was continued into subsequent rounds of selection (see section 1.2). A total of 10 rounds of SELEX were completed for each condition (represented in figure 2.1).

To ensure no amplification of non-specific sequences, the experiment was also undertaken with aptamer alone and fungal cells alone. When visualising resulting PCR products from each elution (see section 2.2.5), if a band was seen in either control this would indicate non-specific amplification and the round of SELEX was repeated from the previous round's elution.

2.2.5 Separation, Visualisation and Purification of PCR products

PCR products were run on a 2% agarose gel prepared with 1x TAE buffer (1.85M Tris, 45mM EDTA and 1M glacial acetic acid), containing 0.002% Gel Red. Samples were prepared by mixing with 1x Orange G (0.2% Orange G, 4% glycerol) and then run at 100volts on an agarose gel with a DNA ladder sample containing DNA fragments of a known size mixed (Thermo Scientific, UK). Gels were then imaged using UV light (Bio-Rad ChemiDoc XRS+ with Image Lab software). Successful amplification was determined by the presence of a band at approx. 105bp, with no bands present in the relevant controls. If non-specific bands were also observed within the reaction, the required band was purified by gel extraction using a Gel Extraction kit (Nucleospin Gel and PCR Clean-up, Machery-Nagel UK) as per the manufacturer's instructions. The final product was then diluted approx. 1/50 and used as a template for PCR amplification of the purified aptamers. The resulting PCR product was then concentrated by ethanol precipitation and continued into the next round of selection.

2.2.6 Ethanol precipitation of PCR products

Following PCR amplification, the purified aptamers were pooled and concentrated by ethanol precipitation. 1/10th the volume of 3M sodium acetate (NaAc) was added along with 2x volume of ice cold ethanol (100%) and incubated at -80°C for 1 hour. Samples were then centrifuged at 17,000g, 4°C for 10 minutes, the supernatant removed, and the DNA pellet washed with 70%

ethanol and centrifuged at 14,000rpm for 5 minutes. 70% ethanol was then removed, and the pellet re-suspended in dH_2O. Concentrations of each sample were determined using the Nanodrop 2000.

2.3 Cloning and Sequencing of Aptamers

2.3.1 Transformation and cloning of Aptamers

After 10 rounds of SELEX, purified DNA aptamers were ligated into a TOPO 2.1 vector (Invitrogen) as per manufacturer's instructions. These ligated plasmids were transformed into chemically competent DH5α *Escherichia coli* (E. *coli*) () (genotype: *F- φ80 (lacZ)ΔM15 ΔlacX74 hsdR (rk-, mk+) ΔrecA1398 endA1 tonA*) prepared by calcium chloride method. Cells were incubated on ice for 1 hour, heat shocked at 42ºC for 90 seconds, snap cooled on ice for 2 minutes and then recovered in LB media (63.5mM tryptone, 0.17 1M sodium chloride (NaCl), 0.5% yeast extract) at 37°C for 1 hour. Recovered E. *coli* were plated onto LB agar (LB broth, 1% agar) containing 25µg/µl ampicillin and incubated overnight at 37°C.

Colonies from the plates were re-suspended in dH_2O, and initially screened for correctly ligated inserts by colony PCR using M13 forward and reverse primers. Results were visualised on a 1% agarose gel (as per section 1.2.3).

Table 2.3 - Reagents used for colony PCR

Reagent	Final Concentration
10x Taq Buffer	1x
$MgCl_2$ (25mM)	0.5mM
dNTPs (10mM)	200µM
M13 forward or Aptfor (100µM)	2µM
M13 Reverse or Aptrev (100µM)	2µM
E. coli Sample	
DNA Taq Polymerase (4U/µl)	0.02U/µl

Table 2.4 – Colony PCR programme.

Action	Time (sec)	Temperature (°C)

Initial Denaturation	300	95
Denaturation	30	95
Annealing	30	45
Extension	30	72
Final Extension	420	72

Positive samples were checked with aptforward and aptreverse primers, then inoculated into LB media with 25µg/µl ampicillin and grown overnight at 37^{o}C with shaking at 180rpm. E. *coli* cells were then harvested by centrifugation at 10,000 x g and the plasmid purified as per manufacturer's instructions using a GeneJet Plasmid Miniprep Kit (Thermo Fisher Scientific). 30 cycles.

2.3.2 Sequencing of Aptamers

Purified plasmids were sent to Source Biosciences (Nottingham, UK) for Sanger sequencing, using M13 forward and reverse primers. Sequences were analysed using Clustal Omega (available at: https://www.ebi.ac.uk/Tools/msa/clustalo/) to determine sequence similarity. Structures of each DNA aptamer were predicted using Mfold software (available at: http://unafold.rna.albany.edu/?q=mfold/DNA-Folding-Form) under the conditions each aptamer binds to its target molecule in (137mM [Na^{+}], 0.25 mM [Mg^{++}] and at either 4^{o}C or 25^{o}C).

2.4 Testing of Purified aptamers

2.4.1 Aptamer Binding using PCR

Isolated aptamers were initially screened for their binding affinity and specificity via PCR. Aptamers were prepared, at a final concentration of 50nM - 200nM, (see section 2.2.2) and incubated for 30 minutes with C. *albicans*, S. *cerevisiae* and A. *fumigatus* separately at either 4^{o}C or room temperature Cells were washed 5 times with washing buffer and resuspended in 200µl of dH_2O. Bound aptamers were eluted by heating to 95°C for 10 minutes and underwent PCR (as described in section 1.2.2). PCR products were then visualised on 2% agarose gel,

alongside 95ng of aptamer library, concentration of 23.75ng/µl. Gels were then analysed by, Bio Rad Chemidoc XRS+, Image Lab+ software and the amount of DNA aptamer from each sample calculated by comparison to the intensity of the band from the aptamer library sample. The exposure time for each image was 0.5 seconds.

2.4.2 Fluorescence microscopy

Isolated aptamers were ordered tagged at the 5' end with a fluorescent tag, either Alexa 488 or Cy5, from IDT (UK). These aptamers were prepared as previously described (section 1.2.2) to a concentration of 200nm and incubated for 30 minutes, at either 4^{o}C or RT with the relevant fungal species (as per section 2.1.1). Cells were then washed five times with washing buffer before being fixed in 3.7% formaldehyde (37% fomaldehyde, 1x PBS) for 15-20 minutes at room temperature, washed with 1x PBS and re-suspended in vectashield with DAPI for mounting onto slides. Cells were then imaged using Zeiss Fluorescent Microscope. For each slide a representative sample was imaged with a Brightfield, DAPI, Alexa 488 and Cy5 filter with a 1.2 second exposure time.

3.0 Results

3.1 Selection of aptamers against *Candida albicans* and *Aspergillus fumigatus* with different incubation conditions.

The SELEX process was previously adapted from the protocol established by Sefah et al. (2010), and optimised to select aptamers specific for the fungi, *C. albicans* and *A. fumigatus*. The SELEX process was carried out at either 4°C or room temperature. This was to enable selection of aptamers specific to either the outside of the cell (wall and membrane) or those internalised into the cell, due to the changes is membrane fluidity caused by the differences in temperature, and the activity of uptake processes in to the cell. After initial amplification, by PCR, and concentration, via ethanol precipitation, the aptamer library was first incubated at 4°C or room temperature for 1 hour with HeLa cells, as a negative selection. Due to the similarities between these eukaryotic species, mammalian cells were used as a negative selection in order to select aptamers more specific to fungal species. Any unbound aptamers were then incubated with the appropriate fungal species at either 4^{o}C or RT, along with controls containing no aptamer to ensure that any amplification is not due to non-specific DNA. At the end of each round of selection, a test PCR was conducted on the elution and the amplified aptamers, of 105bp in size, were purified by gel extraction. This ensured only aptamers of the correct size were amplified and carried through to subsequent rounds of SELEX. Ten rounds of selection were undertaken for each condition and fungal species. Figure 1, shows the PCR amplification from the elution following each round of selection in *C. albicans* and Figure 2 shows this for *A. fumigatus*.

(A) ***Candida albicans* 4°C**

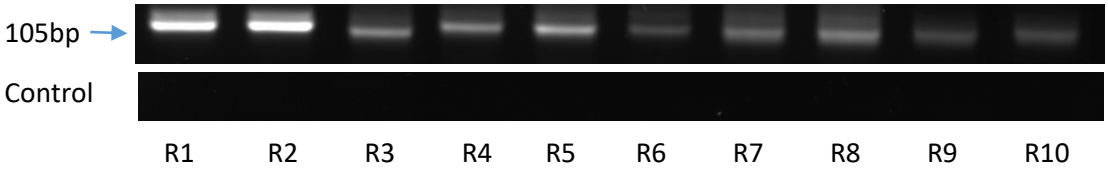

(B) ***Candida albicans* Room Temperature**

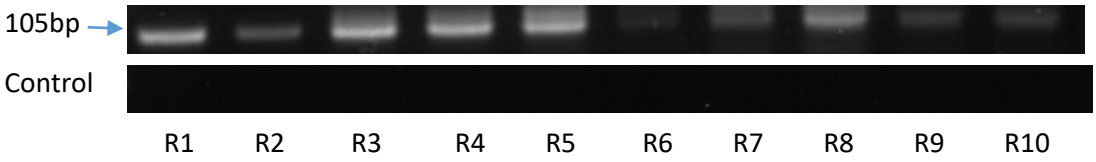

Figure 3.1. Amplification of aptamers from SELEX rounds 1 to 10 of selection in *Candida albicans* at 4°C and room temperature. Aptamer library (round 1) or product from the previous round of selection (each subsequent round) was incubated for 1hr with *C. albicans* at either 4°C (A) or room temperature (B) and a control with no aptamer. Cells were washed and any bound aptamer eluted. A PCR from a sample of each elution was undertaken and run on a 2% agarose gel, imaged at an exposure of 500ms using BioRad ChemiDoc XRS+ Image Lab software.

(A) *Aspergillus fumigatus* 4°C

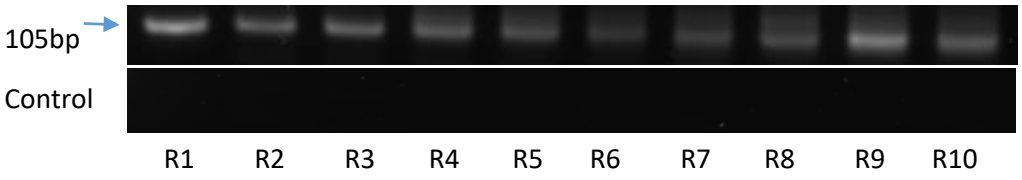

(B) *Aspergillus fumigatus* Room Temperature

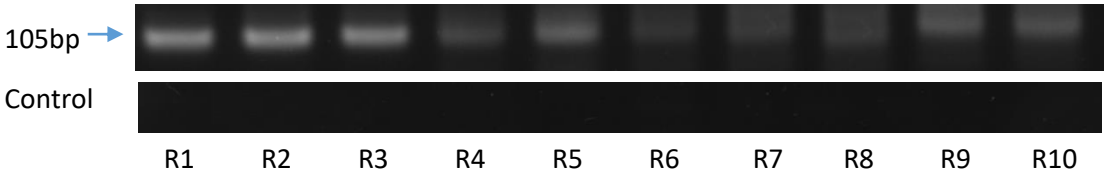

Figure 3.2. Amplification of aptamers from SELEX rounds 1 to 10 of selection in *Aspergillus fumigatus* at room temperature and 4°C. Aptamer library (round 1) or product from the previous round of selection (each subsequent round) was incubated with *A. fumigatus* spores at either 4°C (A) or room temperature (B) and a control with no aptamer. Cells were washed and any bound aptamer eluted. A PCR from a sample of each elution was undertaken and run on a 2% agarose gel, imaged at an exposure of 500ms using BioRad ChemiDoc XRS+ Image Lab software.

Figures 3.1 and 3.2 show the PCR product from each round of selection at 4°C (A) and room temperature (B) along with the no aptamer control from each round. The presence of bands on the agarose gel was used to preliminarily determine whether aptamers had been isolated and whether the amount eluted from cells was sufficient to continue to the next round. The controls were used to confirm the lack of non-specific DNA amplification. In all cases no band was detected in the control indicating that the amplified band was due to the presence of aptamers. For round 1 (figure 3.1A and B and figure 3.2A and B), a clear band at 105bp indicates amplification of aptamers following PCR. The overall intensity of this band decreases for each subsequent round of selection with slight increases in rounds 5, 7 and 8 for figure 1A and rounds 3, 4 and 8 for figure 3.1B. For figure 3.2A the intensity decreases up until round 9, where there was a slight increase, which then decreased again at round 10. Figure 2B shows more of a steady decrease throughout the rounds. Despite the varying intensities, it is still evident that following round 10 of SELEX all conditions have produced elutions that contain aptamers isolated against the target cells through each round of selection.

3.2 Isolation and Sequencing of Aptamers

To isolate these individual aptamers, the PCR product from round 10 was ligated into the TOPO cloning vector (Invitrogen), which relies on the A overhang added by Taq polymerase. After ligation, the resulting plasmids were transformed into chemically competent DH5α *E. coli*. Colonies were grown and selected, before the plasmids were purified. The resulting plasmids were then tested for successful cloning of the aptamer insert by PCR using aptForward and aptReverse primers. The resulting PCR products were run on a 2% agarose gel and visualised using GelRed, positive plasmids give a product of 105bp, as shown in Figure 3.3.

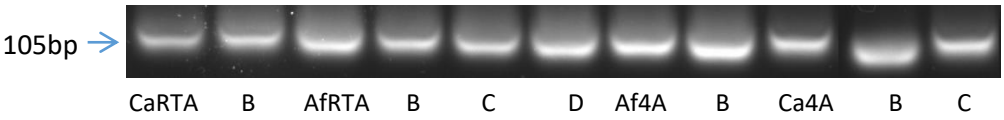

Figure 3.3. Successful cloning of aptamer sequences into TOPO vector was confirmed by PCR. A sample was taken of each mini prep and tested by PCR using aptForward and aptReverse primers, all 11 samples were tested and all 11 were positive for an aptamer insert. CaRTA and B were positive colonies from *C. albicans* at room temperature, AfRTA, B, C and D were positive colonies from *A. fumigatus* at room temperature. Af4A and B were positive colonies from *A. fumigatus* at 4°C and Ca4A, B and C were positive colonies from *C. albicans* at 4°C.

11 colonies in total were obtained and tested, resulting in 3 positive colonies for *C. albicans* at 4°C, 2 positive colonies for *C. albicans* at room temperature, 2 positive colonies for *A. fumigatus* at 4°C and 4 positive colonies for *A. fumigatus* at room temperature. Each positive plasmid was then sent for sequencing using the M13 reverse primer.

Each sequence was then analysed, without the primer sequences, through Clustal Omega analysis software. The analysis from this software shows the similarities between the aptamers allowing for sequence comparisons. Sequences, with the primer sequences, were also analysed by Mfold analysis software to predict secondary folding structure of each aptamer, which is important for target binding.

(A)

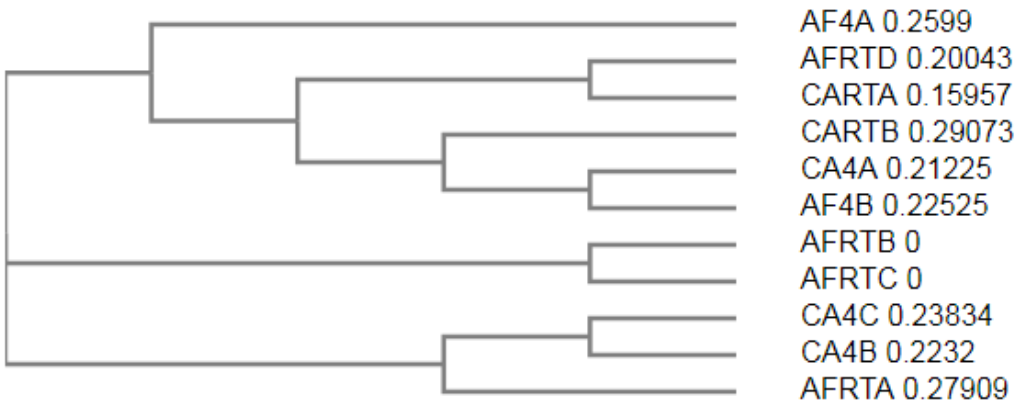
AF4A 0.2599
AFRTD 0.20043
CARTA 0.15957
CARTB 0.29073
CA4A 0.21225
AF4B 0.22525
AFRTB 0
AFRTC 0
CA4C 0.23834
CA4B 0.2232
AFRTA 0.27909

(B)

```
AF4A       -------GCGGGAGAGAATTCAACAACAATGC-AGTCCAGGGACAGAGACAGACAGCAACACGA----------AGCTCCACG---------
AFRTD      ----CCGACGACAGAGTAAGGGGG-GAC--------AATCAGACAG---GAATGACAGGGACAAC----------------------G--
CARTA      ----CGAGAGGGAGAGAGAGGGAGAGAGAGGCAGAGACAGAGACAGAGAGAAAGAGAGAGACAATTCTGCGGTAAACTCGAAGGACAGCC--
CARTB      ----------------------------AGGCAGGAGGGAGATGAGGAGTGGTGAGCGGGATAAGCGTGGGGAG---AGCGGTG--------
CA4A       --------------------GGGCACACGAACAGAAGCGGCAAGACAAGGGGGGAATAACACAAGACGAAGGACCAGGCACGTG--------
AF4B       -------------------AGGCAAGACAAACAAGAGCGAACAGGGAACGGAAA-------------AGCGAACAATGCAC-----------
AFRTB      --------GGGGAGAGGATTCTGGGCACAAGCGAATTTATATAAAGCCCGGCTC--------------------AACTGGCAAAGCAATCGG
AFRTC      --------GGGGAGAGGATTCTGGGCACAAGCGAATTTATATAAAGCCCGGCTC--------------------AACTGGCAAAGCAATCGG
CA4C       TGCCTGGTGTTGTGATTGTCCCCCCCTCGTTG------TTGTTCCCGTGTGCTG--------------------TGC---CGTT--------
AFRTA      --CCTAATACGACTCACTATCCTAA----TACGACTCACTATCCACACGCACAT--------------------CAC--CCGTTG-------
CA4B       ---CTGGTCGTGATTGTTTTCCTTATTTGTTCGTCTTCTTATCCCCACCTTCTC--------------------TTT--GCGTG--------
```

(C)

Aptamer	% Similarity										
	Af4A	AfRTD	CaRTA	CaRTB	Ca4A	Af4B	AfRTB	AfRTC	Ca4C	AfRTA	Ca4B
Af4A	100	37.78	60.00	34.15	32.69	29.27	44.44	44.44	23.40	34.69	30.19
AfRTD	37.78	100	64	42.31	42.42	43.48	45.71	45.71	25	17.14	26.32
CaRTA	60	64	100	39.62	42.19	44.90	45.16	45.16	15.69	25.45	22.41
CaRTB	34.15	42.31	39.62	100	47.17	40.54	24.24	24.24	41.67	20	19.35
Ca4A	32.69	42.42	42.19	47.17	100	56.25	29.55	29.55	31.43	31.58	23.81
Af4B	29.27	43.48	44.90	40.54	56.25	100	35.71	35.71	12.12	27.78	20
AfRTB	44.44	45.71	45.16	24.24	29.55	35.71	100	100	31.91	33.33	38.89
AfRTC	44.44	45.71	45.16	24.24	29.55	35.71	100	100	31.91	33.33	38.89
Ca4C	23.40	25	15.69	41.67	31.43	12.12	31.91	31.91	100	36.73	53.85
AfRTA	34.69	17.14	25.45	20	31.58	27.78	33.33	33.33	36.73	100	49.09
Ca4B	30.19	26.32	22.41	19.35	23.81	20	38.89	38.89	53.85	49.09	100

Figure 3.4. Analysis of aptamer sequences via Clustal Omega (A) Phylogenetic tree of isolated aptamer. Isolated sequences from the SELEX process were put through Clustal Omega software (primer sequences removed) and sequences compared for similarity shown as a phylogenetic tree. **(B) AlignMent of isolated aptamer sequences.** Clustal Omega ouput of sequences aligned. **(C) Percentage similarity of all isolated sequences.** Clustal Omega output of similarity of sequences expressed as percentage values between each sequence.

The phylogenetic tree (figure 3.4A) groups aptamers together based on their similarities in sequences. Sequences were grouped into three main families, which may suggest three distinct epitopes. The first branch contains 6 aptamers, the second branch contains 2 aptamers of the same sequence, AfRTB and AfRTC, and the third branch which contains 3 aptamers. Within the first branch, AFRTD and CARTA are more closely related, as are CA4A and AF4B. In the third branch, CA4C and CA4B are more closely related to each other than AFRTA. Based on the sequence homology, the majority of aptamers showed less than 60% similarity (Figure 3.4B and 3.4C) Ca4C and Af4B show the largest difference with only 12.12% similarity. Within each SELEX condition sequences show varying amounts of similarity. *C. albicans* at 4°C isolated sequences Ca4B and Ca4C show 53.85% similarity but only 23.81% (Ca4B) and 31.43% (Ca4C) to Ca4A. *C. albicans* at room temperature isolated sequences CaRTA and CaRTB show 39.62% similarity, with similar sequence alignments both showing long sequences rich in A and G. However CaRTA is 33 bases longer. Between the 2 conditions again shows varying similarity, with the most similar being Ca4A and CaRTB at 47.17% similarity and the least being Ca4C and CaRTA with a 15.69% similarity. Aptamers selected at room temperature against *A. fumigatus* again show varying levels of similarity with the largest similarity (excluding the 100% similarity between AfRTB and AfRTC) between AfRTB/C and AfRTD at 45.71%, followed by AfRTA and AfRTB/C at 33.33% and finally the lowest similarity between AfRTD and AfRTA at 17.14%. For selection in *A. fumigatus* at 4°C Af4A and Af4B shared a 29.27% similarity.

Figure 3.4B shows the sequence alignments generated by clustal omega, which demonstrates there were very few conserved regions between all aptamers. However, based on the phylogenetic mapping a number of aptamers were found to be closely associated. Therefore, these sequences were analysed separately (Figure 3.5A).

Figure 3.5. Alignment of isolated aptamer sequences using Clustal Omega. (Alignment of two aptamers) (A) AFRTD and CARTA (B) CA4A and AF4B (C) CA4C and CA4B. Conserved regions are indicated in yellow and with a *.

Based on the phylogenetic tree, the closely related sequences AFRTD and CARTA showed 32 consensus bases, with one group of 6, one group of 5 and two groups of 4 conserved bases (Figure 3.5A). CA4A and AF4B, were also shown to be closely related showing 26 consensus bases, with one group of 5 and one group of 4 conserved bases (Figure 3.5B). Finally, CA4C and CA4B showed 25 consensus bases, with one group of 5 conserved bases (Figure 3.5C).

3.3 Predicted Aptamer Folding structures.

(A) **Sequences from *C. albicans* at 4°C predicted folding structure.**

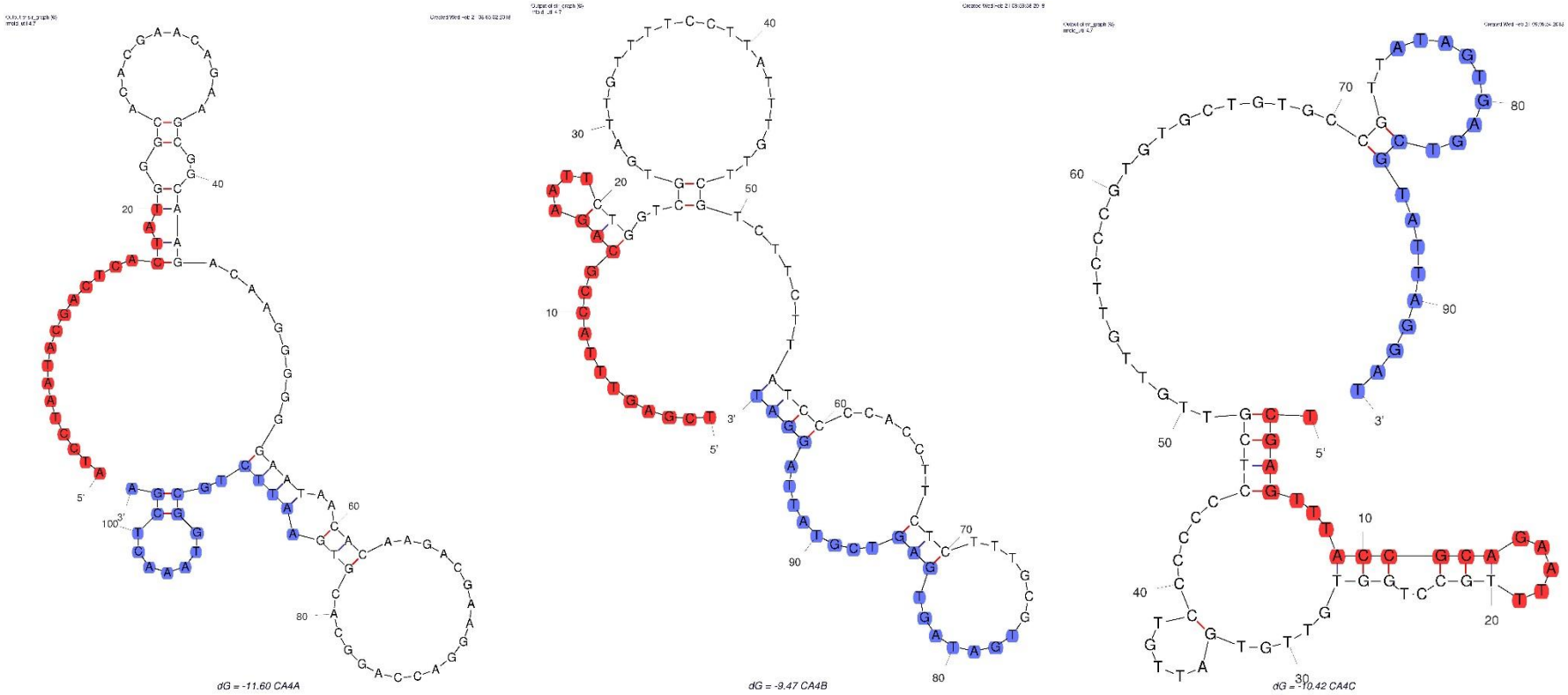

(B). Sequences from *C. albicans* at room temperature predicted folding structure.

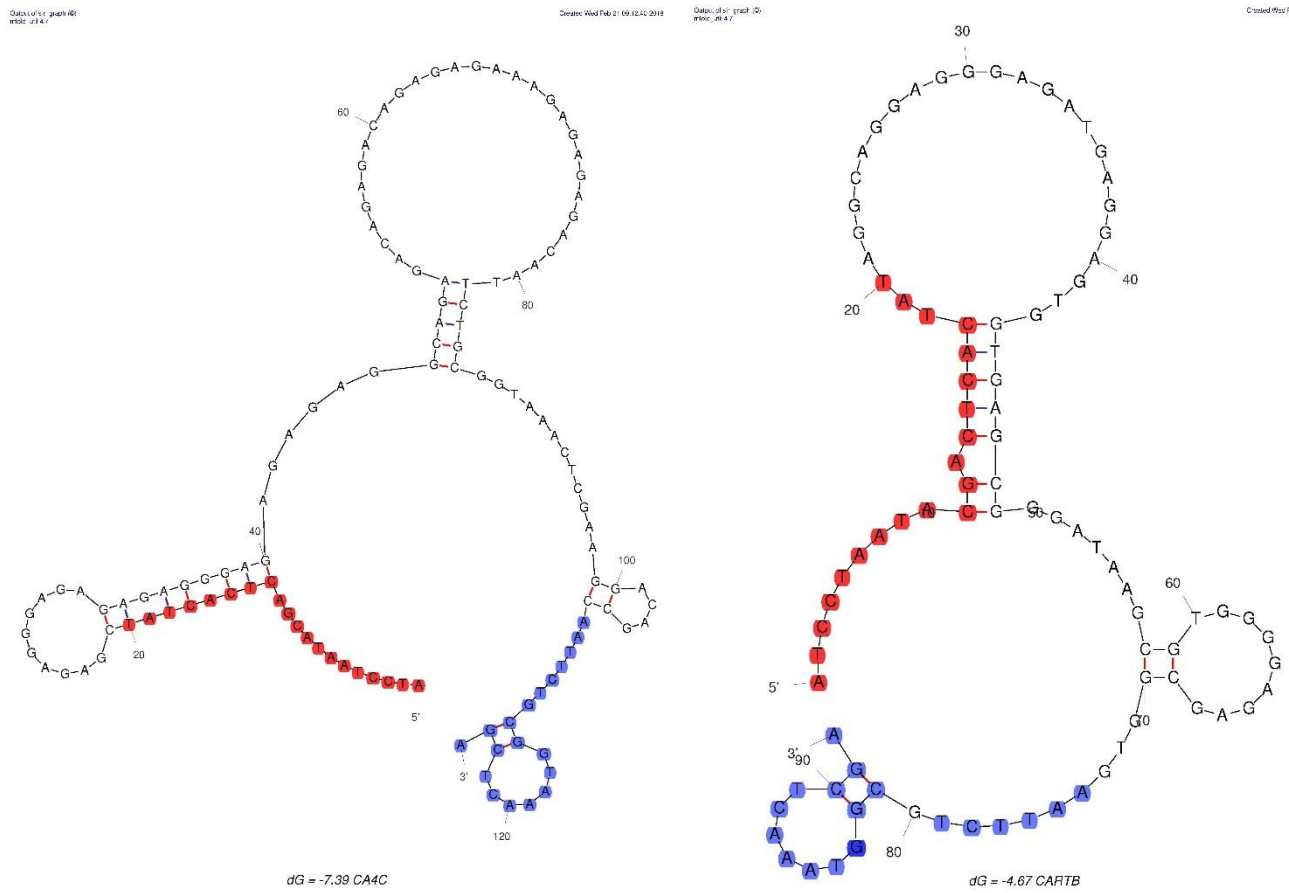

(C). Sequences from *A. fumigatus* at 4°C predicted folding structure.

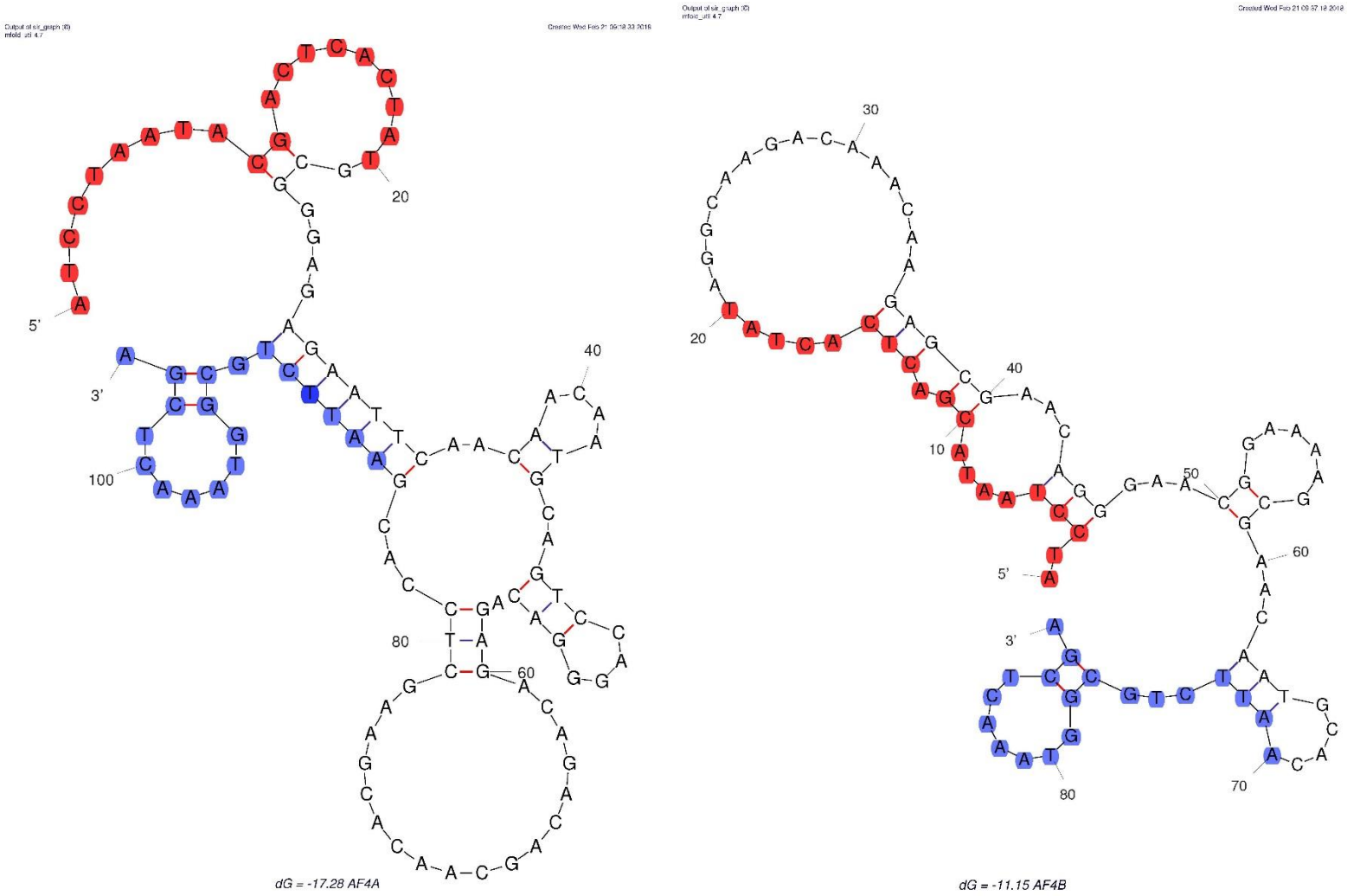

(D). Sequences from *A. fumigatus* at room temperature predicted folding structure.

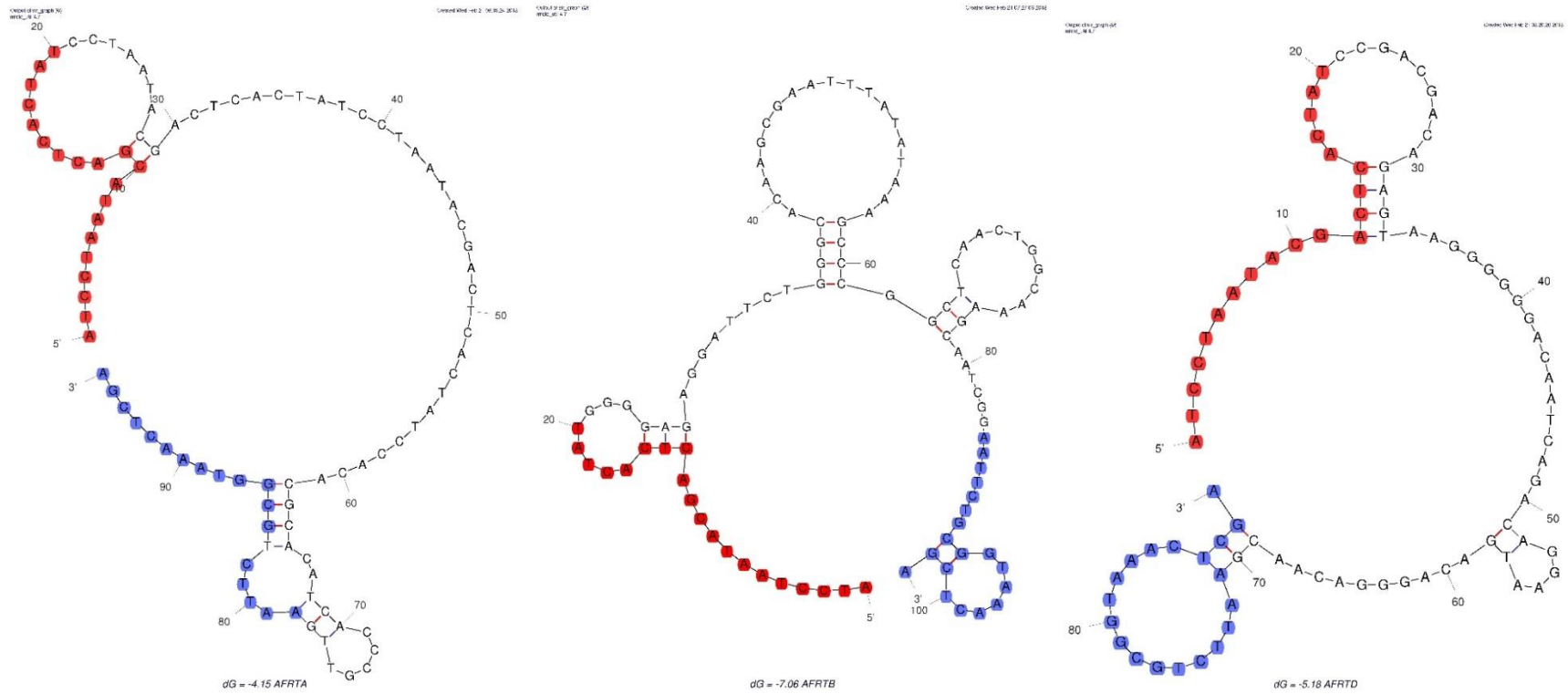

Figure 3.6. Structure Analysis of Aptamer Sequences via Mfold (A) Sequences from *C. albicans* at 4°C predicted folding structure. (B) Sequences from *C. albicans* at room temperature predicted folding structure. (C) Sequences from *A. fumigatus* at 4°C predicted folding structure. (D) Sequences from *A. fumigatus* at room temperature predicted folding structure. All sequences were analysed using Mfold software and folding structure predicted based on SELEX conditions (Na+ 137mM and Mg++ 0.25mM) and 4°C or room temperature based on which SELEX condition. Structures shown are those with the lowest predicted Gibbs free energy. Aptforward primer sequences are highlighted in red and Aptreverse sequences highlights in blue.

3.4 Characterisation of Isolated Aptamer

Aptamers are strands of DNA that are able to fold into a 2D stable structure through complementary base pairing. By predicting the secondary structure of the aptamer, the bases available to bind to the target can be identified. Sequences were analysed using Mfold software and the folding structure based on conditions for each selection (Na+ 137mM and Mg++ 0.25nM and either 4°C or room temperature). These were set by ion concentrations contained within the binding buffer used for incubating aptamers with target cells.

For each structure, the Gibbs free energy (ΔG) is determined, which refers to the amount of energy needed to disrupt the structure and break the bonds formed in each strand of DNA. The structure with the lowest Gibbs free energy was selected as this is most likely structure for the strand to form naturally.

The structures of each aptamer show large similarities within each condition. Both aptamers Ca4B and Ca4C (figure 3.6A) have large loop regions and Ca4A (figure 3.6A) a smaller loop region and have the highest ΔG compared to aptamer structures from the other SELEX conditions. Aptamers from *C. albicans* selections at room temperature (figure 3.6B) again show similarities in structure, both consisting of a larger loop region with 3 stem and loop structures. The predicted secondary structures of aptamers from *A. fumigatus* at 4°C (figure 3.6C) have the lowest ΔG value compared to other conditions. Af4A and Af4B have larger portions of stem structures than other structures. This is stark contrast to aptamers selected against *A. fumigatus* at room temperature (figure 3.6D), which comprise of much larger loop regions with few stem portions. There appear to be no major consistencies between the selection temperature or what species the aptamer was selected against, with the exception of Ca4C which shares more similarities in the large central loop region, branching of with smaller stem loop regions with aptamers AfRTB and AfRTD.

To confirm whether the aptamers where able to bind to the target cells they were isolated against, the purified aptamers were tested to confirm binding and specificity using PCR. All aptamers were amplified by PCR and tested at a concentration of 200nM, as described by Apetkhar *et al.* (2015), both at room temperature and 4°C Aptamers were incubated with each cell type at the required temperature for 30 mins. The reduced incubation time ensured that only aptamers with high affinity to the target were identified. Following incubation, aptamers were eluted from the cells and amplified by PCR before being analysed by gel electrophoresis. Concentration of the amplified aptamer was determined by comparison to a sample of known concentration on the same gel and analysed using ChemiDoc XRS+ software. It was assumed that the concentration of aptamer, following PCR, would be related to the amount of aptamer that bound to the cells. For each species incubated with the various aptamers a previously identified aptamer (C9 for *C. albicans* and Af20 for *Aspergillus*) for that species was also incubated to act as a positive control and a sample with no aptamer as a negative control. Each aptamer was tested twice and the results averaged, and standard error expressed as error bars on each graph. Figure 7 shows the concentration of aptamer in a PCR sample following incubation with *C. albicans* at both 4^{o}C and room temperature.

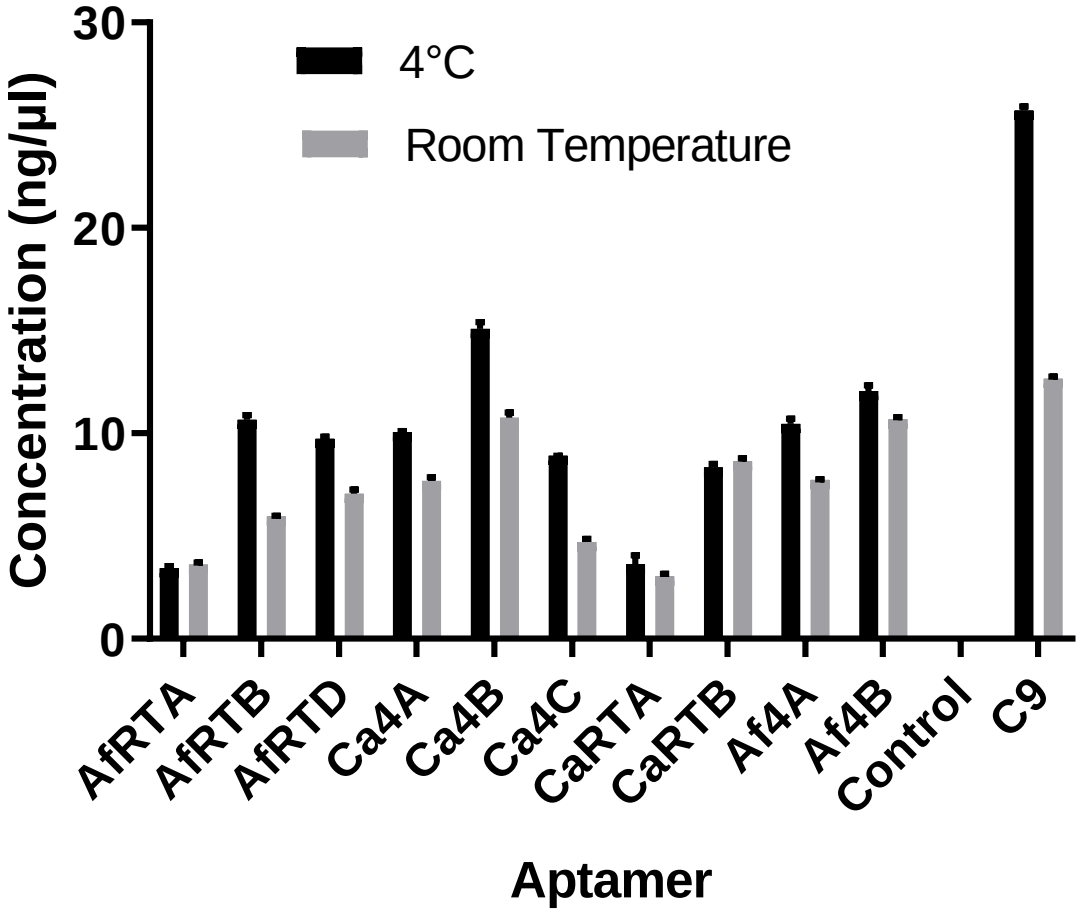

Figure 3.7 Average binding of identified aptamers against *C. albicans* at 4°C and room temperature. 200nM of each identified aptamer was incubated with *C. albicans* for 30 minutes either at room temperature or 4°C, and bound aptamers eluted. Eluted aptamers were amplified by PCR using aptfor and aptrev primers, before being analysed on a 2% agarose gel using a BioRad ChemiDoc XRS+ system with a 500ms exposure. The concentration of amplified aptamer was measured by comparison to a sample of aptamer at a concentration of 171ng/µl. Intensity of the band of DNA was measured by BioRad Image Lab software, and compared to the sample of known concentration to determine the amount of DNA in each band. Repeated twice. Control was a sample of cells incubated with no aptamer, and C9 (a previously identified aptamer) an aptamer with known affinity for *C. albicans*.

Aptamers selected at 4°C for *C. albicans* showed recovery of varied concentrations of aptamer following amplification. Shown in figure 3.7, Ca4B showed the highest concentration following incubation at both at 4°C, 15ng/µl, and room temperature, 10.7ng/µl. Ca4A yielded 10.1ng/µl at 4°C and 7.9ng/µl at room temperature and Ca4C showed the lowest concentration with 8.9ng/µl at 4°C and 4.7ng/µl at room temperature. In all cases, the higher level of binding at 4°C aligns with the selection conditions for these aptamers. Those aptamers selected at room temperature, showed little difference in binding when selected against *C. albicans* at either temperature, CaRTA resulted in a concentration of 3.6ng/µl at 4°C and 3.ng/µl at room temperature and CaRTB 8.3ng/µl at 4°C and 8.6ng/µl at room temperature. Overall, binding of the aptamers selected against *C. albicans* at 4°C was higher than those at room temperature. The 4°C selected aptamers, AF4A and Af4B, both showed binding to *C.albicans* cells at both temperatures. Concentrations of these aptamers following PCR were 10.5ng/µl (4°C) and 7.7ng/µl (RT) for Af4A and 12.1 ng/µl (4°C) and 10.7ng/µl (RT) for Af4B. These were similar levels as seen with Ca4A, Ca4B and CaRTB specifically selected against *C. albicans*. For those *A. fumigatus* aptamers selected at room temperature, AfRTA showed limited binding to *C. albicans* cells, however, AfRTB (10.7ng/µl – 4°C and 6ng/µl – RT) and AfRTD (9.7ng/µl – 4°C and 7.1ng/µl – RT) showed similar levels to the *C.albicans* specific aptamers Ca4A, Ca4C and CaRTB. Aptamers selected against *A. fumigatus* at 4°C showed similar yields to aptamers selected against *C. albicans* at 4°C, with a yield of 10.5ng/µl for Af4A at 4°C and 7.7ng/µl at room temperature and for Af4B, 12.1ng/µl at 4°C and 10.7ng/µl at room temperature. AfRTA yields the least amount of aptamer with 3.4ng/µl at 4°C and 3.6ng/µl at room temperature, whereas AfRTB (10.7ng/µl at 4°C and 6ng/µl at room temperature) and AfRTD (9.7ng/µl at 4°C and 7.1ng/µl at room temperature) show yields more consistent with most other aptamers. As with the *C. albicans* selected aptamers; higher concentrations of *A. fumigatus* aptamer was consistently seen when cells were incubated at 4°C, suggesting better affinity for the target. In all cases, the positive control aptamer (C9) showed significantly higher DNA levels than the test aptamers.

Figure 3.8 shows the concentration of aptamer in a PCR from a sample of elution following aptamer incubation with *A. fumigatus.* The aptamers selected against *A. fumigatus* AfRTB (16.854ng/µl at 4°C and 15.611ng/µl at room temperature) and AfRTD (12.998ng/µl at 4°C and 11.217ng/µl at room temperature) showed the best levels of biding for this condition with the levels of binding from AfRTB the most comparable to the control Af20. AfRTA only yielded 5.502ng/µl and 4°C and 6.324ng/µl at room temperature. *A. fumigatus* selected aptamers at room temperature exhibited lower levels of binding than at 4°C (Af4A 10.464ng/µl at 4°C and 9.126ng/µl at room temperature. Af4B 9.927ng/µl at 4°C and 9.226ng/µl at room temperature) but better levels of binding than AfRTA. Aptamers selected against *C. albicans* at 4°C exhibited levels on binding similar to that of aptamers selected against *A. fumigatus* in either temperature condition. Ca4A yielded 11.165ng/µl at 4°C and 12.149ng/µl at room temperature, Ca4B yielded 7.686ng/µl at 4°C and 10.048ng/µl at room temperature and Ca4C yielded 9.215ng/µl at 4°C and 6.12ng/µl at room temperature following incubation with *A. fumigatus*. *C. albicans* aptamers selected at room temperature exhibited the overall lowest levels of binding to *A. fumigatus* with CaRTA as the lowest (3.363ng/µl at 4°C and 1.308ng/µl at room temperature) and CaRTB (4.834ng/µl at 4°C and 7.149ng/µl at room temperature) more comparable to AfRTA.

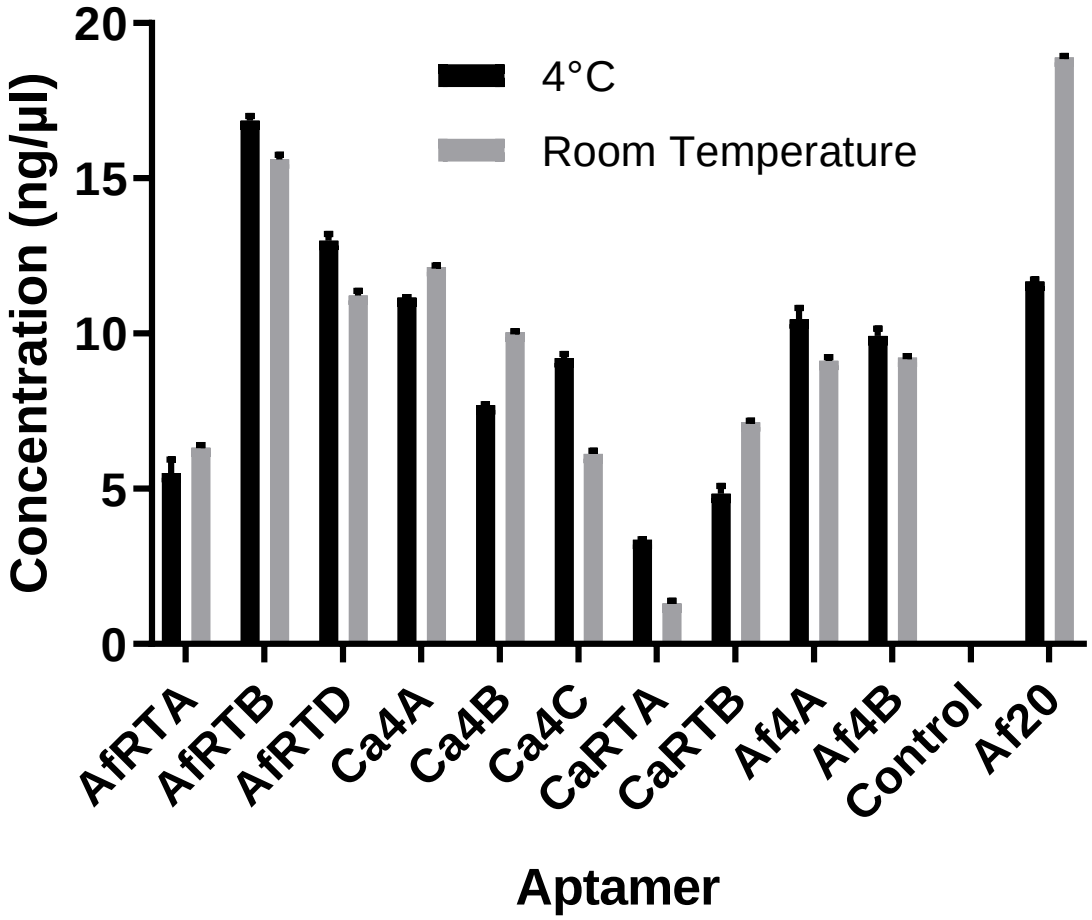

Figure 3.8. Average binding of identified aptamers against *A. fumigatus* at 4°C and room temperature. 200nM of each identified aptamer was incubated with *A. fumigatus* for 30 minutes either at room temperature or 4°C, and bound aptamers eluted. Eluted aptamers were amplified by PCR using aptfor and aptrev primers, before being analysed on a 2% agarose gel using a BioRad ChemiDoc XRS+ system with a 500ms exposure. The concentration of amplified aptamer was measured by comparison to a sample of aptamer at a concentration of 171ng/µl. Intensity of the band of DNA was measured by BioRad Image Lab software, and compared to the sample of known concentration to determine the amount of DNA in each band. Repeated twice. Control was a sample of cells incubated with no aptamer, and Af20 (a previously identified aptamer) an aptamer with known affinity for *C. albicans*.

Across both figures 3.7 and 3.8 there is little difference between the binding of aptamers at 4°C and room temperature regardless of which condition they were selected in. However, there are marked differences between the binding of certain aptamers in *A. fumigatus* and *C. albicans*. Aptamers selected against *C. albicans* Ca4B showed the highest concentration following incubation at both at 4°C, 15.081ng/µl, and room temperature, 10.772ng/µl in *C. albicans* but a concentration of 7.686ng/µl at 4°C and 10.048ng/µ incubated with *A. fumigatus.* Ca4A (*C. albicans* 10.071ng/µl at 4°C and 7.960 ng/µl at room temperature and *A. fumigatus* 11.165ng/µl at 4°C and 12.149ng/µl at room temperature) and Ca4C (8.904 ng/µl at 4°C and 4.715 ng/µl at room temperature and *A. fumigatus* 9.215ng/µl at 4°C and 6.12ng/µl at room temperature) show less affinity for *C. albicans*. For aptamers selected against *C. albicans* at room temperature there were lower levels of binding overall in addition to the lack of specificity (CaRTA *C. albicans* - 3.633 ng/µl at 4°C and 3.049 ng/µl at room temperature, *A. fumigatus* - 3.363ng/µl at 4°C and 1.308ng/µl at room temperature. CaRTB *C. albicans* - 8.341 ng/µl at 4°C and 8.649 ng/µl at room temperature and *A. fumigatus* - 4.834ng/µl at 4°C and 7.149ng/µl at room temperature). Aptamers that were selected against *A. fumigatus* at 4°C showed similarly low levels of specificity with Af4B (*C. albicans* - 10.466ng/µl at 4°C and 7.732ng/µl at room temperature and *A. fumigatus* - 9.927ng/µl at 4°C and 9.226ng/µl at room temperature) and Af4A incubated with *C. albicans* - 12.069 ng/µl at 4°C and 10.686ng/µl at room temperature and *A. fumigatus* - 10.464ng/µl at 4°C and 9.126ng/µl at room temperature) and consistent levels of binding. The most promising levels of specificity were exhibited by AfRTB (10.656ng/µl – 4°C and 5.951ng/µl – room temperature in *C. albicans* but 16.854ng/µl at 4°C and 15.611ng/µl at room temperature in *A. fumigatus*) followed by AfRTD (*C. albicans* - 9.738ng/µl at 4°C and 7.066ng/µl at room temperature and *A. fumigatus* - 12.998ng/µl at 4°C and 11.217ng/µl at room temperature). AfRTA however exhibited a low level of binding over all along with low specificity (*C. albicans* - 5.502ng/µl at 4°C and 6.324ng/µl at room temperature and *A. fumigatus* - 5.502ng/µl and 4°C and 6.324ng/µl at room temperature).

3.5 Further Testing of Shortlisted Aptamers

Aptamers shortlisted for further testing were AfRTB and Ca4B with results indicating that these were one aptamer for each species that exhibited the most promising specificity and levels of binding.

Shortlisted aptamers were further tested by determining their kd through testing binding levels from initial aptamer concentrations of 200nM, 100nM, 50nM and 25nM. This is to determine their affinity for their targets.

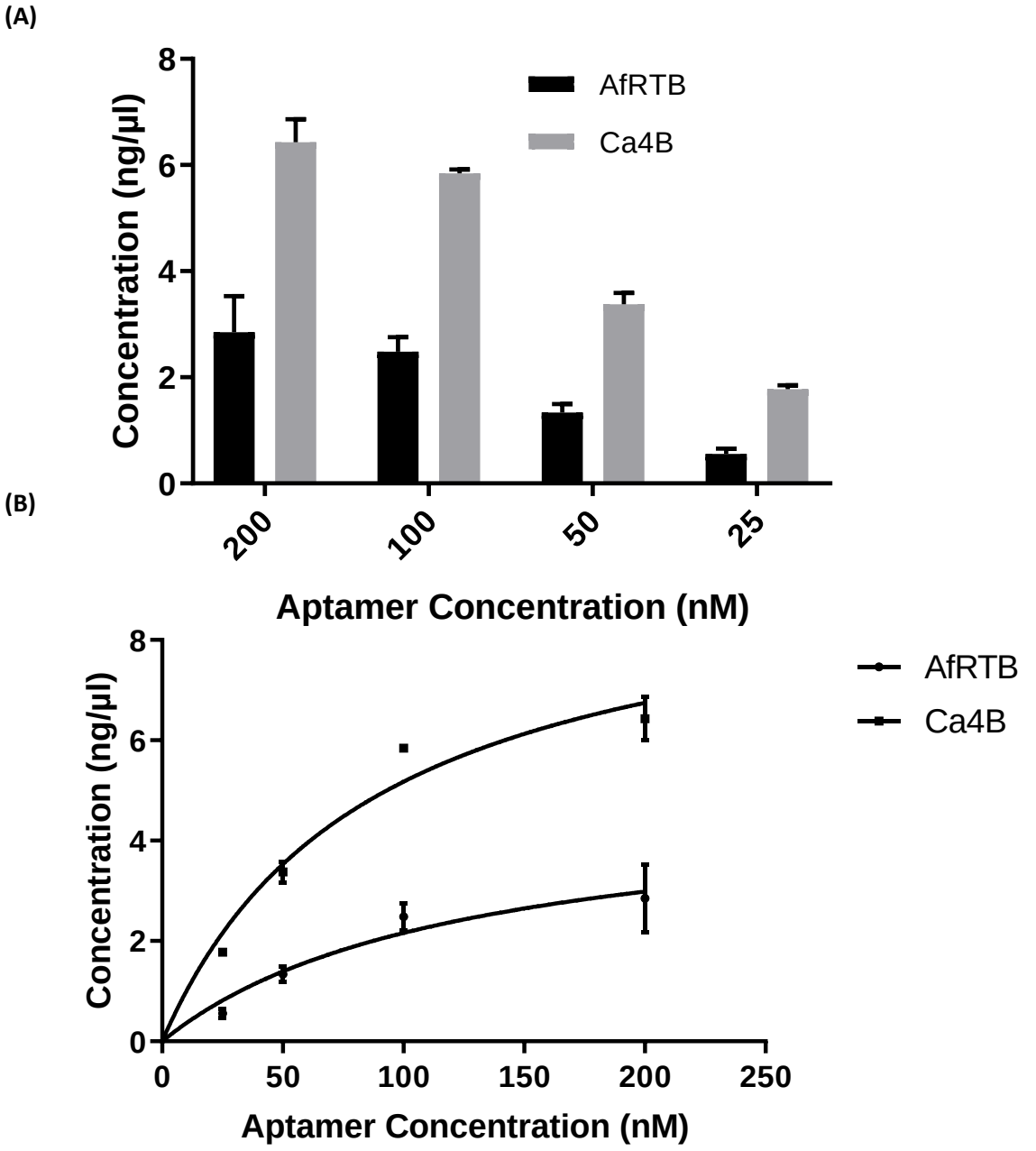

Figure 3.9. Binding of Aptamers, AfRTB and Ca4B, to *C. albicans* at a Variety of Concentrations. (A). Eluted aptamer, amplified by PCR (B) Binding Affinity of aptamer. Identified aptamers AfRTB and Ca4B were both incubated with *C. albicans* at a concentration of 200nM, 100nM, 50nM, and 25nM for 30minutes at room temperature. Aptamers were then eluted. These eluted aptamers were amplified by PCR using aptfor and aptrev primers, before being analysed on a 2% agarose gel using a BioRad ChemiDoc XRS+ system with a 500ms exposure. The concentration of amplified aptamer was measured by comparison to a sample of aptamer at a concentration of 171ng/µl. Intensity of the band of DNA was measured by BioRad Image Lab software, and compared to the sample of known concentration to determine the amount of DNA in each band.

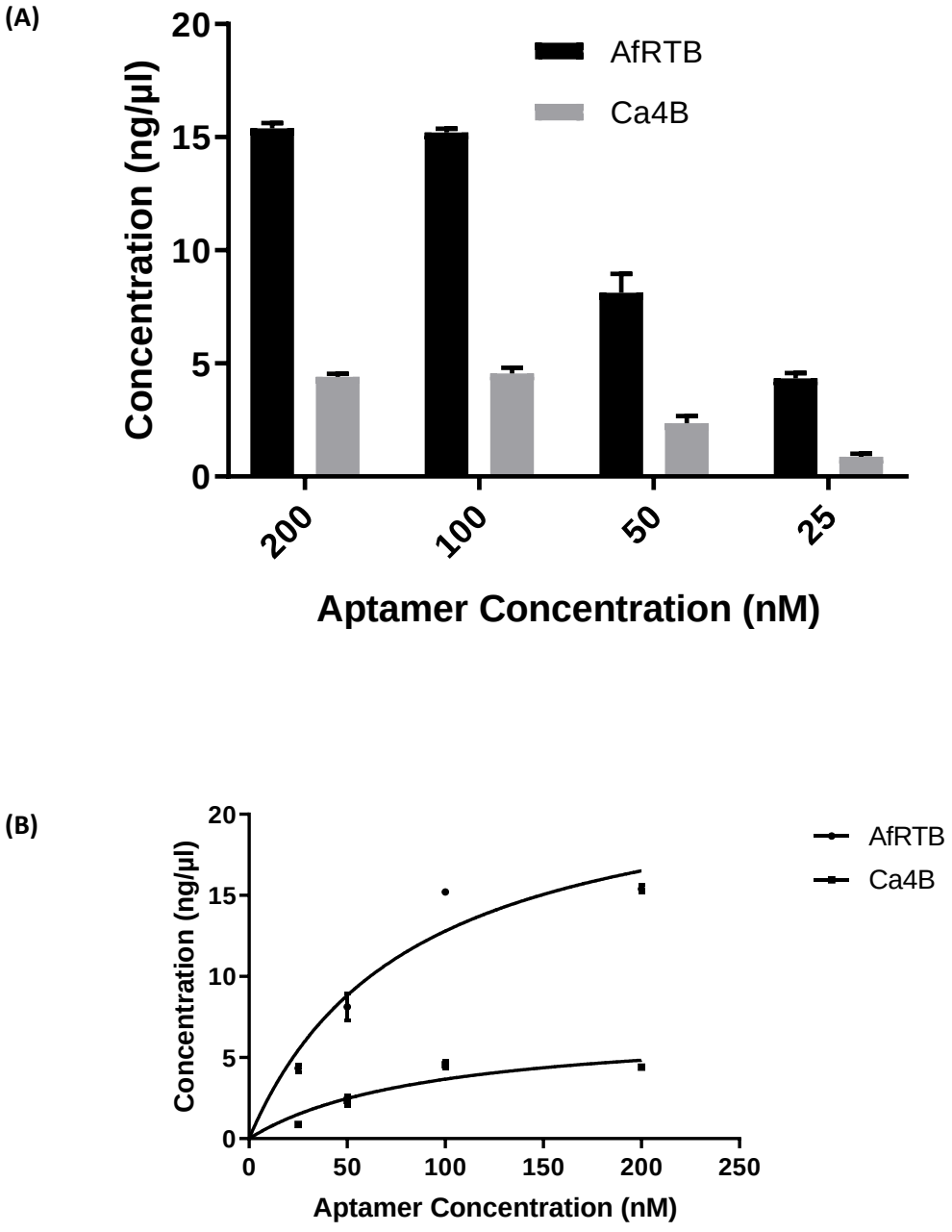

Figure 3.10. Binding of Aptamers, AfRTB and Ca4B, to *A. fumigatus* at a Variety of Concentration. (A) Eluted aptamer, amplified by PCR (B) Binding Affinity of aptamer Identified aptamers AfRTB and Ca4B were both incubated with *A. fumigatus* at a concentration of 200nM, 100nM, 50nM, and 25nM for 30minutes at room temperature. Aptamers were then eluted. These eluted aptamers were amplified by PCR using aptfor and aptrev primers, before being analysed on a 2% agarose gel using a BioRad ChemiDoc XRS+ system with a 500ms exposure. The concentration of amplified aptamer was measured by comparison to a sample of aptamer at a concentration of 171ng/µl. Intensity of the band of DNA was measured by BioRad Image Lab software, and compared to the sample of known concentration to determine the amount of DNA in each band.

Figure 3.9a shows a difference in the binding of AfRTB and Ca4B to *C. albicans* following incubation with varying concentrations of aptamer. The PCR product from *C. albicans* incubation with 200nM AfRTB yielded 2.8ng/µl of aptamer, whereas Ca4B incubated with *C. albicans* yielded 6.4ng/µl. This demonstrates a 3 fold increase in binding in *C.albicans* compared to *A. fumigatus*. As the concentration of AfRTB aptamer decreased, as did the amount of PCR product indicating that less aptamer is being isolated from the cells. However, there was still a clear trend of increased binding in *C. albicans* compared to *A. fumigatus*. Incubation of the aptamer at its lowest concentration of 25nM still displays the same trend with AfRTB yielding 0.5ng/µl, but Ca4B yielding 1.8ng/µl. The graph overall shows that incubation of both aptamers with *C. albicans* resulted in some degree of binding. However, Ca4B appears to show a much higher affinity for *C. albicans*, the target it was selected against with a Kd of 87.3nM whereas AfRTB has a Kd of 123.3nM.

In comparison, when AfRTB was incubated with its target cell (*A. fumigatus*), Figure 3.10, a higher level of binding was observed. 200nM of AfRTB incubated with *A. fumigatus* resulted in a concentration of 15.389ng/µl, this is in contrast to *C. albicans* where there was a 3 fold reduction in binding (Figure 9A) Decreasing the concentration of AfRTB to 100nM resulted in a similar concentration of aptamer being retained on the target cells. As the concentration of AfRTB reduced to 25nM, amplification of the aptamer from *A. fumigatus* was reduced to approximately 4.3ng/µl. A similar reduction trend was also seen in the levels of Ca4B bound to *A. fumigatus.* From this data the Kd of the aptamers was determined in *A. fumigatus*, with AfRTB showing a lower Kd 81.78nM with Ca4B showing a Kd of 93.43nM (Figure 9B).

Comparison of the Kd of the aptamers from each experiment (table 3.1), indicates that there is a clear difference between binding of each aptamer to their target. In *C.albicans* the Ca4B aptamer has a much lower Kd (87.3nM) than is seen in *A. fumigatus* (123.3nM), indicating a higher affinity for *C.albicans*. A similar trend is seen with the AfRTB aptamer when incubated with *A. fumigatus* (81.8nM) compared to *C. albicans* (93.3nM), which also indicates a clear affinity for the target cell.

Fungal species	Kd of Aptamer (nM)	
	Ca4B	**AfRTB**
C. albicans	87.3	93.4
A. fumigatus	123.3	81.8

Table 3.1 Summary of kd of shortlisted aptamers against each target cell. Ca4B and AfRTB were both incubated with both *C. albicans* and *A. fumigatus* at different concentrations. The table summarises data from figures 8B and 9B.

However, when comparing the results from figure 8 and 9, as previously observed, the overall level of aptamer binding is reduced in *C. albicans* compared to *A. fumigatus*, i.e. the highest level of binding in *C. albicans* was approx. 6ng/µl compared with 15ng/µl in *A. fumigatus*. In regards to Ca4B, this means the level of binding seen with the aptamer in *C.albicans* is similar to that in *A. fumigatus*. For example, at 200nM the concentration of aptamer obtained from *C. albicans* is 6.5ng/µl and in *A. fumigatus* it is 4.5ng/µl. This may mean that it would be difficult to identify *C. albicans* using the Ca4B aptamer within a mixed culture of both fungi, due to level of binding of this aptamer to both species, you would be unable to distinguish between them.

3.6 Fluorescence Microscopy

An alternatively way to determine binding of an aptamer to a target cell is visually with a microscopy using a fluorescently tagged aptamer. Both Ca4B and AfRTB were fluorescently tagged at the 5' end with Cy5 by PCR. After incubating 200nM of the tagged aptamers with both *C. albicans* and *A. fumigatus*, the cells were fixed, and mounted on slides with Vectashield mountant containing DAPI counterstain. These were then visualised using a Zeiss fluorescent microscope. Representative images are shown in Figures 3.11 and 3.12.

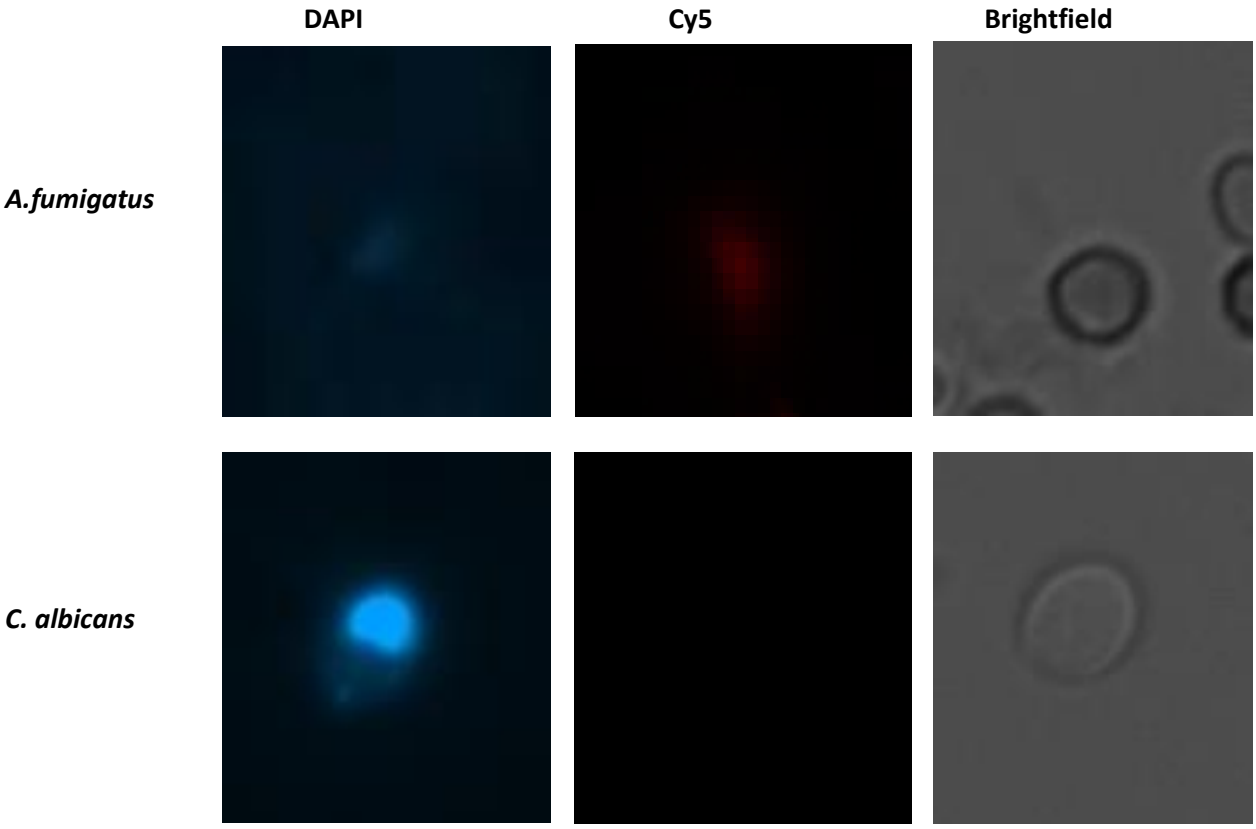

Figure 3.11. Cy5 labelled AfRTB incubated with *A. fumigatus* and *C. albicans.* Shortlisted aptamer AfRTB labelled with Cy5 fluorescent tag (IDT, UK) was incubated with *A. fumigatus* and *C. albicans* for 30 minutes at room temperature using an aptamer concentration of 200nM. Cells were fixed in 3.7% formaldehyde and washed with 1x PBS, before being resuspended in vectashield with DAPI for mounting onto slides. Slides were imaged using Ziess fluorescent microscope, using a DAPI, Cy5 and brightfield filter, exposed for 1.2 seconds.

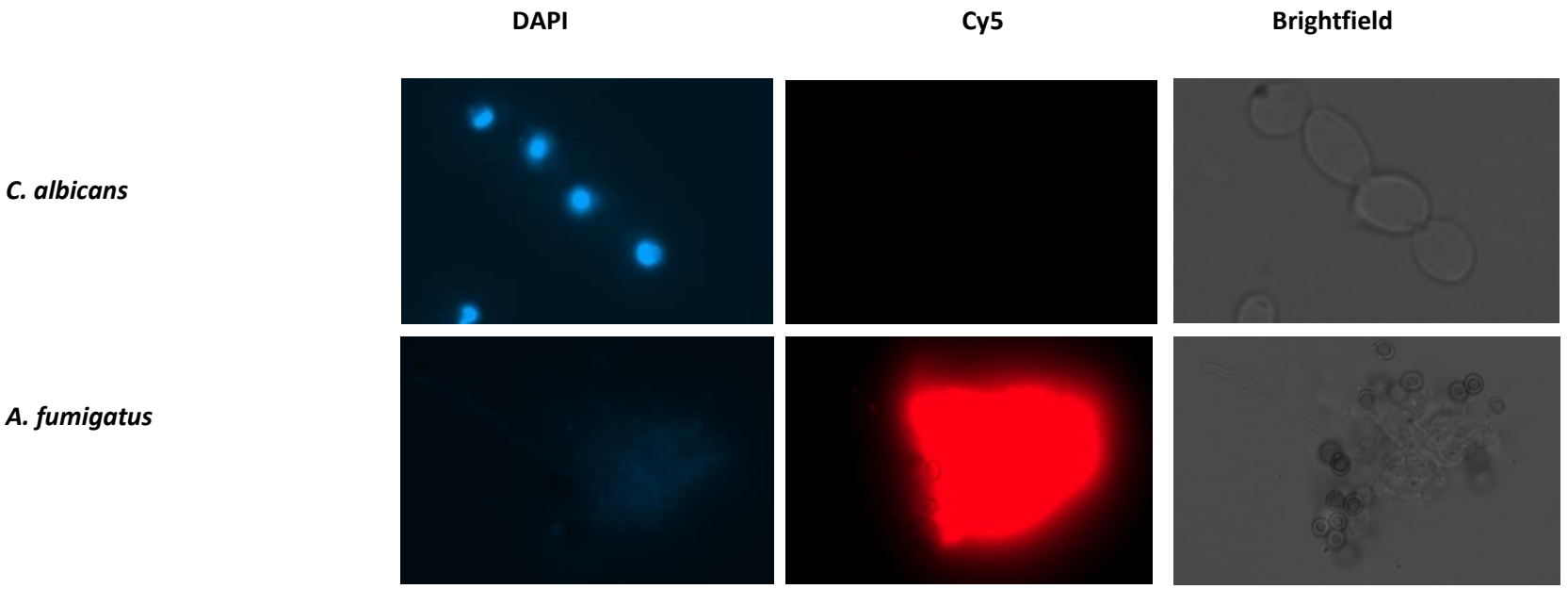

Figure 3.12. Cy5 labelled Ca4B incubated with *A. fumigatus* and *C. albicans*. Shortlisted aptamer Ca4B labelled with Cy5 fluorescent tag (IDT, UK) was incubated with *A. fumigatus* and *C. albicans* at room temperature for 30minutes at a concentration of 200nM. Cells were fixed in 3.7% formaldehyde and washed with 1x PBS before being resuspended in vectashield with DAPI for mounting onto slides. Slides were imaged using Zeiss fluorescent microscope, with DAPI, Cy5 and brightfield filters for an exposure of 1.2 seconds.

Figure 3.11 shows faint staining of *A. fumigatus* with AfRTB within the Cy5 channel, with no fluorescence observed in *C. albicans*. The data seems to suggest binding of AfRTB to its target cell and supports the PCR results (Figures 8A and 8B).

Figure 3.12 shows Cy5 bound Ca4B incubated with *C. albicans,* which seems to indicate no binding. However, when incubated with *A. fumigatus*, several areas of intense fluorescence were observed which corresponded with clumping of the cells. The PCR data suggested that Ca4B was able to bind to both cells types, but with more specificity to *C. albicans*. This result is not supported by the fluorescence data.

3.7 Characterisation of previously Identified Aptamers.

A set of 14 novel aptamers had been previous isolated in the lab against several fungal species. Sixteen rounds of SELEX were undertaken at 4°C against *A. fumigatus*, *C. albicans* and *Saccharomyces cerevisiae* (*S. cerevisiae*) using HeLa cells as a negative selection. These aptamers had yet to be characterised, so were investigated as part of this study.

Initially, each sequence was analysed, without the primer sequences, through Clustal Omega analysis software. The analysis from this software shows the similarities between the aptamers allowing for sequence comparisons. Sequences, with the primer sequences, were also analysed by Mfold analysis software to predict secondary folding structure of each aptamer, which is important for target binding.

(A)

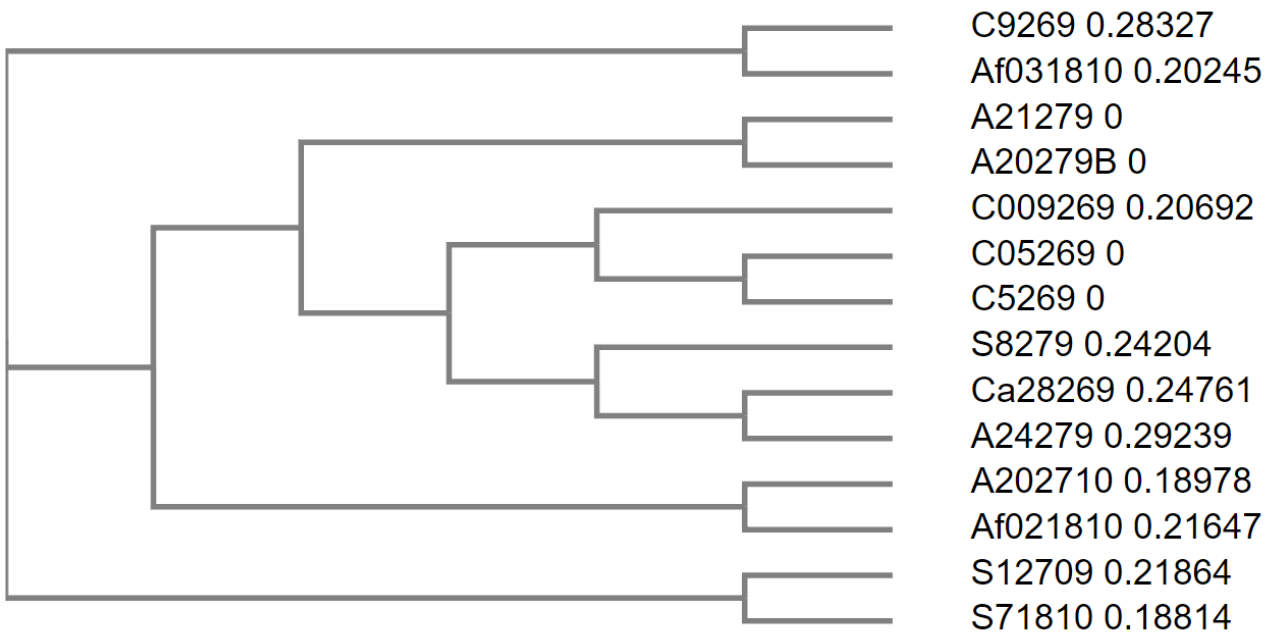

(B)

```
C9269          ------------CCGGGGACGCACCGCATTCAACACGTCGCGAGCACCGCATCA-----   42
A21279         -------CGTACCACCACACGCCCCGACCATTC---------------AGCATCCGCACC   38
A20279B        -------CGTACCACCACACGCCCCGACCATTC---------------AGCATCCGCACC   38
A202710        ---------CCGCGCCAGCACACCACA---------CAGCCATTACCCGGAACCCGTCAC   42
Af021810       ------------------CACAGCGCACACTACCCAACGCCACACACCTGGACCCCCCC-   41
Af031810       TCACCGCTC------------TCCCCACGCTTATCCCG----------CTCACCACTCCT   38
S12709         -----------CCCCGAGTTTACCGCAGAGTTCAGCACACGCCACACTGCCATCCCACAC   49
S71810         CCACCACTGTCCTTCGAGTTTACCGCAGAATTCGCCGATCCACCACACCTCATCACACCC   60
C009269        ------CTG--TCGCTGTTT-GCAGTAGCCATGTGTCGTTCTCTCA---GGCTCC-----   43
C05269         -----CGCG--TCGCTAGTT-GTGTTTGGTTTGTGGTTGTCTTACT---TGGTCT-----   44
C5269          -----CGCG--TCGCTAGTT-GTGTTTGGTTTGTGGTTGTCTTACT---TGGTCT-----   44
S8279          --------------CGGTTG-ATGGCACCAGTGTGTCGCCCATTGGC-GGGGTTG-----   39
Ca28269        ------CTA--CGGACGTCT-TTGCCCTGCGTTCCGCTGCAACTGT---GTGTTC-----   43
A24279         --------C--CCTACGTGC-GTGGCCGCATTGTGCCTTTTGATGG---GTGTTG-----   41


C9269          -----TTCCGTTCCCC--  53
A21279         AGCCTGTCCCTCG-----  51
A20279B        AGCCTGTCCCTCG-----  51
A202710        CATCTGTTCGT-------  53
Af021810       ----------------    41
Af031810       CATCTCCCTCCTGCGC--  54
S12709         CCTGTCCACCCTGC----  63
S71810         CCTCCGTGCC--------  70
C009269        -GGGTGTG----------  50
C05269         -GTGTGTCCCC-------  54
C5269          -GTGTGTCCCC-------  54
S8279          -GATTGTGTCGCGTCCCT  56
Ca28269        -GTG-CTTCCTTCTCCCT  59
A24279         -TCC-TGTCCT-------  50
```

(C)

Aptamer	% Similarity													
	C9269	A21279	A20279B	A202710	Af021810	Af031810	S12709	S71810	C009269	C05269	C5269	S8279	Ca28269	A24279
C9269	100	40	40	43.59	37.84	51.43	39.22	44.69	29.27	25	25	28	32.65	29.55
A21279	40.00	100	100.00	46.34	42.31	41.03	42.55	47.92	41.67	41.03	41.03	40.54	30.00	40.54
A20279B	40.00	100	100	46.34	42.31	41.03	42.55	47.92	41.67	41.03	41.03	40.54	30.00	40.54
A202710	43.59	46.34	46.34	100	59.38	48.39	43.14	50.00	36.84	34.15	34.15	40.00	40.00	25.00
Af021810	37.84	42.31	100.00	59.38	100	46.43	51.22	46.34	33.33	21.21	21.21	31.43	33.33	12.12
Af031810	51.43	41.03	41.03	48.39	46.43	100	51.16	56.25	33.33	29.73	29.73	30.77	37.50	27.27
S12709	39.22	42.55	42.55	43.14	51.22	51.16	100	59.32	38.30	40.00	40.00	30.77	26.92	24.49
S71810	44.69	47.92	47.92	50.00	46.34	56.25	59.32	100	38.00	33.96	33.96	35.42	29.41	28.57
C009269	29.27	41.67	41.67	36.84	33.33	33.33	38.30	38.00	100	54.00	54.00	54.55	34.69	36.17
C05269	25.00	41.03	41.03	34.15	21.21	29.73	40.00	33.96	54.00	100	100	38.30	34.62	32.00
C5269	25.00	41.03	41.03	34.15	21.21	29.73	40.00	33.96	54.00	100	100	38.30	34.62	32.00
S8279	28.00	40.54	40.54	40.00	31.43	30.77	30.77	35.42	54.55	38.30	38.30	100	45.28	47.83
Ca28269	32.65	30.00	30.00	40.00	33.33	37.50	26.92	29.41	34.69	34.62	34.62	45.28	100	46.00
A24279	29.55	40.54	40.54	25.00	12.12	27.27	24.49	28.57	36.17	32.00	32.00	47.83	46.00	100

Figure 3.13. Analysis of aptamer sequences via Clustal Omega (A) Phylogenetic tree of isolated aptamer. Isolated sequences from the SELEX process were put through Clustal Omega software (primer sequences removed) and sequences compared for similarity shown as a phylogenetic tree. **(B) Alignment of isolated aptamer sequences.** Clustal Omega output of sequences aligned. **(C) Percentage similarity of all isolated sequences.** Clustal Omega output of similarity of sequences expressed as percentage values between each sequence.

The phylogenetic tree (figure 3.13A) groups aptamers together based on their similarities in sequences. Sequences were grouped into three main families, which may suggest three distinct epitopes. The first branch contains 2 aptamers, the second branch contains 10 aptamers and the third branch, 2 aptamers. Within the second branch, A21279 and A20279B, have the same sequence, as do C05269 and C5269. Further, Ca28269 and A24279 are very closely related as are A202710 and Af021810. In the third branch, S12709 and S71810 are closely related to each other. Based on the sequence homologue, the majority of aptamers showed less than 60% similarity (Figure 12B and 12C).

Figure 3.13B shows the sequence alignments generated by clustal omega, which demonstrates there were no conserved regions between all aptamers. However, based on the phylogenetic mapping a number of aptamers were found to be closely associated. Therefore, these sequences were analysed separately (Figure 3.14).

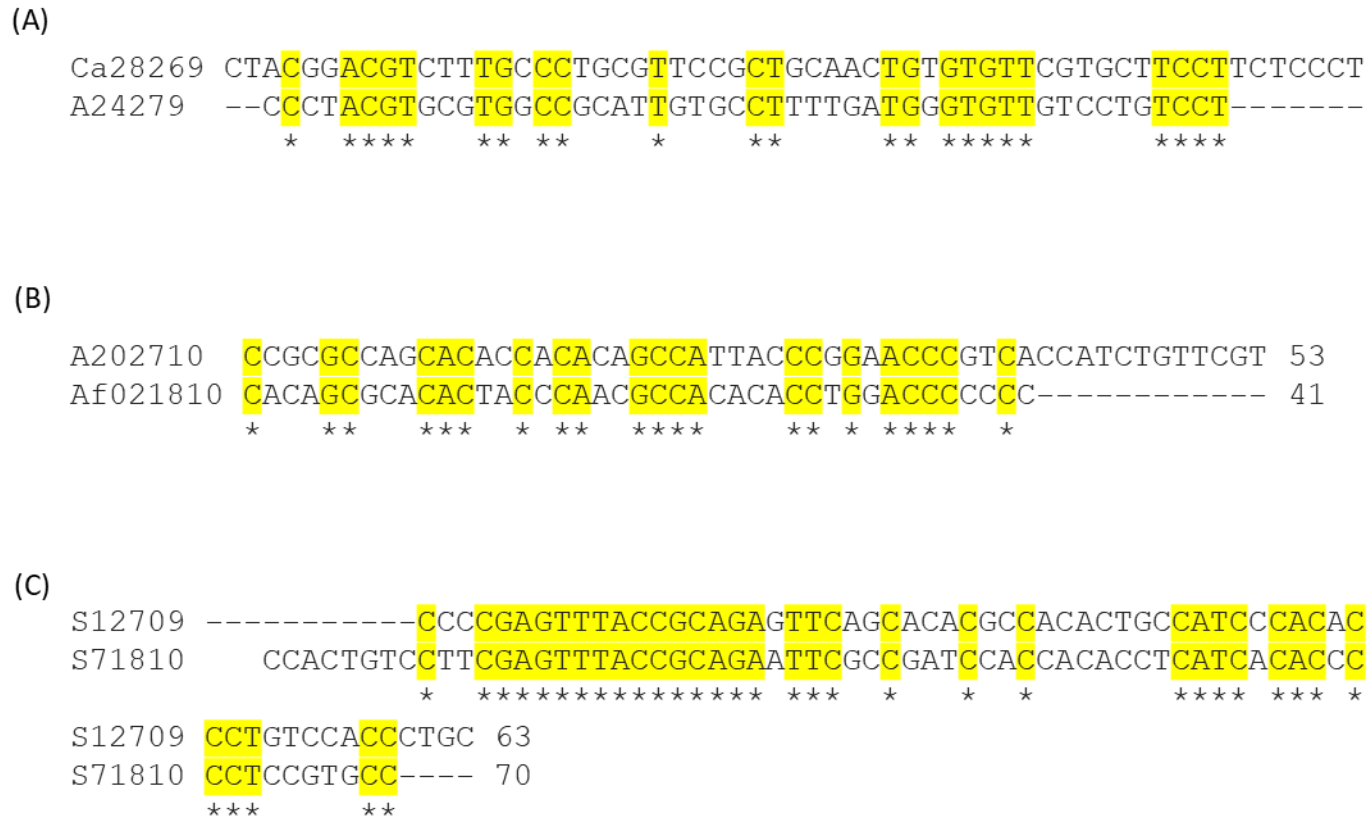

Figure 3.14. Alignment of isolated aptamer sequences using Clustal Omega. Alignment of two aptamers (A) Ca28269 and A24279 (B) A202710 and Af021810 (C) S12709 and S71810. Conserved regions are indicated in yellow and with a *.

Based on the phylogenetic tree, the closely related sequences Ca28269 and A24279 showed 22 consensus bases, with one group of 5 and two groups of 4 conserved bases (Figure 3.14A). A202710 and Af021810, were also shown to be closely related showing 21 consensus bases, with two group of 4 and one group of 3 conserved bases. Finally, S12709 and S71810 showed 35 consensus bases, with one group of 15 and two groups of 4 conserved bases.

3.8 Previously Identified aptamer predicted folding structure.

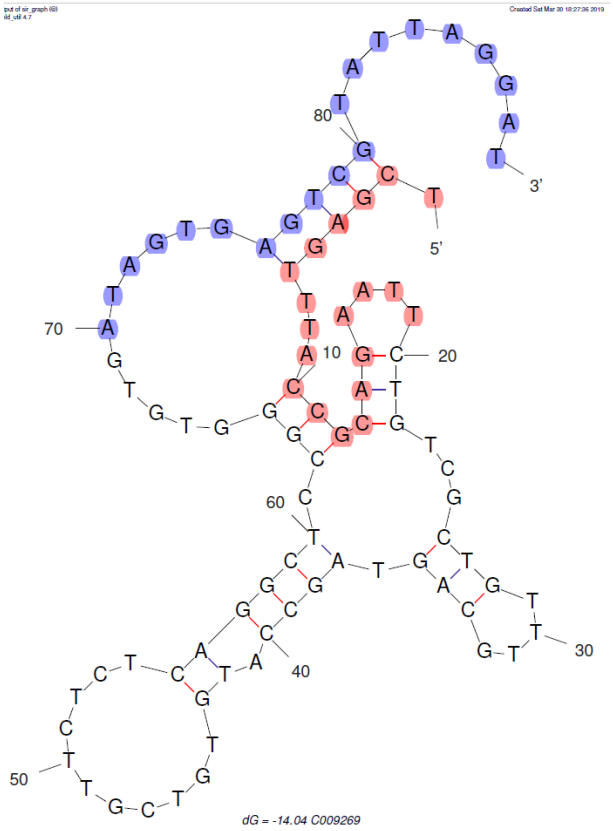
dG = -14.04 C009269

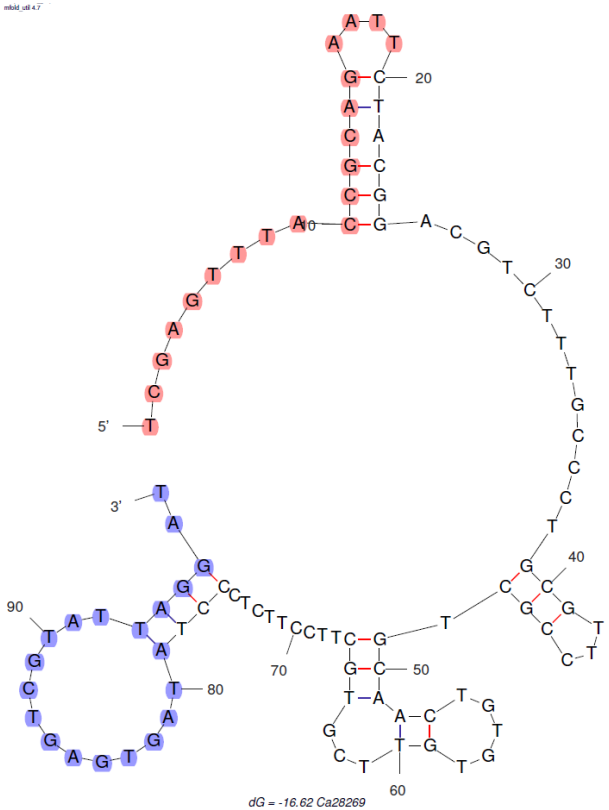
dG = -16.62 Ca28269

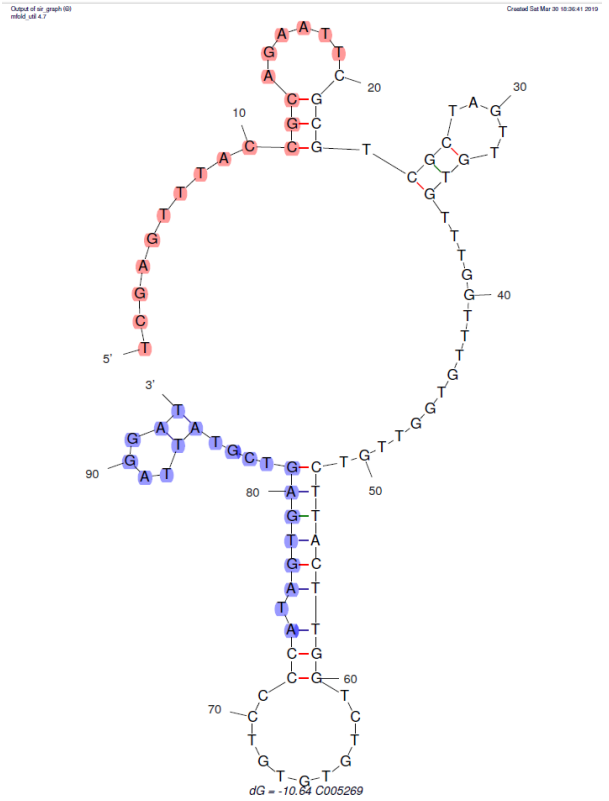
dG = -10.64 C005269

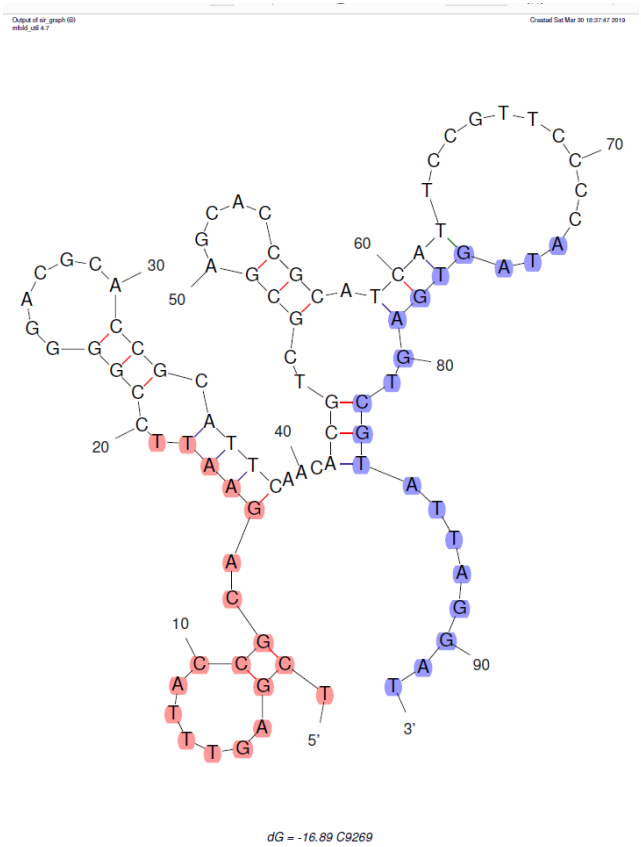
dG = -16.89 C9269

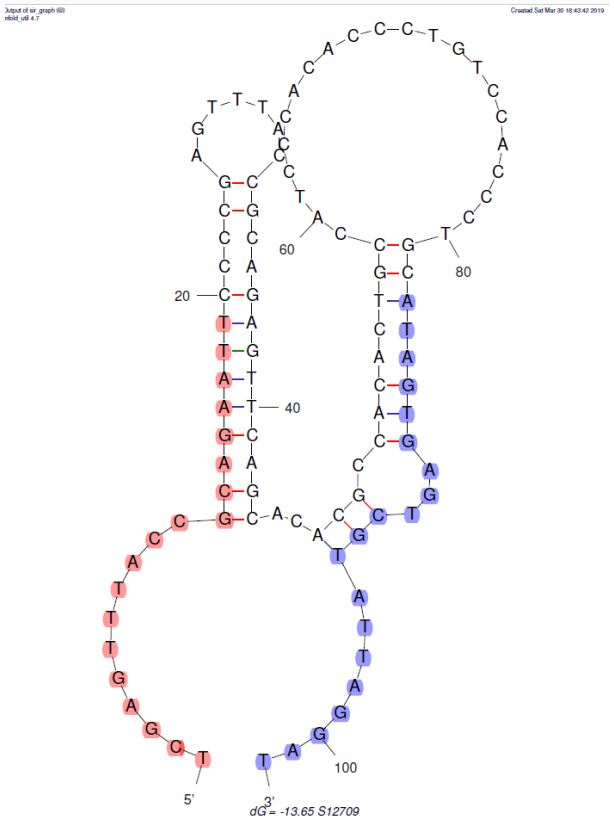
dG = -13.65 S12709

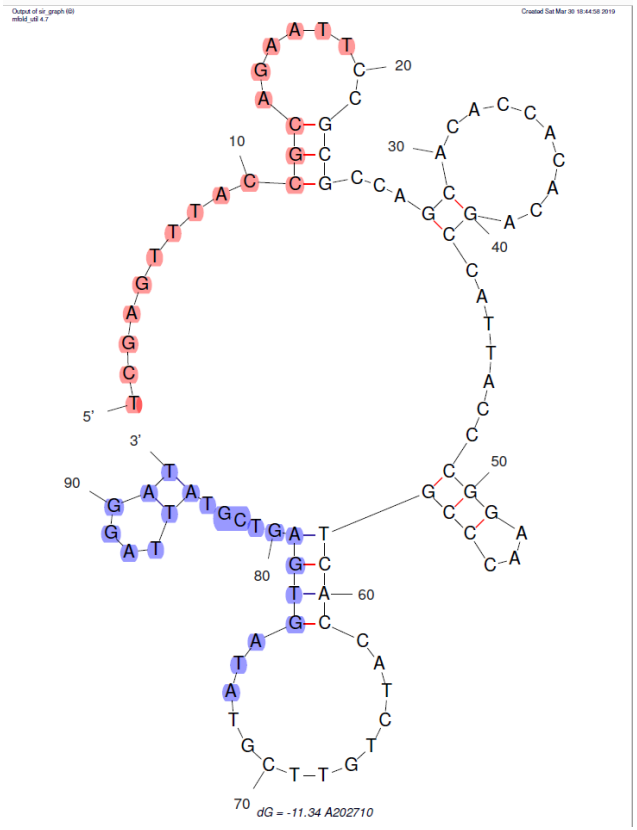
dG = -11.34 A202710

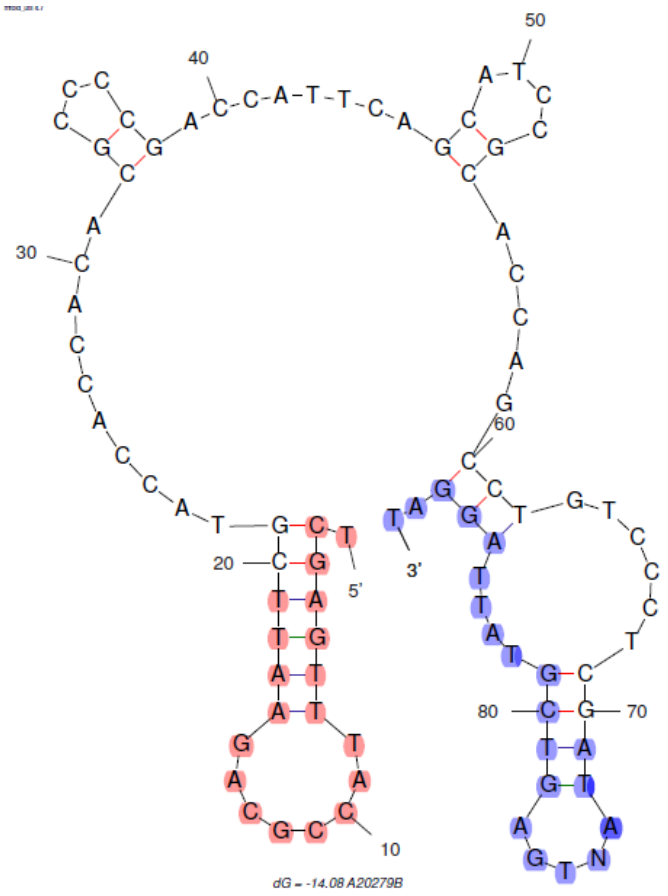
dG = -14.08 A20279B

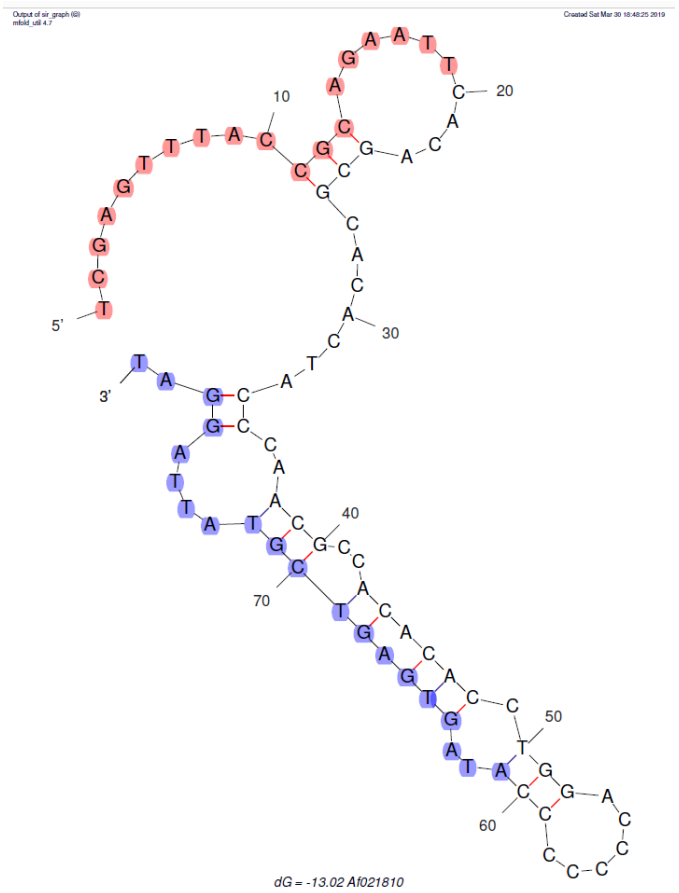
dG = -13.02 Af021810

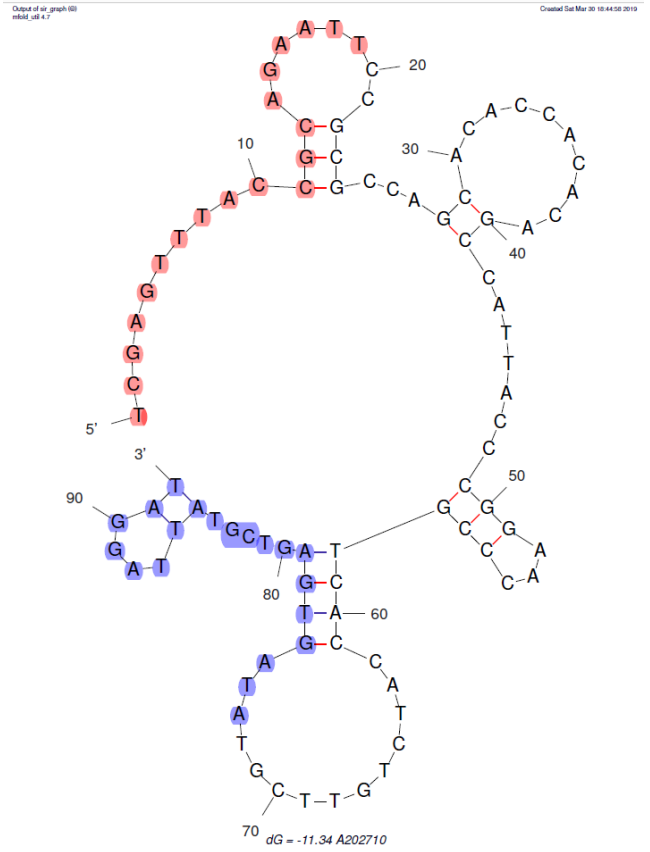
dG = -11.34 A202710

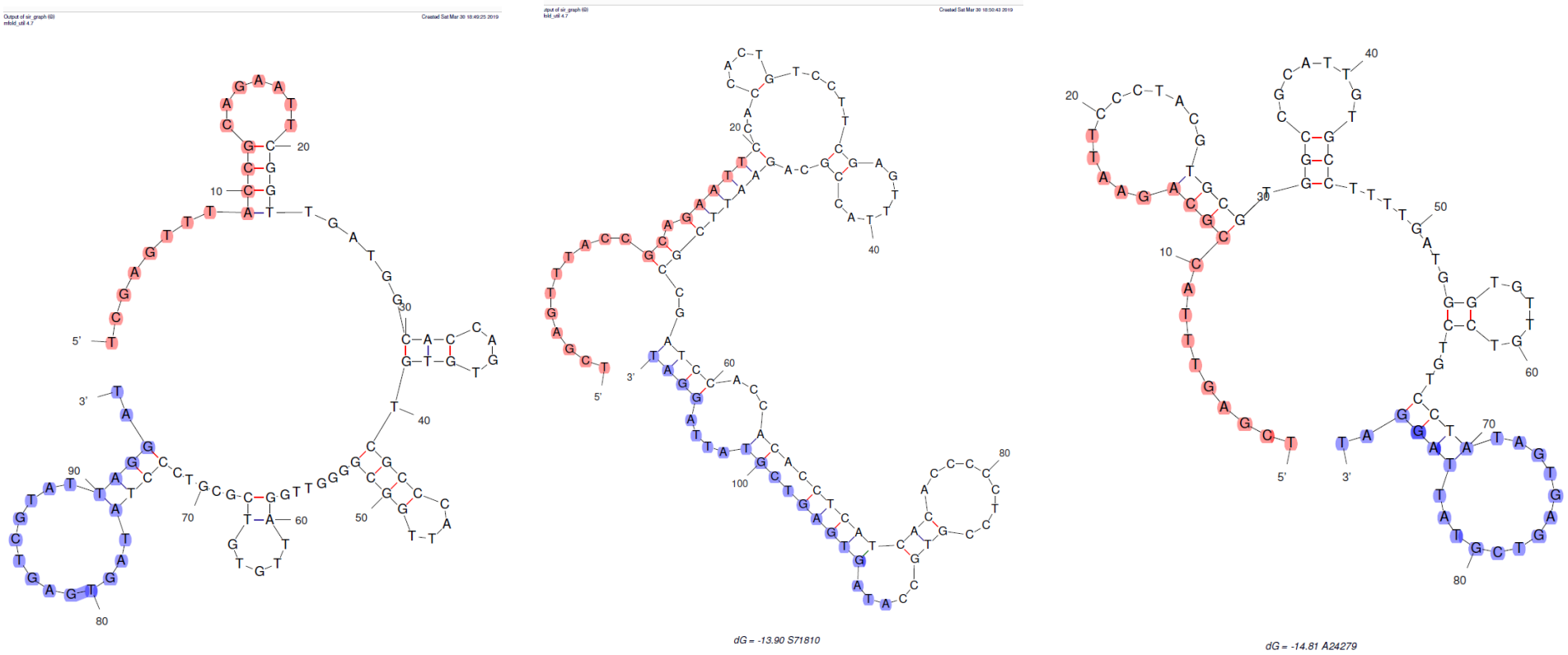

Figure 3.15. Predicted secondary folding structure of previously identified aptamers. All sequences were analysed using Mfold software and folding structure predicted based on SELEX conditions (Na+ 137mM and Mg++ 0.25mM) and 4°C. Structures shown are those with the lowest predicted Gibbs free energy. Aptforward primer sequences are highlighted in red and Aptreverse sequences highlights in blue.

Figure 3.15 shows the predicted secondary structures of the previously identified aptamers. The predicted folding shows some similarities in structures. With aptamers either showing large loop regions, with smaller stem regions or mostly consisting of large stem loop regions.

3.9 Further Testing of Previously Identified aptamers

To determine binding of these novel aptamers to different fungal species, 200nM of each aptamer was incubated with a different fungal cell type at 4^{o}C for 30 minutes. The bound aptamer was then eluted and used as a template for a PCR. It was assumed that the more aptamer bound to the cell, the higher the available template for the PCR, which would result in a higher concentration of the final aptamer product. The resulting product was visualised on an agarose gel and quantified using the ChemiDoc XRS+ software by comparing to a product of known concentration.

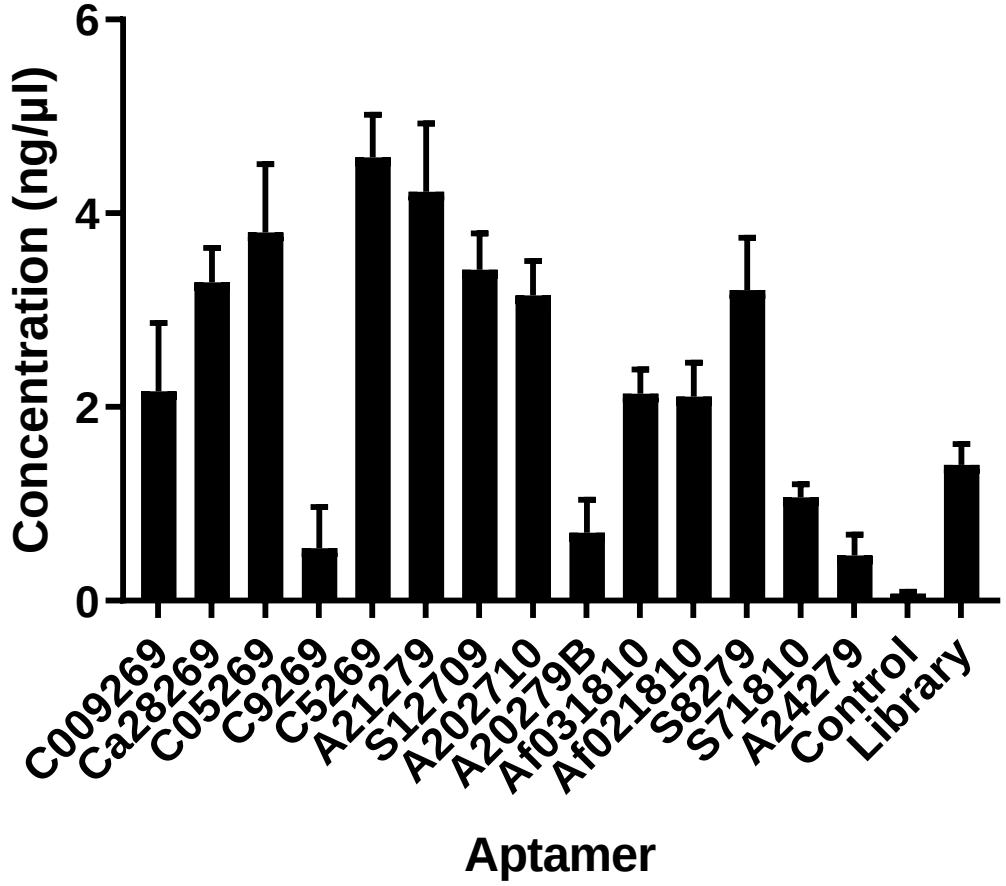

Figure 3.16. *C. albicans* incubated with all previously identified aptamers. *C. albicans* incubated with all previously identified aptamers at a concentration of 200nM, for 30 minutes at 4°C. Cells were then washed with washing buffer, and resuspended in water. Aptamer was then eluted from target cells by heating at 95°C. A sample of eluted aptamer was then amplified by PCR and a sample of the PCR product separated by gel electrophoresis on a 2% agarose gel, and visualised by UV light using the ChemDoc XRS+. A sample of known concentration was run alongside the PCR product sample and the intensity of each band measured. The concentration of aptamer was calculated by comparison to the sample of known concentration (171.1.ng/µl). Each value displayed is an average of 2 repeats, with an amplified aptamer library as a positive control and a sample with no aptamer as a negative control.

Of the aptamers that were selected against C. *albicans* there was varying levels of binding when incubated with *C. albicans*, with C5269 (4.6ng/µl), showing the most binding overall. This was followed by C05269 (3.8ng/µl), which based on the sequence information is the same sequence. The aptamer that appeared to show the lowest level of binding was C9269 (0.5ng/µl). The remaining two aptamers showed intermediate levels of binding, C009269 (2.2ng/µl) and Ca28269 (3.3ng/µl).

Aptamers selected against *A. fumigatus* when incubated with *C. albicans* also showed a wide range of binding, A21279 (4.2ng/µl) was the highest of these aptamers, followed by A202710 (3.1ng/µl), then Af031810 (2.1ng/µl), Af021810 (2.1ng/µl). The lowest levels of binding from this group of aptamers were A20279B (0.7ng/µl) and A24279 (0.5ng/µl). The final aptamers incubated with *C. albicans* in figure 3.16 were those selected against *S. cerevisiae*, again with varied levels of binding. S12709 (3.4ng/µl) being the highest, followed by S8279 (3.2ng/µl) and the lowest being S71810 (1.1ng/µl).

In most cases, the aptamers selected against *S. cerevisiae* and *A. fumigatus*, show significant binding to *C. albicans* when compared to the negative control and the library alone. As previously noted, the overall level of aptamer binding in *C.albicans* was lower than that reported in other fungal species.

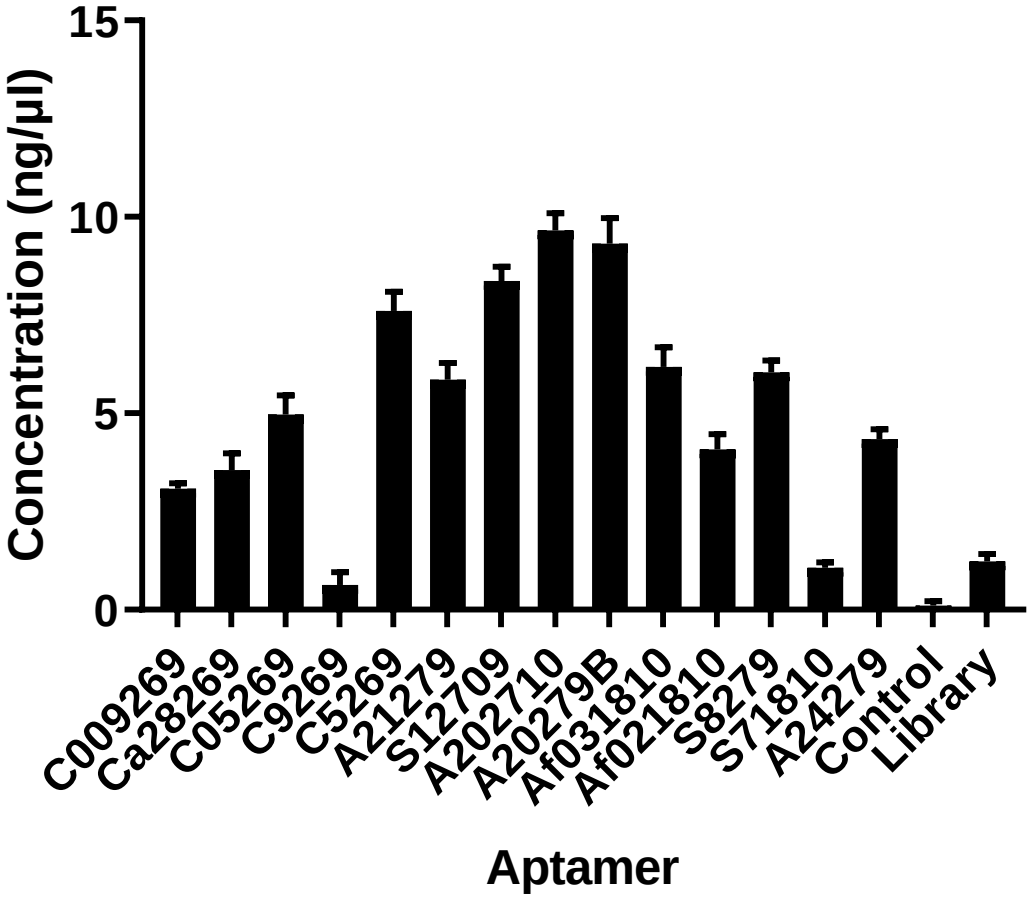

Figure 3.17. *A. fumigatus* incubated with all previously identified aptamers. *A. fumigatus* incubated with all previously identified aptamers at a concentration of 200nM, for 30 minutes at 4°C. Cells were then washed with washing buffer, and resuspended in water. Aptamer was then eluted from target cells by heating at 95°C. A sample of eluted aptamer was then amplified by PCR and a sample of the PCR product separated by gel electrophoresis on a 2% agarose gel, and visualised by UV light using the ChemDoc XRS+. A sample of known concentration was run alongside the PCR product sample and the intensity of each band measured. The concentration of aptamer was calculated by comparison to the sample of known concentration (171.1.ng/µl). Each value displayed is an average of 2 repeats, with an amplified aptamer library as a positive control and a sample with no aptamer as a negative control.

Figure 3.17 shows the previously identified aptamers now incubated with *A. fumigatus*. In most cases, the binding of the aptamers shows a similar trend as that seen in Figure 3.16 however; concentrations of the final aptamer product are consistently higher than seen in *C. albicans*. Aptamers that were selected against *A. fumigatus* generally show the best yield of aptamer after incubation, the highest being A202710 at 9.6ng/µl, followed by A20279 at 9.3ng/µl, then Af031810 at 6.2ng/µl, A21279 at 5.9ng/µl and the lowest A24279 (4.3ng/µl) and Af021810 at 4.086ng/µl). Whereas all aptamers selected against *C. albicans* generally show much lower yields with Ca28269 at 3.5ng/µl, followed byC009269 at 3.1ng/µl and the lowest being C9269 at 0.626ng/µl. With the exception of C5269 (7.6ng/µl) and C05269 (4.9ng/µl) which exhibited levels of binding more comparable to that of Af031810, Af021810 and A24279. Aptamers selected against *S. cerevisiae* show varying yields. S122709 is the highest at 8.4ng/µl followed by S8279 at 6.0ng/µl. S71810 (1.1ng/µl) was the second lowest from all aptamers. The aptamer library control yielded 1.229ng/µl and the no aptamer control 0.111ng/µl. S71810 and C9269 both exhibited binding levels lower than the aptamer library control.

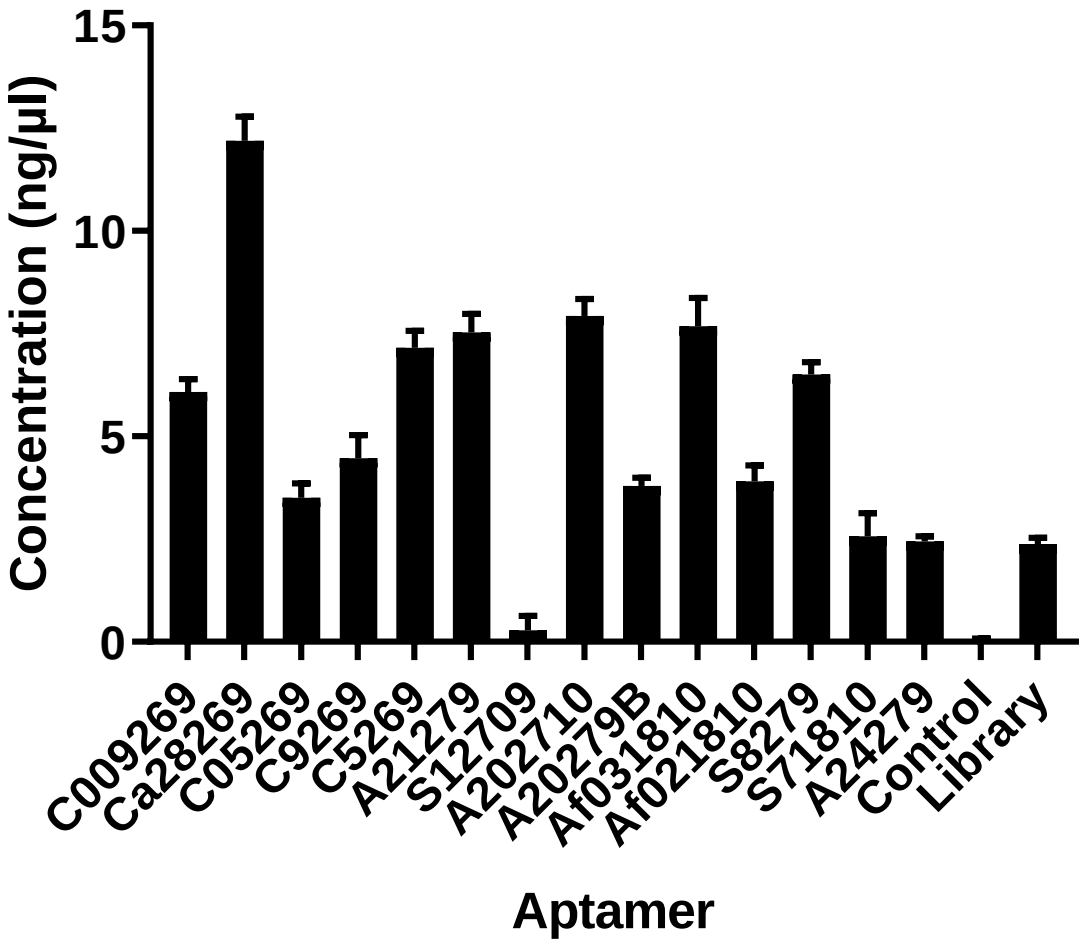

Figure 3.18. *S. cerevisiae* incubated with all previously identified aptamers. *S.* cerevisiae was incubated with all previously identified aptamers at a concentration of 200nM, for 30 minutes at 4°C. Cells were then washed with washing buffer, and resuspended in water. Aptamer was then eluted from target cells by heating at 95°C. A sample of eluted aptamer was then amplified by PCR and a sample of the PCR product separated by gel electrophoresis on a 2% agarose gel, and visualised by UV light using ChemiDoc XRS+. A sample of known concentration was run alongside the PCR product sample and the intensity of each band measured. The concentration of aptamer was calculated by comparison to the sample of known concentration (171.1.ng/µl). Each value displayed is an average of 2 repeats, with an amplified aptamer library as a positive control and a sample with no aptamer as a negative control.

Figure 3.18 shows the data for the aptamers incubated with *S. cerevisiae* cells. Aptamers that were selected against *C. albicans* showed levels of binding similar to their incubation with *C. albicans* with the exception of Ca28269 being considerably higher at 12.2ng/µl. C5269 was the second highest at 7.2ng/µl, followed by C009269 with 6.075ng/µl, then C9269 at 4.5ng/µl and the lowest being C05269 at 3.5ng/µl. Aptamers selected against *A. fumigatus* had a range of levels of binding, the highest being A202710 at 7.9ng/µl, followed by Af031810 at 7.7ng/µl, then A21279 with 7.5ng/µl, then Af021810 with 3.9ng/µl and finally the lowest, Af20279B with 3.8ng/µl. Aptamers selected against *S. cerevisiae* also had varied levels of binding. S8279 had the highest level of binding with 6.5ng/µl, followed by S71810 at 2.6ng/µl and the lowest being S12709 at 0.3ng/µl.

Comparing these aptamers to their incubation in other species it shows they have some specificity fungal species and, in some cases, increased binding to the non-target cell. For example, Ca28269 was isolated at a concentration of 12.2ng/µl when incubated with *S. cerevisiae* but at 3 fold less in its target fungi, *C. albicans*(3.7ng/µl) and 4ng/µl with *A.fumigatus.*. However, a number of aptamers were isolated that where specific for their target cell, for example Af20279B gave a yield of 9.4ng/µl when incubated with its target fungi, *A. fumigatus*, but this was significantly reduced in *C. albicans* and(0.5ng/µl(in and, to some extent, in *S. cerevisiae*(4ng/µl). Whereas some aptamers bind to all the fungal species for example A21279, which bound to all fungi equally well.

Following on from the results of the PCR assay, five aptamers were short listed that showed some specific binding to fungal cells (Table 3.2). These aptamers where C009269 (binding to *A. fumigatus* and *S. cerevisiae*), Ca28269 (high level of binding to *S.cerevisiae)*, C5269 (binding to *C. albicans*, *A. fumigatus* and *S. cerevisiae)*, Af20279B (high level of binding to *A. fumigatus*) and A24279 (binding to *A. fumigatus* and *S. cerevisiae)*.

	Aptamer Binding		
Aptamer	*C. albicans*	*A. fumigatus*	*S. cerevisiae*
C009269	-	✓	✓✓
Ca28269	✓	✓	✓✓✓✓
C05269	✓	✓✓	✓
C5269	✓	✓✓✓	✓✓
C9269	-	-	✓
A21279	✓	✓✓	✓✓✓
A20279B	-	✓✓✓	✓
S12709	✓	✓✓✓	-
A202710	✓	✓✓✓	✓✓✓
Af031810	✓	✓✓	✓✓✓
Af021810	✓	✓	✓
S8279	✓	✓✓	✓✓
S71810	-	-	✓
A24279	-	✓	-

Table 3.2 Summary of Aptamer binding to fungal cells. A summary table of all previously identified aptamers incubated with *C. albicans, A. fumigatus* and *S. cerevisiae* and their level of binding to those species. ✓ indicates 2.5-4.9ng/µl concentration. ✓✓ indicates 5.0-7.4ng/µl concentration. ✓✓✓ indicates 7.5-9.9ng/µl concentration. ✓✓✓✓ indicates 10ng/µl and above concentration.

The binding of the short-listed aptamers was further characterised by testing the aptamers at varying concentrations (200nM to 25nM) with *C. albicans*, *A. fumigatus* and *S. cerevisiae* cells. This would also allow the determination of the Kd, which will help determine their affinity for the target cell. As previously described, following a 30-minute incubation at 4^{o}C with the required aptamer concentration, cells where washed and the bound aptamer was eluted. This was then used as the template DNA for a PCR. Amplified aptamers were analysed by gel electrophoresis and quantified using ChemiDoc software against a control of known concentration.

(A)

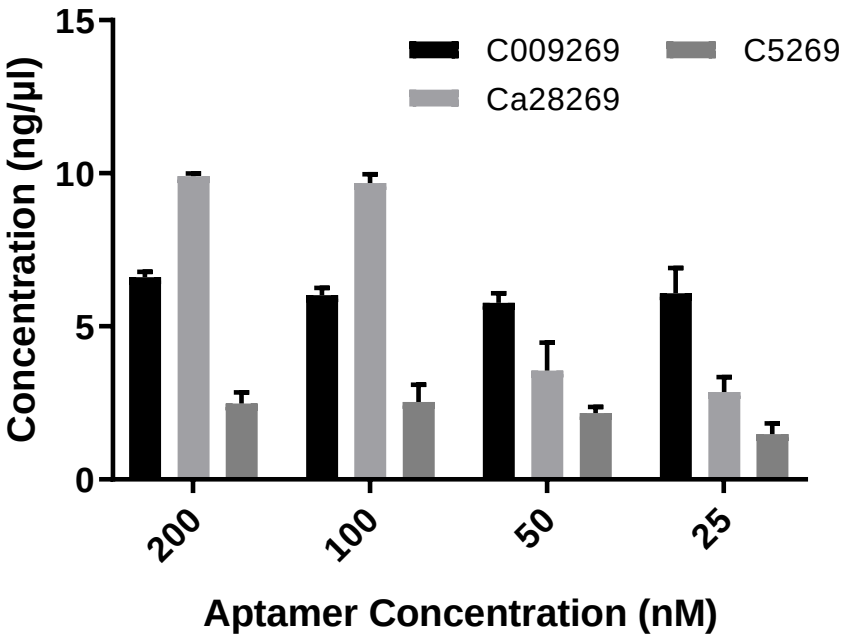

(B)

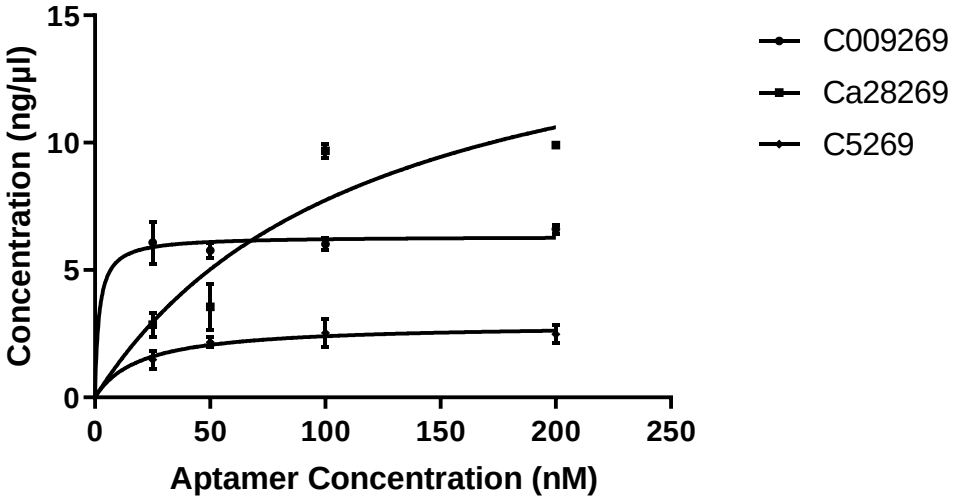

Figure 3.19. *C. albicans* incubated with selected aptamers at differing concentrations. (A) Eluted aptamer, amplified by PCR (B) Binding Affinity of aptamer Shortlisted aptamers C009269, Ca28269 and C5269 were incubated with *C. albicans* for 30minutes at a concentration of 200nM, 100nM, 50nM and 25nM. Cells were washed with washing buffer, and resuspended in water before bound aptamer was then eluted from target cells. A sample of each elution was then amplified by PCR and a sample of this product separated and visualised by gel electrophoresis under UV light using ChemiDoc XRS+ on a 2% agarose gel. A sample of known concentration was also run on the same gel and the concentration of each sample determined by measuring the visual intensity of each band (using ChemiDoc XRS+ Image lab software) in comparison to the sample of known concentration. The Bmax and Kd were calculated using the graph.

Figure 3.19 shows the final concentration of aptamer following incubation with *C. albicans* of the shortlisted aptamers C009269, Ca28269 and C5269 for 30 minutes at 4°C. Ca28269 shows the highest concentration of aptamer with a yield of 9.9ng/µl at 200nM and 9.7ng/µl at 100nM concentrations. The Kd for this aptamer was determined (calculated from data from figure 18, using Graphpad Prism software) to be 117nM. This was much higher than the concentration seen in Figure 12 when *C. albicans* was also incubated with 200nM of this Ca28269. As the initial concentration of aptamer decreased so did the final concentration; 3.6ng/µl at 50nM and 2.9ng/µl at 25nM. Both C009269 (Kd 1.78nM) and C5269 (Kd19.8nM) had less variation in the final aptamer concentration, with values staying constant as the initial aptamer concentration decreased. C009269 was the higher of the two with concentrations of 6.6ng/µl (200nM) 6.0ng/µl (100nM) 5.8ng/µl (50nM) and 6.084ng/µl. C5269 gave a yield of 2.5ng/µl at 200nM and 2.5ng/µl 100nM concentrations, 2.2ng/µl at 50nM and 1.5ng/µl at 25nM.

(A)

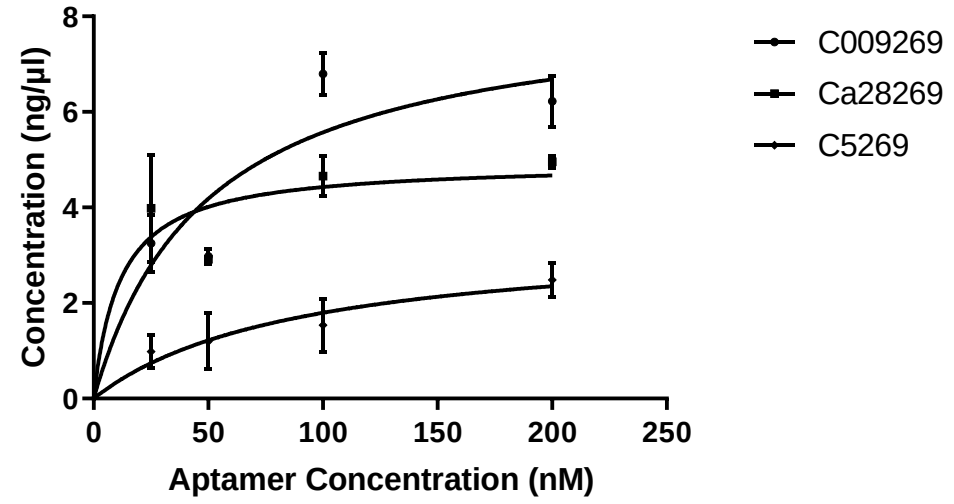

(B)

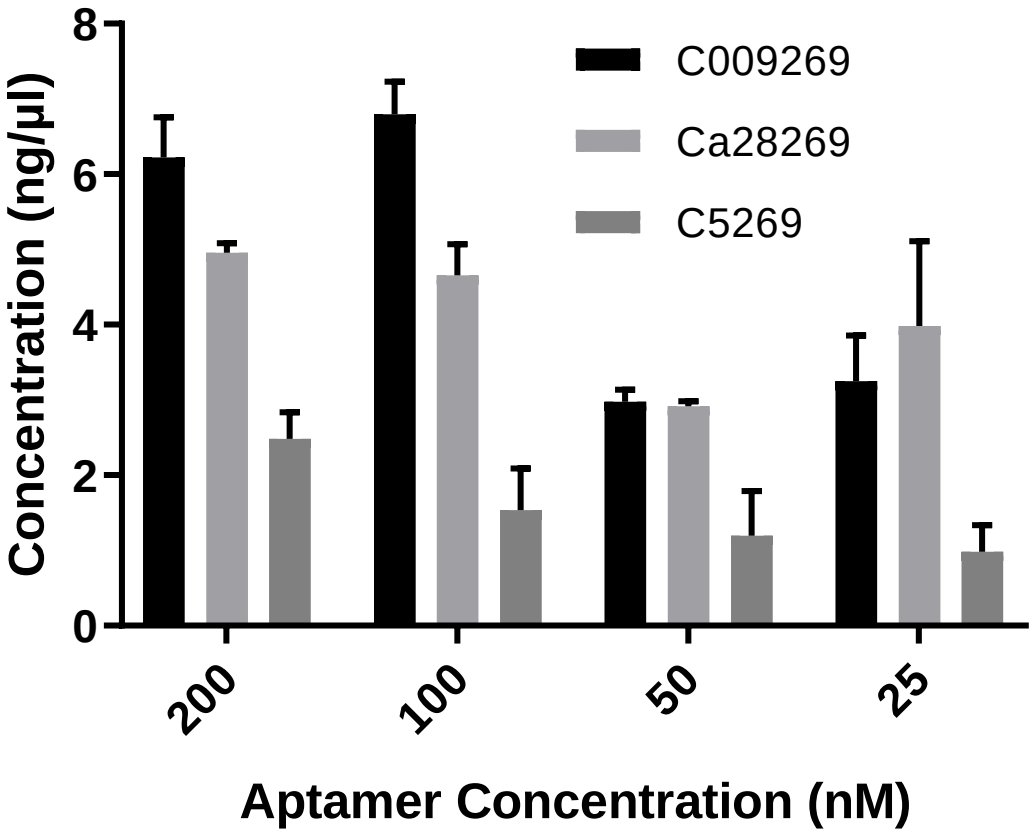

Figure 3.20. *A. fumigatus* incubated with selected aptamers at differing concentrations. Shortlisted aptamers C009269, Ca28269 and C5269 were incubated with *A. fumigatus* for 30minutes at a concentration of 200nM, 100nM, 50nM and 25nM. Cells were washed with washing buffer, and resuspended in water before bound aptamer was then eluted from target cells. A sample of each elution was then amplified by PCR and a sample of this product separated and visualised by gel electrophoresis under UV light using ChemiDoc XRS+ on a 2% agarose gel. A sample of known concentration was also run on the same gel and the concentration of each sample determined by measuring the visual intensity of each band (using ChemiDoc XRS+ Image lab software) in comparison to the sample of known concentration.

Figure 3.20 shows yield of aptamer following incubation with *A. fumigatus* of the shortlisted aptamers C009269, Ca28269 and C5269 for 30 minutes at 4°C. C009269 (Kd 49.78nM) shows the highest yield of aptamer with 6.2ng/µl at a concentration of 200nM and 6.8ng/µl at 100nM, dropping to 2.9ng/µl at 50nM and rising to 3.267ng/µl at 25nM. Ca28269 (Kd 11.55) yielded 4.9ng/µl at 200nM and 4.654ng/µl at 100nM. The yield then drops to 2.9ng/µl at 50nM and then rises slightly to 3.984ng/µl at 25nM. C5269 (Kd 90.01nM) shows the lowest overall yield as it did in figure 3.19, with yields decreasing with decreasing aptamer concentration.

(A)

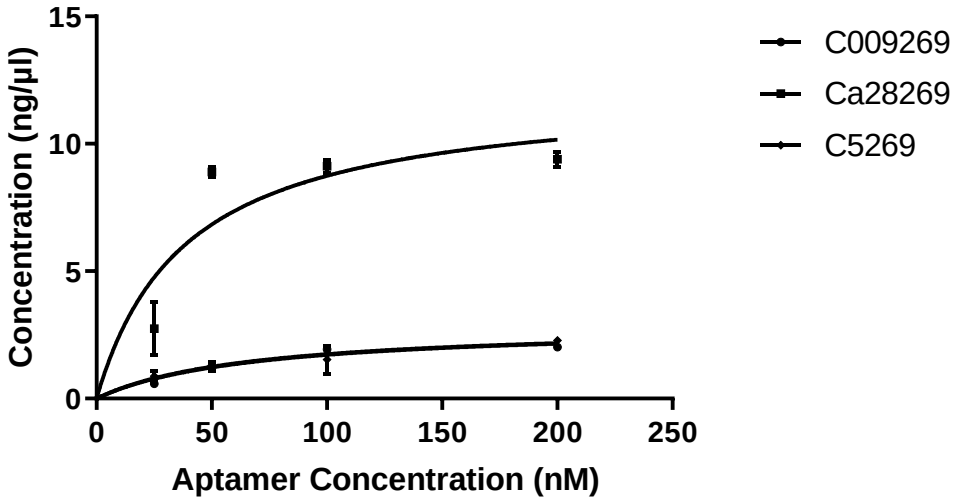

(B)

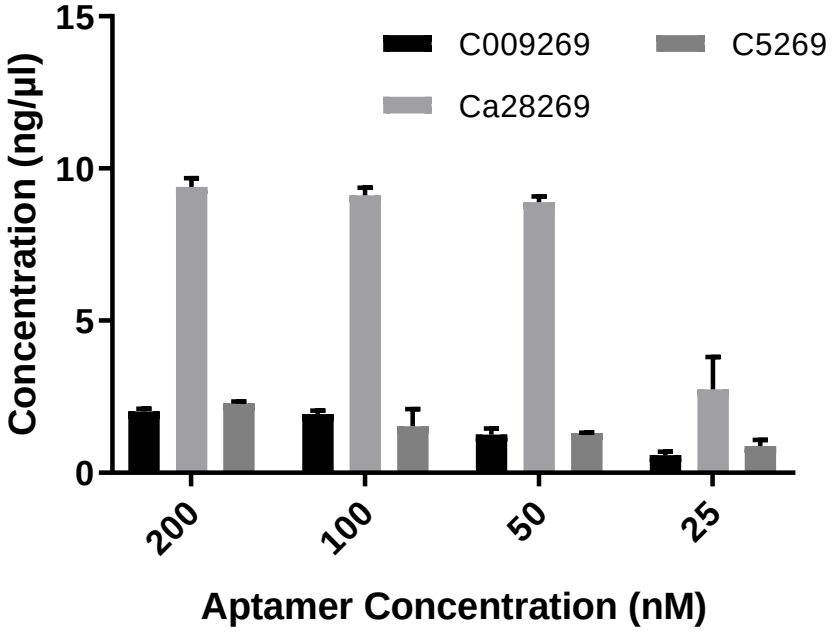

Figure 3.21. *S. cerevisiae* incubated with selected aptamers at different concentrations. (A) Binding Affinity of aptamer (B) Eluted aptamer, amplified by PCR. Shortlisted aptamers C009269, Ca28269 and C5269 were incubated with *S. cerevisae* for 30minutes at a concentration of 200nM, 100nM, 50nM and 25nM. Cells were washed with washing buffer, and resuspended in water before bound aptamer was then eluted from target cells. A sample of each elution was then amplified by PCR and a sample of this product separated and visualised by gel electrophoresis under UV light using ChemiDoc XRS+ on a 2% agarose gel. A sample of known concentration was also run on the same gel and the concentration of each sample determined by measuring the visual intensity of each band (using ChemiDoc XRS+ Image lab software) in comparison to the sample of known concentration.

Figure 3.21 shows yield of aptamer following incubation with *S. cerevisiae* of the shortlisted aptamers C009269, Ca28269 and C5269 for 30 minutes at 4°C. Ca28269 shows the best yield of aptamer with 9.9ng/µl at 200nM, which stayed consistent with decreasing aptamer concentration until 25nM, when the yield dropped to 2.7ng/µl. C009269 and C5269 both have relatively low yields with C009269 at approximately 2.0ng/µl at both 200nM and100nM, before dropping to 1.3ng/µl at 50nM and then 0.576ng/µl at 25nM. A similar trend was observed with C5269, with a maximum yield of 2.3ng/µl at 200nM which gradually reduced with decreasing aptamer concentration.

(A)

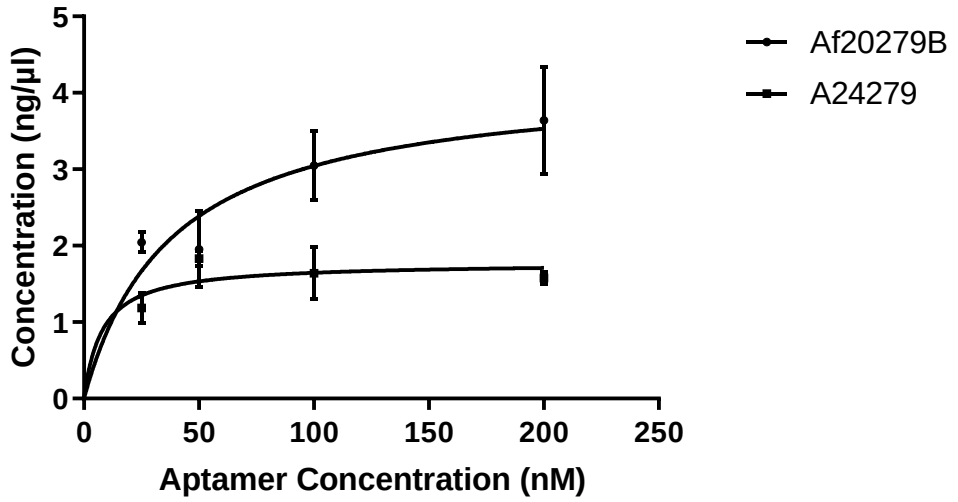

(B)

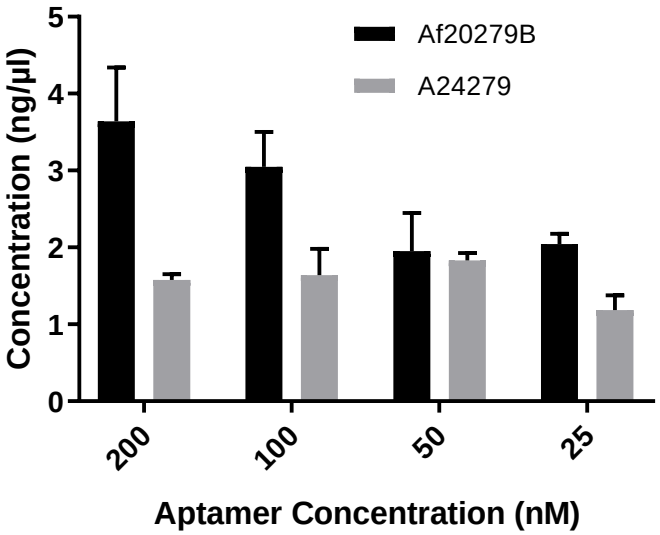

Figure 3.22. *C. albicans* incubated with selected aptamers at differing concentrations. (A) Binding Affinity of aptamer (B) Eluted aptamer, amplified by PCR. Shortlisted aptamers Af20279B and A24279 were incubated with *C. albicans* for 30minutes at a concentration of 200nM, 100nM, 50nM and 25nM. Cells were washed with washing buffer, and resuspended in water before bound aptamer was then eluted from target cells. A sample of each elution was then amplified by PCR and a sample of this product separated and visualised by gel electrophoresis under UV light using ChemiDoc XRS+ on a 2% agarose gel. A sample of known concentration was also run on the same gel and the concentration of each sample determined by measuring the visual intensity of each band (using ChemiDoc XRS+ Image lab software) in comparison to the sample of known concentration.

Figure 3.22 shows the yields of aptamer obtained from the incubation of Af20279B and A24279 with *C. albicans* for 30minutes at 4°C. Af20279B shows a higher yield compared to A24279 with 3.6ng/µl at 200nM, which reduced and plateaued at 50nM to 31.9ng/µl. A24279 gave a much lower yield of 1.575ng/µl at 200nM, which remained relatively consistent as the aptamer concentration reduced to 25nM.

(A)

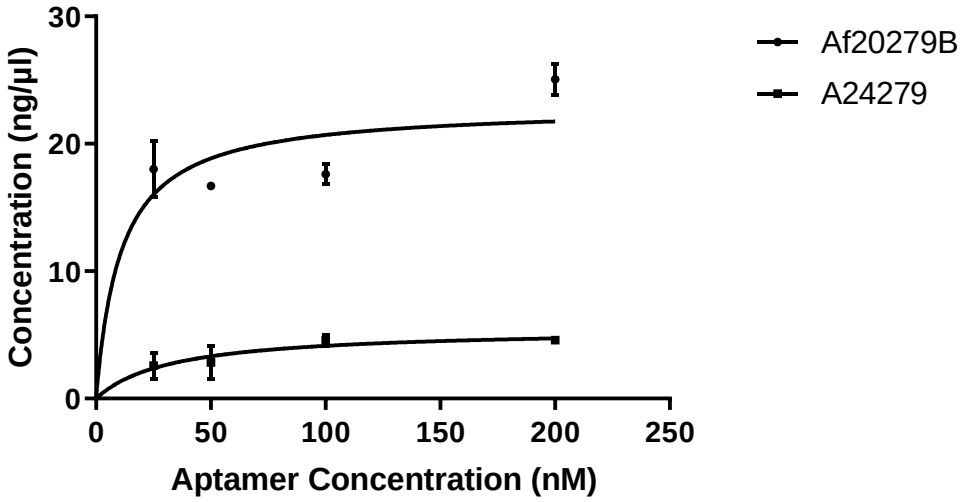

(B)

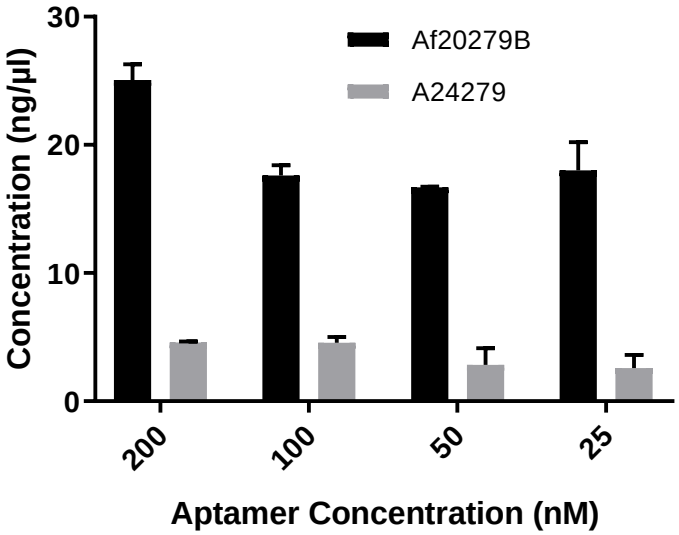

Figure 3.23. *A. fumigatus* incubated with selected aptamers at differing concentrations. (A) Binding Affinity of aptamer (B) Eluted aptamer, amplified by PCR Shortlisted aptamers Af20279B and A24279 were incubated with *A. fumigatus* for 30minutes at a concentration of 200nM, 100nM, 50nM and 25nM. Cells were washed with washing buffer, and resuspended in water before bound aptamer was then eluted from target cells. A sample of each elution was then amplified by PCR and a sample of this product separated and visualised by gel electrophoresis under UV light using ChemiDoc XRS+ on a 2% agarose gel. A sample of known concentration was also run on the same gel and the concentration of each sample determined by measuring the visual intensity of each band (using ChemiDoc XRS+ Image lab software) in comparison to the sample of known concentration.

Figure 3.23 shows the yield of aptamer following incubation of Af20279B and A24279 with *A. fumigatus* for 30minutes at 4°C. Af20279B exhibits the best binding of any of the aptamers selected for further testing for its selected cell type. At 200nM the concentration following incubation was 25.069ng/µl, which reduced slightly at 100nM (17.612ng/µl), before reaching a plateau. Aptamer A24279 showed limited binding to the target cell, with no concentration related change observed.

(A)

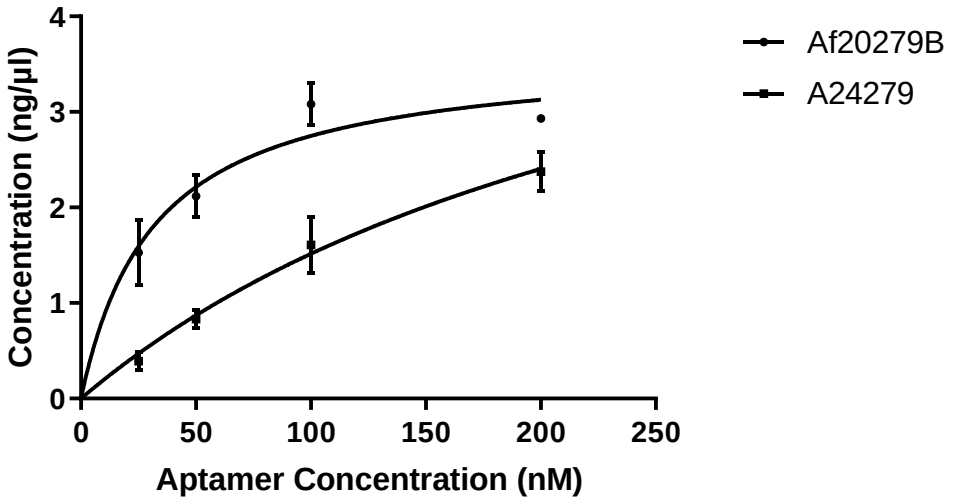

(B)

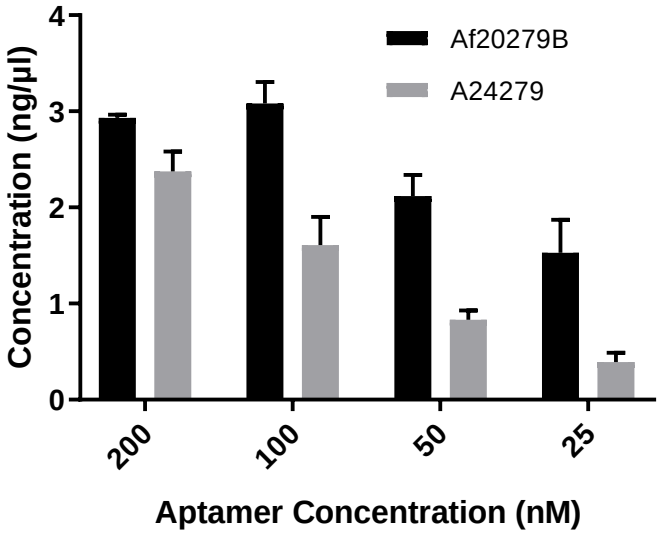

Figure 3.24. *S. cerevisiae* incubated with selected aptamers at differing concentrations. (A) Binding Affinity of aptamer (B) Eluted aptamer, amplified by PCR. Shortlisted aptamers Af20279B and A24279 were incubated with *S. cerevisiae* for 30minutes at a concentration of 200nM, 100nM, 50nM and 25nM. Cells were washed with washing buffer, and resuspended in water before bound aptamer was then eluted from target cells. A sample of each elution was then amplified by PCR and a sample of this product separated and visualised by gel electrophoresis under UV light using ChemiDoc XRS+ on a 2% agarose gel. A sample of known concentration was also run on the same gel and the concentration of each sample determined by measuring the visual intensity of each band (using ChemiDoc XRS+ Image lab software) in comparison to the sample of known concentration.

Figure 3.24 shows the binding affinity of Af20279B and A24279 to *S. cerevisiae*. Af20279B shows the highest binding affinity, but this is still considerably lower than in *A. fumigatus* with 2.9ng/µl at 200nM. . As the concentration decreased below 100nM, the level of binding also reduced until it reached 1.5ng/µl at 25nM. A24279 showed slightly less binding affinity with 2.4ng/µl at 200nM, which also decreased with decreasing aptamer concentration from 1.6ng/µl at 100nM to 0.4ng/µl at 25nM.

Aptamer	Kd of Aptamer (nM)		
	C. albicans	***A. fumigatus***	***S. cerevisiae***
Ca009269	1.78	49.78	67.92
Ca28269	117	11.5	38.82
C5269	19.8	90.01	65.92
Af20279B	38.04	10.84	31.92
A24279	7.95	32.98	284.5

Table 3.3 A summary of the kd of all shortlisted aptamers against each target cell. Each kd was calculated following incubation of each aptamer with each target cell at 200nM, 100nM, 50nM and 25nM. This tables summarises data from figures

Table 3.3 shows a summary of the kd of all shortlisted aptamers against each target cell.
Following the high levels of specificity seen in Af20279 (in figures 3.22, 3.23 and 3.24) the binding affinity was then assessed visually by fluorescence microscopy.

3.10 Confirmation of binding of shortlisted aptamers by fluorescence microscopy

A sample of Af20279 was ordered tagged with alexa488, cells were then incubated with each target for 30minutes using an aptamer concentration of 200nM. Aptamers were not eluted following incubation, and cells were washed and fixed in formaldehyde and mounted onto slides using Vectashield. Slides were then imaged using Ziess fluorescence microscope, with a 1.2 second exposure time.

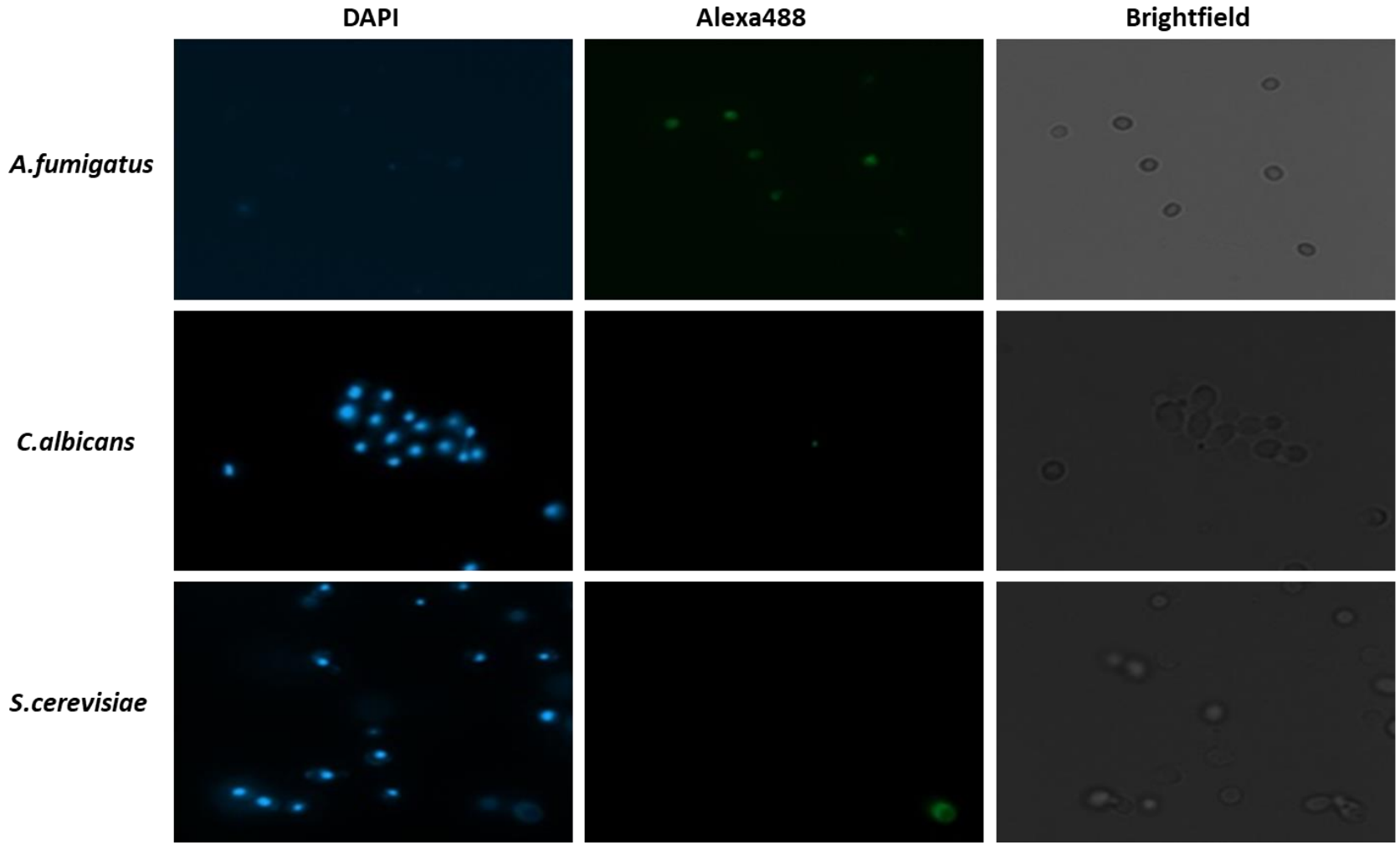

Figure 3.25. Af20279 tagged with Alexa488 and viewed by fluorescence microscopy. Shortlisted aptamer Af20279 labelled with Alex488 fluorescent tag (IDT, UK) was incubated with *A. fumigatus* and *C. albicans* for 30 minutes at room temperature using an aptamer concentration of 200nM. Cells were fixed in 3.7% formaldehyde and washed with 1x PBS, before being resuspended in vectashield with DAPI for mounting onto slides. Slides were imaged using Ziess fluorescent microscope, using a DAPI, Alex488 and brightfield filter, exposed for 1.2 seconds.

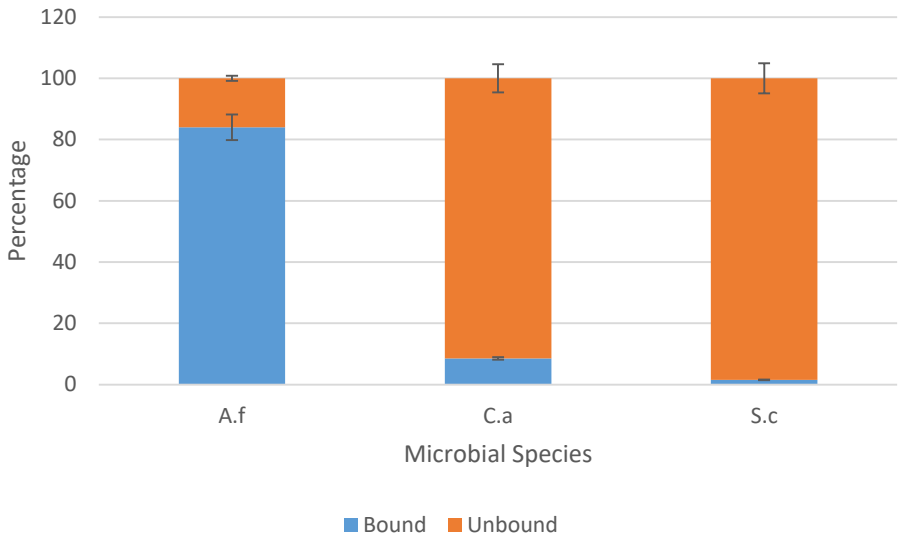

Figure 3.26 Counts of fluorescent/ non-fluorescent cells of each microbial species when incubated with Af20279 tagged with Alexa488.

The results in Figure 3.25, show an increased fluorescence in the Alex488 channel when *A. fumagatius* cells are incubated with this aptamer. This fluorescence is not observed in either of the other two fungal species*, C. albicans* or *S. cerevisiae,* indicating that this aptamer appears to be species specific. This supports the data obtained from the PCR experiments. This data is supported by a cell count that was performed, on this set of slides and another (figure 3.26).

3.11 Outcome of Negative Selections

Figure 3.27. Shortlisted aptamers incubated with HeLa cells. Each shortlisted aptamer was incubated with HeLa cells for 1 hour at room temperature at concentrations of 400nM, 200nM and 100nM. Samples of elution were taken and amplified by PCR, samples of PCR product were then run on a 2% agarose gel by gel electrophoresis. Gels were then viwed under UV light and images taken by ChemiDoc XRS+ image lab software.

Figure 3.27 shows all shortlisted aptamers (A20279, C5269, C28279, C009269, A242710 Ca4B and AfRTB) incubated with HeLa cells to confirm whether any binding to HeLa cells takes place. Each aptamer was incubated for 1 hour at concentrations of 400nM, 200nM and 100nM with HeLa cells. A sample of aptamer library was used as a positive control. No samples of aptamer were yielded by PCR following incubation implying no binding of aptamer.

4.0 Discussion

The aim of this study was to find DNA aptamers that selectively bind to the medically important fungi, *C. albicans* and *A. fumigatus,* as a means of improving both the treatment and diagnosis of infection caused by these microbes. Much like the current issues facing antibacterial treatments, many fungi are now resistant to known antifungal agents. The class of antifungals echinocandins for example have seen reported cases of resistance after just one week of treatment (Lewis *et al.* 2013). There are also specificity issues associated with some antifungal drugs, for instance the commonly used amphotericin B targets ergosterol in the cell membrane causing depolarisation of the membrane, leakage of intercellular components and eventually cell death (Brajtburg *et al*., 1990). However, amphotericin B exhibits high nephrotoxicity (Torrado *et al*., 2008). Amphotericin B is also capable of binding to cholesterol in mammalian cell membranes, which leads to depolarisation of the membrane and leakage of intracellular components. The addition of leaked K^+ and other intracellular ions into the body creates strain on the kidneys to process the excess concentration in the blood in addition to this the cells membranes of nephrons are particularly rich in sterols meaning that the effects of amphotericin B are exaggerated in kidney cells. These adverse effects are not limited to one class of antifungals, Itraconazole for example was found to have a 23% chance of treatment being discontinued due to adverse effects (Wang *et al.* 2010). The high mortality rate associated with invasive fungal infections means that the aggressive side effects are part of a necessary treatment, however, there are ways to dramatically improve this. One way in which this can be done is through the use of targeting molecules such as DNA aptamers. Their high affinity and specificity for a target and their potential for conjugation to drugs means that they can be used in conjunction with current treatments to improve the quality of treatment for patients, without the need for new drug development. As well as treatments, the slow and inefficient means of diagnosis of fungal infections can also be improved with the use of aptamer based assays (Drolet, Moon-McDermott and Romig, 1996, Tang *et al.* 2016) to create

point of care testing kits. Which in turn, lead to faster identification of treatment options and better patient prognosis (Barnes, 2008).

4.1 Optimisation of the SELEX procedure using fungal cells

The SELEX protocol was adapted from the whole cell SELEX protocol set out by Sefah *et al*. (2010). This is a published standardised method for the selection of any aptamers derived from the original aptamer work developed by Tuerk and Gold (1990). An important aspect of SELEX is the optimisation of PCR and influences of initial library amplification, in order to ensure efficiency throughout (Takahashi *et al*., 2016). Previous work had shown that amplification of the aptamer library using the PCR conditions in this paper, resulted in the formation of primer dimers, where primers anneal to each other as opposed to corresponding ends of the template sequence. This can also leads to incorrect formation of the template strand, including the addition of hairpin loops in the template from the strand folding (Tolle *et al*., 2014). Changes were made to the PCR programme to reduce the production of non-specific DNA amplification through the addition of DMSO (Hardjasa *et al*., 2010) and increase in annealing temperature to enhance the specificity of the primers used. DMSO improves amplification of the template in G and C rich sequences by lowering the denaturation temperature between G and C reducing the formation of primer-dimers and increases the accuracy of template reproduction. The ideal concentration of $MgCl_2$ was also optimised to control the folding of template strands during PCR. It is important for the PCR stages of SELEX to be optimised, as aptamer amplification is very different to homogenous DNA amplification (Musheev and Krylov, 2006). An important aspect of this is the choice of enzyme for PCR. In this case Taq polymerase

To ensure the sole amplification of aptamers and not non-specific DNA, target cells were incubated with no aptamers. These samples were then heated, eluted and centrifuged just as the positive selections were and a sample of these put through the same PCR and run on agarose gel. These samples needed to be free of any DNA to ensure that non-specific

amplification had not occurred. Figures 3.1a and 3.1b and 3.2a and 3.2b, show the positive results from each rounds PCR along with negative controls, there is no evidence of amplification of non-specific DNA, which suggests the PCR protocol has been optimised for amplification of the aptamer sequence.

4.1.2 Cell SELEX in fungi

Candida albicans and *Aspergillus fumigatus* are two of the most prevalent invasive fungi to cause infections in humans so this study concentrated on isolating aptamers against these microorganisms.

There are no published papers that detail selection of aptamers against whole cell fungi, however, there are many examples of studies describing the selection of aptamers against whole cell bacteria. Chen *et al*. (2007) found aptamers selected against *Mycobacterium tuberculosis* using 10^8 CFU/ml, decreasing to 10^5 CFU/ml in later rounds to increase selection pressure on the aptamers. Duan *et al*., 2013 also used 10^8 CFU/ml of *Shigella dysenteraie* for selection of aptamers. Initially rounds of one round of selection was undertaken with different numbers of cells, which resulted in the optimal $3x10^6$ CFU/ml *C. albicans* and $7.5x10^6$ CFU/ml of *A. fumigatus* for this study. This was found to provide enough target to narrow the aptamer pool in the initial SELEX rounds, as seen by the presence of aptamer post incubation from round one of selections (Figures 3.1a and b and 3.2a and b).

In terms of fungi there are studies detailing selection against ideal targets for aptamers like Tang *et al.* (2016) selecting aptamers against fungal cell wall component β 1- 3 D Glucan. Purified β -1,3-D glucan was used as the target molecule for rounds of selection. This study resulted in aptamers specific to β, 1-3, D glucan, however testing of the aptamer against whole cells was not performed in this study. Previous studies have indicated that while using an isolated protein as a target is a viable option, there can be problems with the binding of the aptamer when the protein is in its native conformation (Pestourie *et al*., 2006) due to the

specific nature of aptamers and the conditions that can affect protein folding. As well as β-1,3-glucans being present in all species of fungi, potentially leading to incorrect diagnosis, it is also present after some medical procedures. β-1,3- D glucans are present in cellulose membranes used in haemodialysis (leading to an increased concentration patient serum (Kanda *et al*., 2001) and cotton gauze and sponges used in surgeries (Usami *et al*., 2002).

However, aptamers they found with the highest binding affinity were taken forward for use testing patient plasma samples by sandwich ELONA (Enzyme linked oligonucleotide assay, Drolet, Moon-McDermott and Romig, 1996). The ELONA method was developed for use with existing ELISA systems, but with aptamers replacing the antibody component, and is a reliable replacement for ELISA (Toh *et al*., 2015). An industry example of this is the development of an aptamer based assay for the detection of Ochratoxin A, produced by *Aspergillus* and *Penicillium spp.* that grow on agricultural products. This mycotoxin is highly toxic even at low doses, so detection of contamination is very important. Neoventures Biotechnology Inc. commercialised a highly sensitive assay for the detection of this mycotoxin that is now commercially available (Penner, 2012). Methods like this that utilise the reliable binding potential of aptamers make for faster, cheaper and more stable point of care testing, which would help to reduce the long diagnostic processes currently used and aid with earlier detection and treatment leading to better outcomes for the patient.

C. albicans is a yeast like fungus that lives, in a budding yeast form, commensally as part of the gut biome in most healthy individuals. For the purposes of this study, aptamers were selected against the *C. albicans* yeast like form, as many of the proteins needed for hyphal formation are expressed at the cell surface in both hyphal and budding forms. In the case of *C. albicans* infection when *C. albicans* has formed a biofilm it releases cells in their yeast like form to circulate the body and spread the infection. In terms of detection, being able to identify *C. albicans* reliably in a blood test would make for better diagnosis especially because infection is

missed in around 50% of sample from blood culture (Ostrosky-Zeichner, 2012). For future work it may be beneficial to perform selections of aptamers with *C. albicans* in its hyphal form. By growing *C. albicans* in it hyphal form more specific aptamers for the infectious stages could be isolated and could be useful in the diagnosis of systemic *Candida* infections within isolated tissue samples.

For *A. fumigatus* the spores were used for selections as they could be readily re-suspended in solution whereas the whole filamentous cell does not re-suspend in solution as readily. *A. fumigatus* grows in its hyphal form once it has been established in a stationary location; however with the long incubation time of the spores it is difficult to detect infections before they have started. By selecting against the spores this would enable aptamers to be used for diagnostic purposes such as on point testing kits that could provide a quick and simple check for potential infection in patients that are known to be a high risk for infection.

Also due to the melanin coating on the cell wall of the spores, they often go undetected by the body in at risk patients because of failings in other aspects of the immune response. Other studies have detailed the use of aptamer conjugates as a means of improving the bodies non-specific immune response (Bruno, Carrillo and Phillips, 2008).

Preliminary rounds of SELEX were performed to optimise the number of *C. albicans* cells and *A. fumigatus* spores used. *Saccharomyces cerevisiae* was used as part of the initial optimisation of the SELEX procedure (data not shown) due to its similarities to *C. albicans* and its wide use as a model organism (Karathia *et al*., 2011). The number of cells used is a key part of optimisation, too many cells and the likelihood of selecting aptamers with high levels of specificity decreases as cell numbers is a selection pressure, but not enough cells and there would not be enough to isolate aptamers from the library as the selection pressures would be too high (Spill *et al*., 2016 and Wang *et al.,* 2012).

Diagnosis is not the only issue with patient treatment, high toxicity resulting from non-specific action of current antifungal treatments could be reduced with the development of drug aptamer conjugates. For instance an aptamer that would bind specifically to ergosterol in the cell membrane and not affect cholesterol synthesis in surrounding mammalian tissue would greatly improve the efficacy of amphotericin B. Also more specific targeting would reduce the necessary dose and also help to reduce the toxicity of amphotericin B. By using whole cell SELEX the target of the aptamer is not limited, and the addition of negative selections to reduce the number of non-specific aptamers greatly improves the quality of aptamers from the final round.

4.1.3 Temperature as a condition for SELEX in fungal cells.

Fungi have long been used for the transformation of DNA exhibiting their ability to internalise extracellular DNA. Aptamers were selected at 4°C and room temperature. At 4°C cell membrane transport processes are inactive (komai *et al*., 1992) so this limits the internalisation of aptamers thus limiting aptamer targets to the cell membrane. Room temperature selections were also performed to allow active transport processes to continue and aptamers be internalised with the hopes of gaining aptamers that were internalised and aptamers with cell membrane targets. Room temperature selections also served as a more real world applicable condition. As diagnostic tests, on blood culture for example, would be run at room temperature, having an aptamer that's binding has been optimised for room temperature would make the transition from discovery to application easier.

Temperature is also important for the folding of aptamers as temperature affects secondary and tertiary structure of DNA.

4.1.4 Negative Selections in whole cell SELEX

The addition of a negative selection step in the SELEX process allows aptamers that bind with the negative control to be removed from the aptamer library. As suggested by Sefah *et al.* (2010) and carried out by Dwivedi, Smiley and Jaykus, (2013) and Tang *et al.* (2016). A closely related cell type was added and the aptamers that bound to his cell type were removed from selections, this improves specificity of aptamers. This was especially critical for this study as one of the issues associated with antifungals is their non-specific action affecting human tissue. Other aptamer studies have also used a counter selection step to distinguish between closely related targets (Cerchia *et al.*, 2009) and to improve the specificity of aptamers to the target cell (Moon *et al.*, 2015). HeLa cells were used in this study as a negative selection to eliminate binding to mammalian cells. HeLa cells are a well-established and versatile cell line used in many branches of research.

HeLa cells were treated with trypsin to detach them from the surface of the flask to be used for selections. Trypsin is a common method for detaching cells from their surface however trypsin damages the cell membrane in order to detach cells, so prolonged incubation with trypsin causes cell membrane damage, and can affect many of the proteins that are expressed on the membrane of the cell (Huang *et al.*, 2010). This can affect the binding of the aptamer as using damaged cells for a negative selection might only guarantee no binding to the damaged protein. This could mean that, the aptamer could bind to the wild type, expressing a normal version of that protein as very subtle changes in structure of the target can differentiate between a binding and non-binding aptamer. 10,000 HeLa cells were used in this study, to provide sufficient exclusion of binding aptamers.

4.1.5 Isolating aptamers against *A. fumigatus* and *C. albicans* using cell SELEX

A total of ten rounds of selections were undertaken for this study. Through each round of selection the amount of aptamer amplification is monitored (shown in figures 3.1 and 3.2) to show whether amplification of binding aptamers has occurred between rounds. There were instances where bands of varying sizes were separated during gel electrophoresis, to eliminate the DNA from these bands and to reduce the amplification of non-specific DNA (Tolle *et al*., 2014 and Musheev and Krylov, 2006) a gel extraction was performed (Dwivedi, Smiley and Jaykus, 2013) between each round to carry forward amplification of aptamers of the correct size. However there are issues associated with gel extraction, the yield of the desired size DNA sample following gel extraction can reduce dramatically (Langridge, Langridge and Bergquist, 1980). This can be due to the improper melting of the agarose gel, or loss during the many washing steps involved with a gel extraction. In future it may be beneficial to limit the number of gel extractions performed throughout the selection process, to reduce the potential loss of aptamers.

The apparent decrease in the amount of aptamers through each round could be caused by the narrowing of the aptamer pool as each round further excludes non-binding aptamers. However, there are variations in each selection, most studies expect to see a decrease in the amount of aptamer amplified as the aptamer pool narrows as non-binding aptamers are eliminated from the pool. This is expected to then be followed by an increase in PCR product concentrations as the binding aptamers remaining in the pool are amplified. *A. fumigatus* at room temperature (figure 3.2b) reflects this pattern the best out of all conditions, and was the only condition to produce 4 positive colonies at the cloning stage, and also the only conditions to produce 2 of the same sequence, suggesting this condition was more abundant in binding aptamers. Figure 3.2a shows the PCR products of rounds of selection in *A. fumigatus* at 4°C, the concentration of PCR product appears to decline up to round 9, where is suddenly

increases. This suggests that the process of narrowing the aptamer pool took more rounds of selection in this condition, and that to improve the quality of aptamers gained from this condition it would be beneficial to carry out more rounds of selection to allow sufficient amplification of binding sequences. Figures 3.1a and b show selections in *C. albicans* at both temperature selections, these are far more varied and do not seem to show the same pattern that figures 3.2a and b show. There are a number of uncertainties during the SELEX procedure, one of which is the unexpected loss of aptamers

4.1.6 Determining levels of aptamer binding

However other studies use different methods of measuring their post selections amplification. Shangguan, Bing and Zhang (2015) used flow cytometry binding assays to determine the levels of binding after certain rounds of selection. They also saw a much more consistent level of amplification throughout the rounds of selection. Duan *et al*. (2013) used fluorescence intensity as a measure of aptamer binding as part of their second stage testing to calculate the Kd for their aptamers. For future work it would be worth considering using fluorescence intensity to confirm the viability of the method used and better monitor the amount of amplification following each round.

4.1.7 Isolating aptamers by TOPO Cloning

The product from round 10 of each selection condition was amplified by PCR as previously described and then cloned into a TOPO vector. These vectors were then transformed in chemically competent *E. coli* and grown. Only 11 colonies in total were obtained from all four selection conditions, considerably less than expected. This may have been due to the fact that the TOPO vector relies on an A overhang on the end of each sequence which must be added post PCR. A different vector like JetClone could have been used which relies on blunt ends, and therefore does not rely on additions during PCR.

4.2 Characterisation of isolated aptamers

4.2.1 Sequencing of isolated aptamers

The primary structure of DNA is made up of a series of nucleotides, the sequence of which is important for folding and, therefore, binding of the aptamer to its target.

The isolated aptamers, obtained following cloning from SELEX round 10 of, were sent for sequencing. The sequences were then analysed through the Clustal Omega software (with primer sequences removed) and an output of percentage similarities between each sequence was analysed.

The phylogenetic tree (figure 3.4a) groups the sequences into three main families, suggesting three distinct epitopes. Aptamers that were selected at the same temperature appear to be more closely related than aptamer that were selected against the same species. Within the first branch, AFRTD and CARTA are more closely related, as are CA4A and AF4B, than CaRTA to Ca4A or AfRTD to Af4B. In the third branch, CA4C and CA4B are closely related to each other than AFRTA.

For instance aptamers Ca4B and Ca4C share 53.85% similarity whereas between other aptamers from *C. albicans* at 4°C it is below 35%. Between conditions, within *C. albicans* varies again with the highest homologue being between Ca4A and CaRTB at 47.17% and the lowest Ca4C and CaRTA at 15.69%. For *A. fumigtus* sequences AfRTB and AfRTC were found to be the same sequence implying that this sequence was more abundant following isolation against this condition. These sequences also had their own distinct epitope in figure 4a, meaning they are not closely related to any of the other aptamers.

Sequences were also aligned by Clustal Omega to show any conserved regions between aptamers, as this may indicate whether aptamers share similar targets or whether there are

regions of aptamers that are important for binding. The aptamers indicated to be closely related by the phylogenetic tree (figure 3.4a) were aligned, AfRTD and CaRTA showed a total of 32 consensus bases, with one group six, one group of five and two groups of four. CA4A and AF4B, were also shown to be closely related showing 26 consensus bases, with one group of 5 and one group of 4 conserved bases. Finally, CA4C and CA4B showed 25 consensus bases, with one group of 5 conserved bases.

4.2.2 Secondary Structure of isolated aptamers

Secondary structure was predicted using Mfold software, as this can indicate key regions of aptamers for binding. Conditions set for folding were based on the ion concentration dictated by the binding buffer used during incubation of aptamers and target cells, as the folding during incubation heavily influences the aptamers binding ability. Mg^{++} concentration was 0.25mM in binding buffer. Hamula *et al.* (2008) used a binding buffer with 1mM Mg^{++}, this study opted for a much lower concentration as aptamers with a higher binding affinity rely less on Mg^{++} concentration (Carothers *et al*., 2010). Predicted secondary structure has been used to identify specific regions of aptamers, key for binding, based on the comparison of several aptamers secondary structures (Mei *et al.*, 2012). These predictions have also been used in the modification of identified aptamers to improve binding. Kaur and Yung (2012), after determining the structure of an aptamer against VEGF165, truncated stem loop regions of the aptamer and found that a truncation of one of the stem loop regions led to a dramatic increase in binding affinity of the aptamer. However, tertiary structure is also important for aptamer binding (Wang *et al*., 1993) as many targets are complex three dimensional structures, aptamers must fold to fit these structures for better binding affinity (Choi and Ban, 2016).

The predicted structures of identified aptamers vary considerably in similarity. Figure 4a shows aptamers selected against *C. albicans* at 4°C, Ca4A and Ca4B show similarities in predicted folding, with both aptamers having predicted stem loop structures which have been shown to

be important for aptamer binding (Kaur and Yung 2012). For aptamers selected against *C. albicans* at room temperature there is less stem structures than seen in the 4°C aptamers, with larger loop regions comprising the main structure. The aptamers selected at 4°C in *C. albicans* share more similarities in structure with aptamers selected at 4°C in *A. fumigatus*, with these aptamers also containing more stem regions. Aptamers selected against *A. fumigatus* at room temperature show the largest loop regions of all of the structures, but bearing most similarity to *C. albicans* at room temperature aptamers.

4.2.3 Characterisation of Identified Aptamers

All identified aptamers were further tested in both temperature conditions and against each target cell. Incubation time was reduced from 1 hour to 30minutes to increase selective pressure (as performed by Meyer *et al*., 2013). 200nm of each aptamer was incubated with both *C. albicans* and *A. fumigatus* at 4°C and room temperature. PCR samples from each elution was then run on agarose gel and visualised by UV light. To enable quantification of the bound aptamer, a sample of aptamer library at a concentration of 171ng/µl was used a reference.

Each aptamer was tested at both room temperature and 4°C despite the selection. When testing all aptamers some showed little to no difference between binding levels at 4°C and room temperature, CaRTB, AfRTA, CaRTA and Af4B for example in figure 6 all show a difference of less that 2ng/µl in aptamer binding between 4°C and room temperature.

The aptamers with the highest yield following incubation in their target cells, but limited product in the opposing cell type, were considered for further testing. This was determined by comparing the yields of aptamers to each other, aptamers were judged based on the levels of binding they exhibited between species of targets and also compared to a control of an aptamer with known specificity for that species. For instance Ca4A yielded 10ng/µl at 4°C, which implies recovery from elution and thus binding to *C. albicans*, however, when incubated

with *A. fumigatu*s yielded 11.2ng/µl showing that this aptamer also binds to *A. fumigatus*. So although this aptamer shows levels of binding, it was not to be tested further as it does not exhibit the desired level of specificity. Aptamers CaRTA and AfRTA showed relatively poor binding in both *C. albicans* and *A. fumigatus* with a minimum 4 fold decrease in binding compared to Af20 and C9. AfRTD and Ca4A showed very little difference in their binding between species, both at around 9ng/µl in *C. albicans* and around 12ng/µl in *A. fumigatus*. Aptamers Af4A and Af4B also followed the same pattern. This may be due to the targets that the aptamer has bound to. A common target in fungal cells for antifungals is the cell wall component β 1-3 D Glucans and their abundance throughout the cell wall, and non-existence in mammalian cells makes them an easy target. It is likely that a lot of the aptamers have this as their target or other cell wall components and thus no matter the selection temperature were not taken up into the cell meaning they would bind just as well at room temperature than 4°C.

The aptamers that were taken forward for further testing were AfRTB and Ca4B. AfRTB showed promising amounts of specificity to *A. fumigatus* with a yield of only 5.9ng/µl after incubation with *C. albicans* but a near threefold increase in binding after incubation with *A. fumigatus*. This was also the most comparable to the control aptamer Af20 which 19ng/µl at room temperature and was also the highest yield from aptamers incubated with *A. fumigatus*. Ca4B was also selected because of its promising specificity for *C. albicans*, yielding 7.6ng/µl after incubation with *A. fumigatus* at 4°C but yielding double that (15ng/µl) after incubation with *C. albicans*. Despite the control aptamer C9 exhibiting double the levels of binding this Ca4B showed the best levels of specificity in comparison to other identified aptamers selected against *C. albicans*.

4.2.4 Further Testing of Selected Aptamer

Aptamers that showed the most specificity and affinity in binding by PCR were selected to move forward to further testing. Aptamers were tested at different concentrations to determine the limitations of their binding, allowing the Kd for each aptamer to be calculated. The Kd (disassociation constant) represents the concentration of a ligand that binds to half of the receptor population. In this case, half the concentration of aptamer required to bind to all of its targets. By testing the binding of the isolated aptamers at 200nM, 100nM, 50nM and 25nM a pattern of binding potential can be determined and the kd calculated. In this instance kd was calculated using Graphpad Prism software, from the determined concentration of aptamer in each band of DNA following elution and PCR (as described in section 4.2.3). The kd could have been calculated using fluorescence intensity. An aptamer tagged with a fluorescent molecule, incubated with target cells and processed by flow cytometry would mean a larger number of cells could be processed, at a larger number of different aptamer concentrations and a more accurate representation of binding in the target gained.

Each of the aptamers shortlisted for further testing were incubated with HeLa cells for 1 hour at concentrations of 400nm, 200nm and 100nm. Covering a range of concentrations both above and below the selection concentration and incubating aptamers with HeLa cells for longer meant that the conditions for aptamers to potentially bind were favourable. However no binding occurred of the aptamers to HeLa cells indicating the effectiveness of the use of a negative selection. Although only on one cell line, shows the potential use of aptamers as a means of clearly distinguishing between fungal cells components and their similar mammalian counterparts.

4.3 Visualisation of Binding

Binding was visualised by use of fluorescence microscopy. Aptamers were conjugated with either Alexa488 or Cy5 fluorescence molecule and the SELEX protocol carried out as previously

described without removal of the aptamer from target cells. Cells were then fixed with formaldehyde and mounted on slides with Vectasheild.

Figure 10 shows very faint fluorescence AfRTB tagged with Cy5 in *A. fumigatus*, with no fluorescence observed in *C. albicans*. The data seems to suggest binding of AfRTB to its target cell and supports the PCR results (Figures 8A and 8B). However it is very faint, and

Figure 11 shows Cy5 bound Ca4B incubated with *C. albicans,* which seems to indicate no binding. However, when incubated with *A. fumigatus*, several areas of intense fluorescence were observed which corresponded with clumping of the cells. The PCR data suggested that Ca4B was able to bind to both cells types, but with more specificity to *C. albicans*. This result is not supported by the fluorescence data. This image when viewed with DAPI stain and brightfield, appears to shows a large clump of *A. fumigatus* cells, a mixture of spores and the hyphae. Before use, spores of *A. fumigatus* were cultivated by loop transfer from an SAB agar plate, washed, and vortexed to ensure free suspension of the spores. However, it is possible that in this process, an amount of hyphal cells were inadvertently included in transfer. These hyphal cells are very difficult to separate, so it is likely that they would maintain this structure even with rigorous vortexing. The images are representative of this set of data and a repeat, where the same results were observed. Controls with no aptamer were imaged to account for and remove background fluorescence.

4.4 Future Improvements

The selected aptamers show some specificity but this is limited. A potential solution to this would be to include each of the other cell types as negative selections. As done by Bachtiar, Srisawat and Bachtiar, (2019) who used *S. cerevisiae* as a counter selection. This study would benefit from the use of the same, using *S. cerevisiae* as a counter selection for *C. albicans* and also *A. fumigatus*. This would improve the specificity issues between species.

4.5.1 Characterisation of Previously Identified Aptamers

A set of 14 aptamers had been previously identified following 16 rounds of selection against *A. fumigatus*, *C. albicans* and *S. cerevisiae* at 4°C, with a negative selection against HeLa cells. These aptamers hadn't been characterised, so they were tested to determine their specificity to the relevant fungal species. Each aptamer was incubated with each target cell for 30minutes before the concentration of the bound aptamer was determined by PCR. These concentrations of aptamer following incubation were compared to the elution concentration of aptamer library sample incubated with each cell type. In order for an amount to be considered a good level of binding it must be higher than the amount from the aptamer library sample to demonstrate the higher abundance of binding sequences.

4.5.2 Sequencing of Previously Identified Aptamers

As with the above set of aptamers, this set was sent for sequencing following isolation. The phloygenetic tree (figure 12a) suggests three distinct epitopes. Two of the branches containing two aptamers each (C9269 and Af031810 together and S12709 and S71810 together) and a third branch containing the remaining 10 aptamers, within this Ca28269 and A24279 are very closely related, and the sequences A21279 and A20279B are the same, as are C005269 and C5269. The sequences grouped as closely related were aligned to highlight any conserved regions between them. Based on the phylogenetic tree, the closely related sequences Ca28269 and A24279 showed 22 consensus bases, with one group of 5 and two groups of 4 conserved bases (Figure ?A). A202710 and Af021810, were also shown to be closely related showing 21 consensus bases, with two group of 4 and one group of 3 conserved bases. Finally, S12709 and S71810 showed 35 consensus bases, with one group of 15 and two groups of 4 conserved bases.

4.5.3 Secondary structures of previously identified aptamers

The predicted secondary structures of the previously identified aptamers vary considerably regardless of the target cell they were selected against. *C. albicans* selected aptamers C009269 and C9269 show a majority of stem loop structures, whilst Ca28269 consists of a larger middle loop region with 4 smaller stems. C5269 again shows a middle loop region, but much smaller than that of Ca28269 and 4 stem loop structures, with one much longer stem. S1279 and S71810 (both selected against *S. cerevisiae*) both show long stem regions with small loops. When these two sequences were aligned they showed 59% similarity with 35 consensus bases, one group of 15 and two groups of four. However both aptamers did not share consistent similarities in binding properties. Incubated with *S. cerevisae* S12709 yielded the lowest aptamer following incubation (0.3ng/µl) and S71810 the second lowest (2.6ng/µl). The aptamer library control was 2.3ng/µl, meaning that S71810 is deemed as showing very poor binding and S12709 shows poor binding being barely above the control. However, S12709 shows better levels of binding in *C. albicans* (3.4ng/µl) and considerably better levels of binding in *A. fumigatus* (8.4ng/µl) whilst S71810 remains below the levels of aptamer library control binding for all targets. This could indicate that the consensus bases, more probably the larger group of 15 consensus bases (as this would likely have the largest impact on structure) could be detrimental to binding of this aptamer to *S. cerevisiae*.

Aptamers selected against *A. fumigatus* appear to show less variation in the predicted secondary structure than described in the previous aptamers. All appear to form a large loop in the middle, with 4-5 small stem loop structures. With the exception of Af021810, which is mainly comprised of a long stem loop region, and a smaller loop, with another stem loop region attached. Af021810 was grouped closely with A202710 on the phylogenetic tree (figure12A) and shares 21 consensus bases. As summarised on table 3.2, Af021810, shows less

affinity against all target cell types than Af202710, this suggests that the consensus regions highlighted are not crucial for binding.

4.5.4 Binding of previously identified aptamers

Figure 15 shows all the aptamers tested against *C. albicans*. The aptamers that were originally selected against *C. albicans* showed relatively low levels of binding compared to the levels of binding seen with aptamers selected against *A. fumigatus* of *S. cerevisiae*. For example all aptamers selected against *C. albicans* yield less than 5ng/µl, whereas aptamers incubated with *A. fumigatus* range from no binding, to just under 10ng/µl and aptamers incubated with *S. cerevisiae* range from no binding to over 10ng/µl. There is also an abundance of aptamers that show degrees of binding across species. Af021810 and S8279 show similar levels of binding across species, whereas C5269 shows binding across species but with even more binding to *A. fumigatus*. As previously mentioned, all species of fungi share the general composition of the cell wall and membrane. However there are differences in the levels that these components are expressed at. Chitin for example, represents a relatively low proportion of fungi cell wall, however it is far more abundant in *S. cerevisiae* (Lesage and Bussey, 2006). This could explain the binding of Ca28269, where there were relatively low levels of binding in *C. albicans* and *A. fumigatus* but much higher levels of binding in *S. cerevisiae*. Chitin is present in the membrane of *C. albicans* and therefore a viable target for aptamer binding during selection.

Figure 16 shows the binding of all previously identified aptamers against *A. fumigatus*. As previously stated the aptamers incubated showed more varied levels of binding than in *C. albicans*. The aptamers C5269, C05269 and C009269 all showed higher levels of binding affinity despite the fact that they were selected against *C. albicans*.

All of the aptamers incubated with *C. albicans* for figure 15 appear to have a much lower yield than those incubated in *A. fumigatus* and *S. cerevisiae*. For instance, C009269 was taken forward for further testing, in figure 15 the yield of this aptamer is 2.2ng/µl whereas when incubated at a 200nM concentration (figure 15) to determine its Kd the yield was much higher at 6.6ng/µl. The same is also true for Ca28269 which yielded 9.867ng/µl in figure 14 compared to just 3.1ng/µl in figure 15. Each incubation was repeated twice and controls containing cells with no aptamer and aptamer with no cells gave the expected results. This suggests that there was no non-specific amplification occurring and that there was sufficient amplification of DNA during PCR. This would then leave the inconsistencies to have occurred during incubation. There are many points at which error could occur. The amount of aptamer bound to target cells was measured by comparing the intensity of visualised PCR samples at the end of each round to DNA aptamer of known concentration. This method relies on the elution of all bound aptamers from the cell (if not all then a similar percentage of each sample) which was not investigated. This could affect yields of aptamer between the same samples. However, the same aptamer PCR programme and conditions were used for every PCR so the amplification of each sample is kept at a constant. Also the measuring of each sample was always compared to the same sample of known concentration, and was run on every gel. So variations in overall intensity of bands on the agarose gel following electrophoresis was accounted for. In addition to this, according to other sources 95°C heating followed by centrifugation is sufficient to elute enough aptamers to use in subsequent rounds of SELEX (Mozioglu et al., 2015 and Turek, 2013) so with this assumption the amount of aptamer remaining within the discarded cells should not make a large difference to the aptamer pool.

4.5.5 Af20279B

Af20279B was determined as having the best affinity for *A. fumigatus* and the best specificity, with a kd of The aptamer Af202710 showed good levels of affinity and specificity and when

analysed under fluorescence microscope showed good binding to *A. fumigatus* and low levels of binding to *C. albicans* and *S. cerevisiae*. The fluorescence data is supported by a cell count of 100 cells, and their fluorescence for each target species, this was repeated twice, and the images shown in figure

4.5.6 Further Testing

In order to take the testing of these aptamers further a target of each aptamer would need to be defined, done by Aptoprecipitation as performed by Aptekhar et al. (2015). This uses the isolated aptamer to bind to separated proteins from the target cell. Whichever proteins bind can then be characterised and therefor the target determined.

An important aspect of this study would be to determine kd of the aptamers from this study compared to aptamers identified by published literature. Currently in this study there is only reference to each of the aptamers for how well each aptamer binds, in order to gain a better picture of overall binding, and how well the binding of these aptamers would be used in the real world a comparison to the binding affinity of other aptamers would have to be performed.

References

Abe, F., Usui, K. and Hiraki, T. (2009). Fluconazole Modulates Membrane Rigidity, Heterogeneity, and Water Penetration into the Plasma Membrane inSaccharomyces cerevisiae. *Biochemistry*, 48(36), pp.8494-8504.

Arendrup, M., Prakash, A., Meletiadis, J., Sharma, C. and Chowdhary, A. (2017). Comparison of EUCAST and CLSI Reference Microdilution MICs of Eight Antifungal Compounds for Candida auris and Associated Tentative Epidemiological Cutoff Values. *Antimicrobial Agents and Chemotherapy*, 61(6).

Armstrong-James, D., Meintjes, G. and Brown, G. (2014). A neglected epidemic: fungal infections in HIV/AIDS. *Trends in Microbiology*, 22(3), pp.120-127.

Aptekar, S., Arora, M., Lawrence, C., Lea, R., Ashton, K., Dawson, T., Alder, J. and Shaw, L. (2015). Selective Targeting to Glioma with Nucleic Acid Aptamers. PLOS ONE, 10(8), p.e0134957.

Bachtiar, B., Srisawat, C. and Bachtiar, E. (2019). RNA aptamers selected against yeast cells inhibit Candida albicans biofilm formation in vitro. *MicrobiologyOpen*, p.e812.

Barnes, R. (2008). Early diagnosis of fungal infection in immunocompromised patients. *Journal of Antimicrobial Chemotherapy*, 61(Supplement 1), pp.i3-i6.

Beauvais, A. and Latgé, J. (2015). Aspergillus Biofilm In Vitro and In Vivo. *Microbiology Spectrum*, 3(4).

Beffa T., Staib F., Lott Fischer J., Lyon P.-F., Gumowski P., Marfenina O. E., DunoyerGeindre S., Georgen F., Roch-Susuki R., Gallaz L., Latgé J.P. (1998). Mycological control and surveillance of biological waste and compost. Medical Mycology, 36 (suppl.I), 137-145.

Bénet, T., Voirin, N., Nicolle, M., Picot, S., Michallet, M. and Vanhems, P. (2013). Estimation of the incubation period of invasive aspergillosis by survival models in acute myeloid leukemia patients. *Medical Mycology*, 51(2), pp.214-218.

Brajtburg, J., Powderly, W., Kobayashi, G. and Medoff, G. (1990). Amphotericin B: current understanding of mechanisms of action. *Antimicrobial Agents and Chemotherapy*, 34(2), pp.183-188.

Brogden, K., Phillips, M., Thurston, J. and Richard, J. (1984). Electron microscopic examination of ribosome preparations from germinated spores of Aspergillus fumigatus. *Mycopathologia*, 86(1), pp.59-64.

Brown, G., Denning, D. and Levitz, S. (2012). Tackling Human Fungal Infections. *Science*, 336(6082), pp.647-647

Brown, G., Denning, D., Gow, N., Levitz, S., Netea, M. and White, T. (2012). Hidden Killers: Human Fungal Infections. *Science Translational Medicine*, 4(165), pp.165rv13-165rv13.

Bruno, J., Carrillo, M. and Phillips, T. (2008). In Vitro antibacterial effects of antilipopolysaccharide DNA aptamer-C1qrs complexes. *Folia Microbiologica*, 53(4), pp.295-302.

Bukhary ZA. Candiduria: A review of clinical significance and management. Saudi J Kidney Dis Transpl. 2008;19(3):350–60

Carothers, J., Goler, J., Kapoor, Y., Lara, L. and Keasling, J. (2010). Selecting RNA aptamers for synthetic biology: investigating magnesium dependence and predicting binding affinity. *Nucleic Acids Research*, 38(8), pp.2736-2747.

Cassone, A. and Cauda, R. (2012). Candida and candidiasis in HIV-infected patients. *AIDS*, 26(12), pp.1457-1472.

Cerchia, L., Esposito, C., Jacobs, A., Tavitian, B. and de Franciscis, V. (2009). Differential SELEX in Human Glioma Cell Lines. *PLoS ONE*, 4(11), p.e7971.

Chen, F., Zhou, J., Luo, F., Mohammed, A. and Zhang, X. (2007). Aptamer from whole-bacterium SELEX as new therapeutic reagent against virulent Mycobacterium tuberculosis. *Biochemical and Biophysical Research Communications*, 357(3), pp.743-748.

Choi, S. and Ban, C. (2016). Crystal structure of a DNA aptamer bound to PvLDH elucidates novel single-stranded DNA structural elements for folding and recognition. *Scientific Reports*, 6(1).

Chowdhary, A., Sharma, C. and Meis, J. (2017). Candida auris: A rapidly emerging cause of hospital-acquired multidrug-resistant fungal infections globally. *PLOS Pathogens*, 13(5), p.e1006290.

Cools H. J, Fraaije B. A. , Pest Manag. Sci. 64, 681–684 (2008)

Cruz, M., Graham, C., Gagliano, B., Lorenz, M. and Garsin, D. (2013). Enterococcus faecalis Inhibits Hyphal Morphogenesis and Virulence of Candida albicans. *Infection and Immunity*, 81(1), pp.189-200.

Diasio RB, Bennett JE, Myers CE. Mode of action of 5-fluorocytosine. Biochem Pharmacol 1978; 27(5):703–707

Drolet, D., Moon-McDermott, L. and Romig, T. (1996). An enzyme-linked oligonucleotide assay. *Nature Biotechnology*, 14(8), pp.1021-1025.

Duan, N., Ding, X., Wu, S., Xia, Y., Ma, X., Wang, Z. and Chen, J. (2013). In vitro selection of a DNA aptamer targeted against Shigella dysenteriae. *Journal of Microbiological Methods*, 94(3), pp.170-174.

Dwivedi, H., Smiley, R. and Jaykus, L. (2013). Selection of DNA aptamers for capture and detection of Salmonella Typhimurium using a whole-cell SELEX approach in conjunction with cell sorting. *Applied Microbiology and Biotechnology*, 97(8), pp.3677-3686.

Ellepola, A. and Morrison, C. (2005). Laboratory diagnosis of invasive candidiasis. *The Journal of Microbiology*, 43(1), pp.65-84.

Gow, N., van de Veerdonk, F., Brown, A. and Netea, M. (2011). Candida albicans morphogenesis and host defence: discriminating invasion from colonization. *Nature Reviews Microbiology*, 10(2), pp.112-122.

Greenspan, D. and Greenspan, J. (1996). HIV-related oral disease. *The Lancet*, 348(9029), pp.729-733.

Hall, R., De Sordi, L., MacCallum, D., Topal, H., Eaton, R., Bloor, J., Robinson, G., Levin, L., Buck, J., Wang, Y., Gow, N., Steegborn, C. and Mühlschlegel, F. (2010). CO2 Acts as a Signalling Molecule in Populations of the Fungal Pathogen Candida albicans. *PLoS Pathogens*, 6(11), p.e1001193.

Hamula, C., Zhang, H., Guan, L., Li, X. and Le, X. (2008). Selection of Aptamers against Live Bacterial Cells. *Analytical Chemistry*, 80(20), pp.7812-7819.

Hardjasa, A., Ling, M., Ma, K. and Yu, H. (2010). Investigating the Effects of DMSO on PCR Fidelity Using a Restriction Digest-Based Method. *Journal of Experimental Microbiology and Immunology*, 14, pp.161-164.

Hornby, J., Jensen, E., Lisec, A., Tasto, J., Jahnke, B., Shoemaker, R., Dussault, P. and Nickerson, K. (2001). Quorum Sensing in the Dimorphic Fungus Candida albicans Is Mediated by Farnesol. *Applied and Environmental Microbiology*, 67(7), pp.2982-2992.

Huang, H., Hsing, H., Lai, T., Chen, Y., Lee, T., Chan, H., Lyu, P., Wu, C., Lu, Y., Lin, S., Lin, C., Lai, C., Chang, H., Chou, H. and Chan, H. (2010). Trypsin-induced proteome alteration during cell subculture in mammalian cells. *Journal of Biomedical Science*, 17(1), p.36.

Jöchl, C., Loh, E., Ploner, A., Haas, H. and Hüttenhofer, A. (2009). Development-dependent scavenging of nucleic acids in the filamentous fungus Aspergillus fumigatus. *RNA Biology*, 6(2), pp.179-186.

Kanda, H., Kubo, K., Hamasaki, K., Kanda, Y., Nakao, A., Kitamura, T., Fujita, T., Yamamoto, K. and Mimura, T. (2001). Influence of various hemodialysis membranes on the plasma (1→3)-β-D-glucan level. *Kidney International*, 60(1), pp.319-323.

Kaur, H. and Yung, L. (2012). Probing High Affinity Sequences of DNA Aptamer against VEGF165. *PLoS ONE*, 7(2), p.e31196.

Karathia, H., Vilaprinyo, E., Sorribas, A. and Alves, R. (2011). Saccharomyces cerevisiae as a Model Organism: A Comparative Study. *PLoS ONE*, 6(2), p.e16015.

Kathiravan, M., Salake, A., Chothe, A., Dudhe, P., Watode, R., Mukta, M. and Gadhwe, S. (2012). The biology and chemistry of antifungal agents: A review. *Bioorganic & Medicinal Chemistry*, 20(19), pp.5678-5698.

Kaur S., and Singh S. (2014) Biofilm formation by *Aspergillus fumigatus* . Med Mycol, 52(1), pp.2–9

komai, T., Shigehara, E., Tokui, T., Koga, T., Ishigami, M., Kuroiwa, C. and Horiuchi, S. (1992). Carrier-mediated uptake of pravastatin by rat hepatocytes in primary culture. *Biochemical Pharmacology*, 43(4), pp.667-670.

Langridge, J., Langridge, P. and Bergquist, P. (1980). Extraction of nucleic acids from agarose gels. *Analytical Biochemistry*, 103(1), pp.264-271.

Latgé, J. (1999). Aspergillus fumigatus and Aspergillosis. *Clinical Microbiology Reviews*, 12(2), pp.310-350.

Leberer, E., Harcus, D., Dignard, D., Johnson, L., Ushinsky, S., Thomas, D. and Schröppel, K. (2001). Ras links cellular morphogenesis to virulence by regulation of the MAP kinase and cAMP signalling pathways in the pathogenic fungus Candida albicans. *Molecular Microbiology*, 42(3), pp.673-687.

Lesage, G. and Bussey, H. (2006). Cell Wall Assembly in Saccharomyces cerevisiae. *Microbiology and Molecular Biology Reviews*, 70(2), pp.317-343.

Lewis, J., Wiederhold, N., Wickes, B., Patterson, T. and Jorgensen, J. (2013). Rapid Emergence of Echinocandin Resistance in Candida glabrata Resulting in Clinical and Microbiologic Failure. Antimicrobial Agents and Chemotherapy, 57(9), pp.4559-4561

Lim, C., Seo, J., Park, S., Hwang, H., Lee, H., Lee, S., Chae, E., Do, K., Song, J., Kim, M. and Kim, S. (2012). Analysis of initial and follow-up CT findings in patients with invasive pulmonary aspergillosis after solid organ transplantation. *Clinical Radiology*, 67(12), pp.1179-1186.

Lo, H., Köhler, J., DiDomenico, B., Loebenberg, D., Cacciapuoti, A. and Fink, G. (1997). Nonfilamentous C. albicans Mutants Are Avirulent. *Cell*, 90(5), pp.939-949.

Lu, Y., Su, C. and Liu, H. (2014). Candida albicans hyphal initiation and elongation. *Trends in Microbiology*, 22(12), pp.707-714.

Matsubara, V., Wang, Y., Bandara, H., Mayer, M. and Samaranayake, L. (2016). Probiotic lactobacilli inhibit early stages of Candida albicans biofilm development by reducing their growth, cell adhesion, and filamentation. *Applied Microbiology and Biotechnology*, 100(14), pp.6415-6426.

Mei, H., Bing, T., Yang, X., Qi, C., Chang, T., Liu, X., Cao, Z. and Shangguan, D. (2012). Functional-Group Specific Aptamers Indirectly Recognizing Compounds with Alkyl Amino Group. *Analytical Chemistry*, 84(17), pp.7323-7329.

Meyer, S., Maufort, J., Nie, J., Stewart, R., McIntosh, B., Conti, L., Ahmad, K., Soh, H. and Thomson, J. (2013). Development of an Efficient Targeted Cell-SELEX Procedure for DNA Aptamer Reagents. *PLoS ONE*, 8(8), p.e71798.

Mircescu, M., Lipuma, L., van Rooijen, N., Pamer, E. and Hohl, T. (2009). Essential Role for Neutrophils but not Alveolar Macrophages at Early Time Points followingAspergillus fumigatusInfection. *The Journal of Infectious Diseases*, 200(4), pp.647-656.

Mora, C., Tittensor, D., Adl, S., Simpson, A. and Worm, B. (2011). How Many Species Are There on Earth and in the Ocean?. *PLoS Biology*, 9(8), p.e1001127.

Morgan, J., Wannemuehler, K., Marr, K., Hadley, S., Kontoyiannis, D., Walsh, T., Fridkin, S., Pappas, P. and Warnock, D. (2005). Incidence of invasive aspergillosis following hematopoietic stem cell and solid organ transplantation: interim results of a prospective multicenter surveillance program. Medical Mycology, 43(s1), pp.49-58.

Moyes, D., Wilson, D., Richardson, J., Mogavero, S., Tang, S., Wernecke, J., Höfs, S., Gratacap, R., Robbins, J., Runglall, M., Murciano, C., Blagojevic, M., Thavaraj, S., Förster, T., Hebecker, B., Kasper, L., Vizcay, G., Iancu, S., Kichik, N., Häder, A., Kurzai, O., Luo, T., Krüger, T., Kniemeyer, O., Cota, E., Bader, O., Wheeler, R., Gutsmann, T., Hube, B. and Naglik, J. (2016). Candidalysin is a fungal peptide toxin critical for mucosal infection. *Nature*, 532(7597), pp.64-68.

Mozioglu, E., Gokmen, O., Tamerler, C., Kocagoz, Z. and Akgoz, M. (2015). Selection of Nucleic Acid Aptamers Specific for Mycobacterium tuberculosis. *Applied Biochemistry and Biotechnology*, 178(4), pp.849-864.

Moon, J., Kim, G., Park, S., Lim, J. and Mo, C. (2015). Comparison of Whole-Cell SELEX Methods for the Identification of Staphylococcus Aureus-Specific DNA Aptamers. *Sensors*, 15(4), pp.8884-8897.

Musheev, M. and Krylov, S. (2006). Selection of aptamers by systematic evolution of ligands by exponential enrichment: Addressing the polymerase chain reaction issue. *Analytica Chimica Acta*, 564(1), pp.91-96.

Nanteza, M., Tusiime, J., Kalyango, J. and Kasangaki, A. (2014). Association between oral candidiasis and low CD4+ count among HIV positive patients in Hoima Regional Referral Hospital. *BMC Oral Health*, 14(1).

Nobile, C. and Mitchell, A. (2005). Regulation of Cell-Surface Genes and Biofilm Formation by the C. albicans Transcription Factor Bcr1p. *Current Biology*, 15(12), pp.1150-1155.

Nobile, C., Andes, D., Nett, J., Smith, F., Yue, F., Phan, Q., Edwards, J., Filler, S. and Mitchell, A. (2006). Critical Role of Bcr1-Dependent Adhesins in C. albicans Biofilm Formation In Vitro and In Vivo. *PLoS Pathogens*, 2(7), p.e63.

Ostrosky-Zeichner, L. (2012). Invasive Mycoses: Diagnostic Challenges. *The American Journal of Medicine*, 125(1), pp.S14-S24.

Pegorie, M., Denning, D. and Welfare, W. (2017). Estimating the burden of invasive and serious fungal disease in the United Kingdom. *Journal of Infection*, 74(1), pp.60-71.

Penner, G., 2012. Commercialization of an aptamer-based diagnostic test. *IVD Technol*, *18*(4), pp.31-37.

Perlin, D. (2011). Current perspectives on echinocandin class drugs. *Future Microbiology*, 6(4), pp.441-457.

Pestourie, C., Cerchia, L., Gombert, K., Aissouni, Y., Boulay, J., Franciscis, V., Libri, D., Tavitian, B. and Ducongé, F. (2006). Comparison of Different Strategies to Select Aptamers Against a Transmembrane Protein Target. *Oligonucleotides*, 16(4), pp.323-335.

Public Health England (2018). Laboratory surveillance of candidaemia in England, Wales and Northern Ireland: 2017. *Health Protection Report*, 12(34).

Rajendran, R., Williams, C., Lappin, D., Millington, O., Martins, M. and Ramage, G. (2013). Extracellular DNA Release Acts as an Antifungal Resistance Mechanism in Mature Aspergillus fumigatus Biofilms. *Eukaryotic Cell*, 12(3), pp.420-429.

Rast, T., Kullas, A., Southern, P. and Davis, D. (2016). Human Epithelial Cells Discriminate between Commensal and Pathogenic Interactions with Candida albicans. *PLOS ONE*, 11(4), p.e0153165.

Satoh, K., Makimura, K., Hasumi, Y., Nishiyama, Y., Uchida, K. and Yamaguchi, H. (2009). Candida aurissp. nov., a novel ascomycetous yeast isolated from the external ear canal of an inpatient in a Japanese hospital. *Microbiology and Immunology*, 53(1), pp.41-44.

Sefah, K., Shangguan, D., Xiong, X., O'Donoghue, M. and Tan, W. (2010). Development of DNA aptamers using Cell-SELEX. *Nature Protocols*, 5(6), pp.1169-1185.

Shangguan, D., Bing, T. and Zhang, N. (2015). Cell-SELEX: Aptamer Selection Against Whole Cells. *Aptamers Selected by Cell-SELEX for Theranostics*, pp.13-33.

Shapiro, R., Robbins, N. and Cowen, L. (2011). Regulatory Circuitry Governing Fungal Development, Drug Resistance, and Disease. *Microbiology and Molecular Biology Reviews*, 75(2), pp.213-267.

Sobel, J. (2007). Vulvovaginal candidosis. *The Lancet*, 369(9577), pp.1961-1971.

Spill, F., Weinstein, Z., Irani Shemirani, A., Ho, N., Desai, D. and Zaman, M. (2016). Controlling uncertainty in aptamer selection. *Proceedings of the National Academy of Sciences*, 113(43), pp.12076-12081.

Staab, J., Bradway, S., Fidel Jr., P. and Sundstrom, P. (1999). Adhesive and Mammalian Transglutaminase Substrate Properties of Candida albicans Hwp1. *Science*, 283(5407), pp.1535-1538.

Taha, M., Pollard, S., Sarkar, U. and Longhurst, P. (2005). Estimating fugitive bioaerosol releases from static compost windrows: Feasibility of a portable wind tunnel approach. *Waste Management*, 25(4), pp.445-450.

Takahashi, M., Wu, X., Ho, M., Chomchan, P., Rossi, J., Burnett, J. and Zhou, J. (2016). High throughput sequencing analysis of RNA libraries reveals the influences of initial library and PCR methods on SELEX efficiency. *Scientific Reports*, 6(1).

Tang, X., Hua, Y., Guan, Q. and Yuan, C. (2016). Improved detection of deeply invasive candidiasis with DNA aptamers specific binding to (1→3)-β-D-glucans from Candida albicans. *European Journal of Clinical Microbiology & Infectious Diseases*, 35(4), pp.587-595.

Thompson, D., Carlisle, P. and Kadosh, D. (2011). Coevolution of Morphology and Virulence in Candida Species. *Eukaryotic Cell*, 10(9), pp.1173-1182.

Toh, S., Citartan, M., Gopinath, S. and Tang, T. (2015). Aptamers as a replacement for antibodies in enzyme-linked immunosorbent assay. *Biosensors and Bioelectronics*, 64, pp.392-403.

Tolle, F., Wilke, J., Wengel, J. and Mayer, G. (2014). By-Product Formation in Repetitive PCR Amplification of DNA Libraries during SELEX. *PLoS ONE*, 9(12), p.e114693.

Torrado, J., Espada, R., Ballesteros, M. and Torrado-Santiago, S. (2008). Amphotericin B Formulations and Drug Targeting. *Journal of Pharmaceutical Sciences*, 97(7), pp.2405-2425.

Turek, D. (2013). Molecular recognition of live methicillin-resistant staphylococcus aureus cells using DNA aptamers. *World Journal of Translational Medicine*, 2(3), p.67.

Usami, M., Ohata, A., Horiuchi, T., Nagasawa, K., Wakabayashi, T. and Tanaka, S. (2002). Positive (13)-beta-d-glucan in blood components and release of (13)-beta-d-glucan from depth-type membrane filters for blood processing. *Transfusion*, 42(9), pp.1189-1195.

Uppuluri, P., Chaturvedi, A., Srinivasan, A., Banerjee, M., Ramasubramaniam, A., Köhler, J., Kadosh, D. and Lopez-Ribot, J. (2010). Dispersion as an Important Step in the Candida albicans Biofilm Developmental Cycle. *PLoS Pathogens*, 6(3), p.e1000828.

van Leeuwen, P., van der Peet, J., Bikker, F., Hoogenkamp, M., Oliveira Paiva, A., Kostidis, S., Mayboroda, O., Smits, W. and Krom, B. (2016). Interspecies Interactions between Clostridium difficile and Candida albicans. *mSphere*, 1(6).

Vazquez, J., Miceli, M. and Alangaden, G. (2013). Invasive fungal infections in transplant recipients. *Therapeutic Advances in Infectious Disease*, 1(3), pp.85-105.

Waldorf AR, Polak A. Mechanisms of action of 5-fluorocytosine. Antimicrob Agents Chemother 1983; 23(1):79–85

Wang, K., Krawczyk, S., Bischofberger, N., Swaminathan, S. and Bolton, P. (1993). The tertiary structure of a DNA aptamer which binds to and inhibits thrombin determines activity. *Biochemistry*, 32(42), pp.11285-11292.

Wang, J., Rudzinski, J., Gong, Q., Soh, H. and Atzberger, P. (2012). Influence of Target Concentration and Background Binding on In Vitro Selection of Affinity Reagents. *PLoS ONE*, 7(8), p.e43940.

Wang, J., Chang, C., Young-Xu, Y. and Chan, K. (2010). Systematic Review and Meta-Analysis of the Tolerability and Hepatotoxicity of Antifungals in Empirical and Definitive Therapy for Invasive Fungal Infection. Antimicrobial Agents and Chemotherapy, 54(6), pp.2409-2419.

White, T. (2004). R.A. Calderone, ed. Candida and Candidiasis. *Mycopathologia*, 157(4), pp.389-390.

Zhao, X. (2004). ALS3 and ALS8 represent a single locus that encodes a Candida albicans adhesin; functional comparisons between Als3p and Als1p. *Microbiology*, 150(7), pp.2415-2428.